

## Discovery of a Bromodomain and Extraterminal Inhibitor with a Low Predicted Human Dose through Synergistic Use of Encoded Library Technology and Fragment Screening

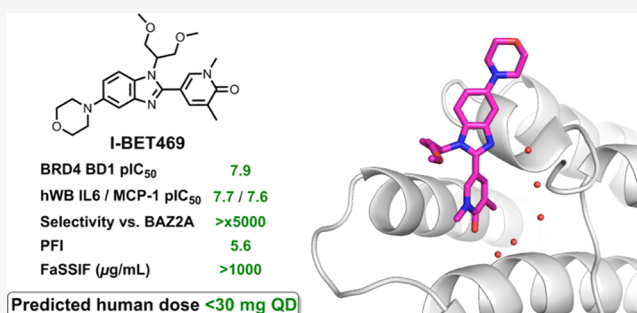
Christopher R. Wellaway,<sup>\*,†</sup> Dominique Amans,<sup>†</sup> Paul Bamborough,<sup>†</sup> Heather Barnett,<sup>†</sup> Rino A. Bit,<sup>†</sup> Jack A. Brown,<sup>†</sup> Neil R. Carlson,<sup>‡</sup> Chun-wa Chung,<sup>†</sup> Anthony W. J. Cooper,<sup>†</sup> Peter D. Craggs,<sup>†</sup> Robert P. Davis,<sup>†</sup> Tony W. Dean,<sup>†</sup> John P. Evans,<sup>†</sup> Laurie Gordon,<sup>†</sup> Isobel L. Harada,<sup>†</sup> David J. Hirst,<sup>†</sup> Philip G. Humphreys,<sup>†</sup> Katherine L. Jones,<sup>†</sup> Antonia J. Lewis,<sup>†</sup> Matthew J. Lindon,<sup>†,§</sup> Dave Lugo,<sup>†</sup> Mahnoor Mahmood,<sup>†</sup> Scott McCleary,<sup>†</sup> Patricia Medeiros,<sup>‡</sup> Darren J. Mitchell,<sup>†</sup> Michael O'Sullivan,<sup>†</sup> Armelle Le Gall,<sup>†</sup> Vipulkumar K. Patel,<sup>†</sup> Chris Patten,<sup>†</sup> Darren L. Poole,<sup>†</sup> Rishi R. Shah,<sup>†</sup> Jane E. Smith,<sup>†</sup> Kayleigh A. J. Stafford,<sup>†</sup> Pamela J. Thomas,<sup>†</sup> Mythily Vimal,<sup>†</sup> Ian D. Wall,<sup>†</sup> Robert J. Watson,<sup>†</sup> Natalie Wellaway,<sup>†</sup> Gang Yao,<sup>‡</sup> and Rab K. Prinjha<sup>†</sup>

<sup>†</sup>GSK, Gunnels Wood Road, Stevenage, Hertfordshire SG1 2NY, U.K.

<sup>‡</sup>GSK, 200 Cambridge Park Drive, Cambridge, Massachusetts 02140, United States

**S** Supporting Information

**ABSTRACT:** The bromodomain and extraterminal (BET) family of bromodomain-containing proteins are important regulators of the epigenome through their ability to recognize *N*-acetyl lysine (KAc) post-translational modifications on histone tails. These interactions have been implicated in various disease states and, consequently, disruption of BET–KAc binding has emerged as an attractive therapeutic strategy with a number of small molecule inhibitors now under investigation in the clinic. However, until the utility of these advanced candidates is fully assessed by these trials, there remains scope for the discovery of inhibitors from new chemotypes with alternative physicochemical, pharmacokinetic, and pharmacodynamic profiles. Herein, we describe the discovery of a candidate-quality dimethylpyridone benzimidazole compound which originated from the hybridization of a dimethylphenol benzimidazole series, identified using encoded library technology, with an *N*-methyl pyridone series identified through fragment screening. Optimization via structure- and property-based design led to I-BET469, which possesses favorable oral pharmacokinetic properties, displays activity in vivo, and is projected to have a low human efficacious dose.

**INTRODUCTION**

Protein transcription is a tightly regulated process and is controlled, in part, by proteins which “read” post-translational modifications (PTMs) on flexible histone tails.<sup>1</sup> One important class of the reader module, known as bromodomains, recognizes *N*-acetyl lysine (KAc) PTMs, and dysregulation of their function can lead to pathological conditions.<sup>2</sup> Of the 46 bromodomain-containing proteins (BCPs) identified,<sup>3</sup> the bromodomain and extraterminal domain (BET) family (BRD2, BRD3, BRD4, and BRDT) have been the most extensively studied, with links established to a diverse range of disease states such as cancer, inflammation, and viral infection.<sup>4</sup> Because of these associations, abrogation of BET–KAc interactions is a burgeoning field of research with an increasing number of small molecule inhibitors being described, several of which are currently under clinical

investigation.<sup>5</sup> Most of these inhibitors bind to each of the four BET isoforms and their tandem bromodomain modules with similar affinity, that is, pan-inhibition, but reports of molecules selective for either the first [(*N*-terminal) bromodomain, BD1] or second [(*C*-terminal) bromodomain, BD2] set of bromodomains have emerged,<sup>6–9</sup> as well as isoform-selective inhibitors<sup>10</sup> and compounds selective for one out of the eight BET bromodomains.<sup>11</sup> Furthermore, the BET family has been targeted using contemporary approaches such as bivalent inhibition of the tandem bromodomain modules,<sup>12–14</sup> degradation via the proteasome using proteolysis targeting chimera technology,<sup>15–19</sup> and through covalent inhibition.<sup>20</sup>

Received: October 8, 2019

A key goal in the development of BET inhibitors toward medicines has been to establish activity in preclinical species, and success in this area was demonstrated early in the field. For example, a seminal study with I-BET762 **1** (Figure 1)

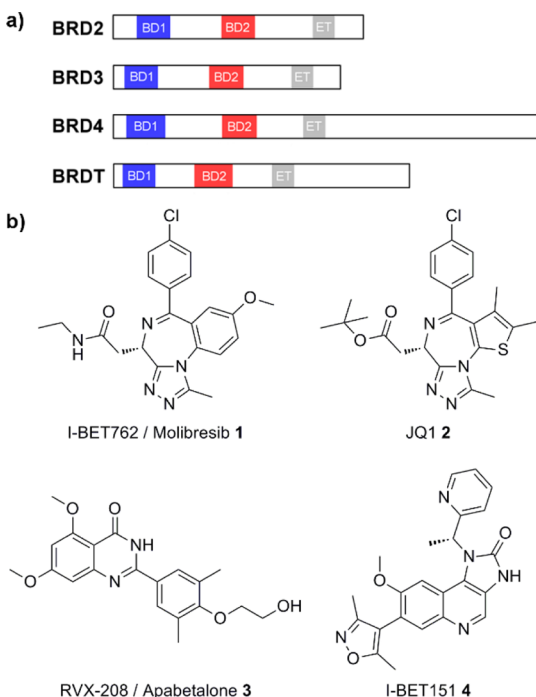


**Figure 1.** (a) Domain architecture of BET highlighting the eight bromodomains. (b) Early generation BET inhibitors with *in vivo* capability.

demonstrated its ability to protect mice against death in models of endotoxic shock and sepsis,<sup>21</sup> and it was subsequently shown to inhibit ear swelling in a rat model of delayed-type hypersensitivity.<sup>22</sup> The related BET inhibitor, JQ1 **2**, was first shown to reduce the tumor size and promote survival in mouse xenograft models of nuclear protein in testis midline carcinoma,<sup>23</sup> and has since been evaluated in a range of animal models including male contraception,<sup>24</sup> bleomycin-induced lung fibrosis,<sup>25,26</sup> and cardiac hypotrophy.<sup>27</sup> Another molecule first published at the start of the last decade, RVX-208 **3**, has been shown to increase apolipoprotein A-1 and high-density lipoprotein cholesterol in monkeys<sup>28</sup> and reduce atherosclerosis in hyperlipidemic apolipoprotein E-deficient mice.<sup>29</sup> The early generation BET inhibitor, I-BET151 **4**, promoted survival in mouse models of leukemia<sup>30</sup> and, similarly to I-BET762 **1**, suppressed cytokine production and protected against death in acute inflammatory mouse models.<sup>31,32</sup> Data from *in vivo* studies with newer inhibitors are emerging,<sup>33–46</sup> but such reports often disclose response data without the corresponding drug concentrations, which prevents full understanding of pharmacokinetic/pharmacodynamic (PKPD) effects and can hinder modeling predictions for humans. Furthermore, some inhibitors have been reported to display solubility-limited absorption following oral dosing<sup>32</sup> and short half-lives<sup>22,23,39</sup> and are at risk of not engaging the mechanism in humans if poor systemic exposure translates. For these reasons, there remains scope for the development of BET inhibitors with sufficient exposure in multiple preclinical test species to provide confidence that the mechanism can be engaged in humans. Furthermore, inhibitors need to possess

both favorable pharmacokinetic parameters and high potency for the target to achieve a low predicted human efficacious dose and minimize the risk of idiosyncratic toxicity. Accordingly, we herein report the development of a potent and soluble dimethylpyridone benzimidazole BET inhibitor exhibiting PK profiles which, after single species scaling based on the allometric principles, correspond to low predicted human doses of <30 mg once every day (QD). Hybridization of a dimethylphenol benzimidazole series identified using encoded library technology (ELT) with a methyl pyridone series discovered by fragment screening resulted in an improved dimethylpyridone benzimidazole scaffold. Subsequent optimization of off-target bromodomain selectivity was carried out alongside frequent PKPD modeling to deliver an inhibitor which fully engaged the BET mechanism and demonstrated immunomodulatory effects *in vivo*.

## RESULTS AND DISCUSSION

Our overall goal was to discover an orally bioavailable BET inhibitor that was structurally distinct from our existing clinical candidates.<sup>22,47</sup> We set approximate potency criteria of <50 nM in a BET biochemical fluorescence resonance energy transfer (FRET) assay and <100 nM in an LPS-stimulated human whole blood (WB) assay measuring inhibition of the proinflammatory cytokines monocyte chemoattractant protein 1 (MCP-1) and interleukin 6 (IL-6), a phenotype of BET inhibition.<sup>20</sup> We also required 100-fold selectivity over other BCPs and over representative targets from other target classes. To minimize the risk of compound-based attrition, we aimed for a property forecast index (PFI [ChromLog $D_{7.4}$  + number of aromatic rings])<sup>48</sup> <6, solubility in FaSSIF >100  $\mu\text{g}/\text{mL}$ , and a predicted human daily dose <100 mg. This was in accordance with our oral candidate quality criteria,<sup>49</sup> and these parameters guided the optimization process.

To identify a novel BET inhibitor chemotype, we embarked on a screening campaign using ELT which has proven to be an important lead generation platform for various therapeutic targets.<sup>50–55</sup> A 6His-BRD4 (1–477) tandem bromodomain construct was screened against a panel of DNA-encoded small-molecule libraries using affinity-based selection technology, and a hit series was identified from a three-cycle benzimidazole core library (Figure 2). This specific library was constructed using a split-and-pool strategy with three cycles of building blocks (BBs) to provide a total warhead diversity of 117 million compounds as previously reported.<sup>53–55</sup> Nucleophilic aromatic substitution of DNA-appended 4-fluoro-3-nitrobenzoate with 65 monoprotected diamines at cycle 1 was followed by nitro reduction to afford 65 benzenediamines (Figure 2a). These diamines were condensed with 922 aldehydes at cycle 2 to form benzimidazole ring systems. After amine deprotection, the library was reacted with 1960 amine capping groups (carboxylic acids, isocyanates, sulfonyl chlorides, and heterocyclic halides) to afford the final library. DNA tags were added after each cycle of reaction to unambiguously encode each warhead in the library. Interpretation of the affinity selection from this library was viewed in a cubic scatter plot (Figure 2b), where each axis corresponds to a BB cycle. Examination of these data revealed enrichment of a specific BB1 (piperidin-4-ylmethanamine, **5**) and BB2 (4-hydroxy-3,5-dimethylbenzaldehyde, **6**) combination which corresponded to 1,2,5-substituted benzimidazole **7**. The cycle 3 amine capping groups were predominately carboxylic acids of diverse structure, and the appearance of a highly populated

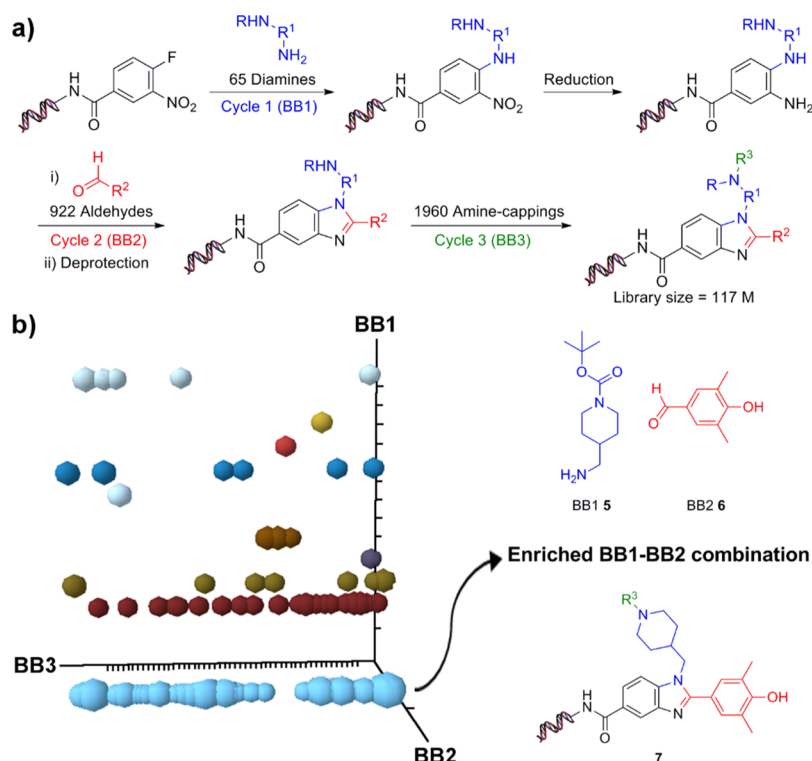
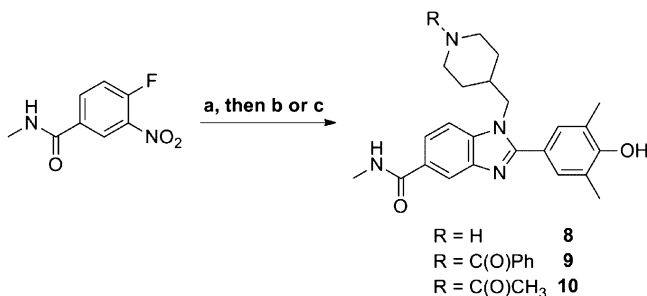


**Figure 2.** (a) Scheme of the hit DNA-encoded benzimidazole library where BB1, BB2, and BB3 refer to cycle 1, 2, and 3 BBs, respectively. (b) Result of the BRD4 screen of the benzimidazole library. Compounds on the highlighted horizontal line (light blue) in the cubic scatter plot shared the common BB1–BB2 combination (5 and 6, respectively) with BB3 as a variable component resulting in the generic hit structure 7. The sphere size is proportional to the DNA tag copy number. Library members with less than 5 copies were removed to simplify visualization.

(light blue) line along the x-axis indicated no preference for any particular carboxylic acid, suggesting that BB3 contributed little to the binding.

Having identified a hit series, we prepared several 1,2,5-substituted benzimidazoles without DNA tags as exemplars of the hit BB1–BB2 combination 7 in a similar manner to that outlined in Figure 2a (Scheme 1). The synthetic sequence commenced with reaction of 4-fluoro-*N*-methyl-3-nitrobenzamide with *tert*-butyl 4-(aminomethyl)piperidine-1-carboxylate (5) leading to the nucleophilic aromatic substitution product which was used without purification in the formation of the benzimidazole ring. Construction of the heterocycle was

#### Scheme 1. Synthesis of Dimethylphenol Benzimidazole Analogues 8–10<sup>a</sup>

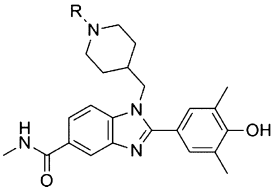


<sup>a</sup>Reagents and conditions: (a) (i) *tert*-butyl 4-(aminomethyl)piperidine-1-carboxylate (5), DIPEA, EtOH, 80 °C; (ii) 4-hydroxy-3,5-dimethylbenzaldehyde, Na<sub>2</sub>S<sub>2</sub>O<sub>4</sub>, EtOH/H<sub>2</sub>O (4:1), 80 °C; (iii) TFA, DCM, rt; (b) PhCO<sub>2</sub>H, HATU, DIPEA, DMF, rt; (c) (i) Ac<sub>2</sub>O, pyr, THF/MeCN; (ii) 2 M LiOH, THF/MeOH (4:1), rt.

carried out in one pot, whereby the *ortho*-nitroaniline was reacted with 4-hydroxy-3,5-dimethylbenzaldehyde in the presence of sodium dithionite in a nitro reduction–aromatization sequence according to the method of Yang et al.<sup>56</sup> Subsequent *N*-Boc removal provided amine 8 which was acylated to provide the target amides 9 and 10. The activities of these compounds were measured in a historical fluorescence polarization (FP) assay format and/or a routine FRET assay format using a mutant BRD4 construct which determined activity at BD1 and was used as a surrogate for activities at all BET bromodomains (Table 1). Lipophilicities were measured using a chromatographic method at pH = 7.4 (Chrom-LogD<sub>7.4</sub>),<sup>48</sup> and the corresponding PFI values were calculated.

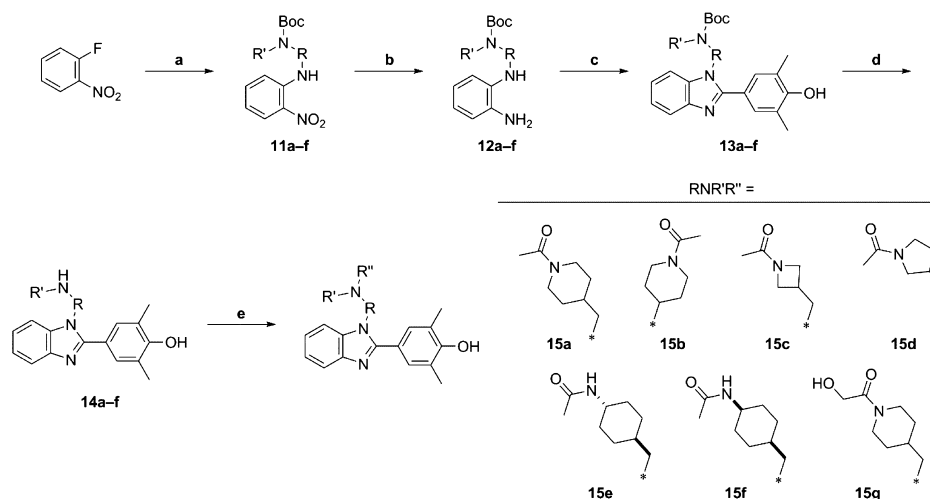
Piperidine 8 was weakly active at BRD4 but potency was increased by capping as the benzamide 9 and acetamide 10, indicating a basic center was not optimal for binding to the target at this position in the molecule. While acetamide 10 was the slightly less potent amide, it was less lipophilic than benzamide 9 leading to a more desirable PFI and higher LLE. Therefore, exploration of alternative benzimidazole N1 substituents was generally conducted with acetamides in place. First, however, we were interested in assessing the importance of the benzimidazole 5-position amide toward binding affinity, given its role as the linking functionality to DNA during ELT hit identification. Accordingly, we prepared benzimidazole 15a lacking the 5-amide following Scheme 2 and, after biochemical testing, found only a slight lowering in activity versus its amide-substituted congener 10 (BRD4 FP pIC<sub>50</sub> = 6.3 and 6.6, respectively). Therefore, further exploration of SAR at the benzimidazole N1-position was conducted without the 5-amide in place (compounds 15b–g, Scheme 2); BRD4 FRET assay results are shown in Table 2.

Table 1. Data for Dimethylphenol Benzimidazole N1 Analogues 8–10



compound	R	BRD4 pIC <sub>50</sub> <sup>a</sup>		ChromLogD <sub>7,4</sub>	PFI	LE <sup>b</sup>	LLE <sup>b,c</sup>
		FP	FRET				
8	H	NT	5.7	0.8	3.8	—/0.27	—/2.1
9	PhC(O)	6.9	6.7	3.2	7.2	0.26/0.25	2.5/2.3
10	CH <sub>3</sub> (O)	6.6	NT	2.0	5.0	0.28/—	4.0/—

<sup>a</sup>Expressed as the mean from at least two test occasions. NT = Not tested. <sup>b</sup>Calculated from FP/FRET pIC<sub>50</sub> values. <sup>c</sup>Defined as BRD4 pIC<sub>50</sub> – clog P.

Scheme 2. Synthesis of Dimethylphenol Benzimidazole N1 Analogues 15a–g<sup>a</sup>

<sup>a</sup>Reagents and conditions: (a) RNH<sub>2</sub>, K<sub>2</sub>CO<sub>3</sub>, MeCN, 80–110 °C; (b) H<sub>2</sub>, Pd/C, DMF, 30 °C; (c) 4-hydroxy-3,5-dimethylbenzaldehyde, Na<sub>2</sub>S<sub>2</sub>O<sub>5</sub>, DMF, 100 °C; (d) 4 M HCl in MeOH, rt–50 °C; (e) AcOH or 2-hydroxyacetic acid, BOP, NEt<sub>3</sub>, DCM, rt.

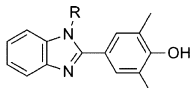
BRD4 activity for 4-piperidine acetamide **15b** was threefold less than that for 4-methylene piperidine acetamide **15a** and highlighted the importance of a linking methylene between the pendant heterocycle and the benzimidazole core. The size of the heterocycle also affected activity, underscored by the lower potencies for azetidine **15c** and racemic pyrrolidine **15d** compared to piperidine **15a**. Transposition of the amide in piperidine acetamide **15a** to an exocyclic position gave the cyclohexyl acetamides **15e** and **15f**, and activity was maintained with the latter *cis*-isomer. Finally, it was demonstrated that the acetamide **15a** could be substituted with a hydroxyl group to give the more polar hydroxy acetamide **15g** without lowering BRD4 activity.

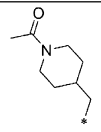
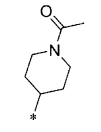
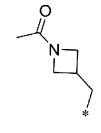
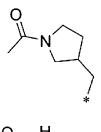
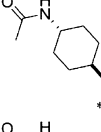
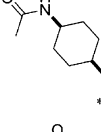
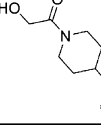
During these investigations, we pursued efforts to obtain an X-ray crystal structure of acetamide **10**. Gratifyingly, cocrystallization with BRD4 BD1 resulted in a 1.5 Å structure and revealed the dimethylphenol moiety positioned in the KAC binding site (Figure 3).

The 2,6-dimethylphenol group replicated the interactions of KAC<sup>3</sup> and bound in the same manner as other 2,6-dimethylphenol-containing BET ligands.<sup>57</sup> Specifically, the hydroxyl accepted a hydrogen bond from Asn140 and donated a hydrogen bond via water to Tyr97, while an ortho-methyl substituent occupied a lipophilic pocket adjacent to Phe83.

The phenyl ring of the benzimidazole bicyclic system was positioned between Leu92 and Trp81 (a region known as the ZA channel) and formed an edge-to-face interaction with the latter residue. The benzimidazole N1 position provided an appropriate vector for the 4-methylene piperidine to bind to the lipophilic region flanking the Trp81-Pro82-Phe83 triad, commonly referred to as the WPF shelf, and occupying this part of the binding site has generally been associated with increased potency.<sup>58</sup> The relatively small Ile146 residue in BRD4 BD1, located near the start of the C-helix, permitted access to the WPF shelf but larger residues at this position in other BCPs preclude access, and thus, binding to the WPF shelf in BRD4 BD1 was expected to impart selectivity over certain BCPs.<sup>58</sup> The acetamide was directed out of the WPF shelf toward the solvent, and this was consistent with SARs demonstrating that alterations to the amide did not profoundly affect potency. The methylamide substituent at the 5-position of the benzimidazole was directed out of the ZA channel toward the solvent, and this positioning was consistent with its role as the linker to DNA during hit identification. A final observation was that the benzimidazole N3 atom was sufficiently close (2.7 Å) to accept a hydrogen bond from an adjacent water molecule, which in turn formed contacts to

**Table 2.** BRD4 Activities and PFI Values of Dimethylphenol Benzimidazole N1 Analogues 15a–g



Compound	R	BRD4 FRET pIC <sub>50</sub> <sup>a</sup>	PFI
15a		6.3	6.2
15b		5.8	6.1
15c		5.8	5.7
15d		5.6	5.6
15e		5.8	6.2
15f		6.3	6.2
15g		6.2	5.9

<sup>a</sup>Expressed as the mean from at least three test occasions.

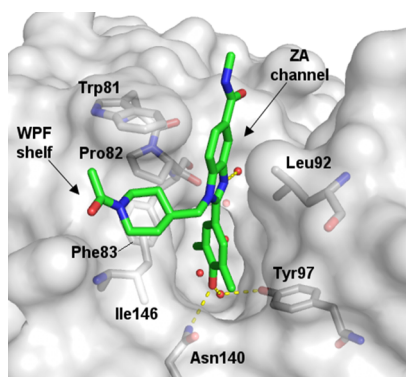


**Figure 3.** X-ray crystal structure of acetamide **10** (carbon = green) in BRD4 BD1 (carbon = gray, PDB 6TPX). Water molecules at the base of the binding pocket are shown as red spheres, and selected hydrogen bonds are shown as yellow dashed lines.

other water molecules and Pro82 and was therefore deemed an important interaction.

With the binding mode and opportunity for structure-based design established, we were keen to investigate this series further and identify any issues requiring optimization. Our primary concern at this early stage was the reliance on the 2,6-dimethylphenol moiety as the KAc mimetic. Given the general requirement for BET inhibitors to possess a KAc mimetic,<sup>5</sup> the 2,6-dimethylphenol was deemed integral to achieve high potency but represented a potential liability because of the propensity of phenols to be rapidly metabolized by phase II enzymes. Therefore, dimethylphenol **10** was assessed in a mouse PK experiment where clearance from the blood (346 mL/min/kg) was found to be greater than liver blood flow, and a short half-life (0.37 h) was observed after iv dosing (see the [Supporting Information](#)). Based on these results, we commenced investigations to replace the 2,6-dimethylphenol KAc mimetic.

To find suitable alternative KAc-binders and integrate additional information for optimal lead generation,<sup>59</sup> we turned to our extensive collection of bromodomain fragment data. We have previously described our first screen of a fragment library against the BET family bromodomains, which generated multiple chemically diverse low-molecular-weight starting points that bind in the KAc site.<sup>60</sup> These are ligand-efficient starting points, and we have shown that they can be optimized for BET bromodomains using structure-based design to build in the extra pharmacophoric components needed for high-affinity binding.<sup>61</sup> In addition, we have found the pool of multiple bromodomain/fragment crystal structures to be a valuable source of ideas for isosteric replacements and hybridization during optimization of leads from other sources including high-throughput screening and ELT.

One of the fragments emerging from this work was the low-affinity ligand-efficient *N*-methyl pyridone-containing compound **16** (BRD4 FRET pIC<sub>50</sub> = 4.9, LE = 0.42) ([Figure 4a](#)). A 1.9 Å X-ray crystal structure of this fragment in BRD2 BD1 showed the pyridone group binding in the KAc-site, with its carbonyl group forming a direct hydrogen bond interaction with Asn156 and through the water network to Tyr113 ([Figure 4b](#)). The methoxyphenyl group partially occupied the ZA channel without completely filling it.

A substructure search for related *N*-methyl pyridone analogues in the GSK compound collection identified the imidazole **17** (BRD4 FRET pIC<sub>50</sub> = 5.2, LE = 0.36). A 2.3 Å X-ray crystal structure of this compound was also obtained in BRD2 BD1 ([Figure 4c](#)) and confirmed that the interactions of the *N*-methylpyridone are the same as those made by fragment **16**. The imidazole pointed toward the ZA channel with one of its nitrogens forming a hydrogen bond to water. Although the fluorophenyl ring did not occupy the WPF shelf, this substituent position on the imidazole offered a vector to access the shelf and potentially gain potency.

[Figure 4d](#) shows the superimposed crystal structures of pyridone **17** in BRD2 BD1 and the phenol **10** in BRD4 BD1. Unusually, in bromodomain-inhibitor complexes, the phenolic OH group of **10** probably acts as a hydrogen bond donor toward the W1 water. This contrasts with the carbonyl of pyridone **17** which can only act as a more typical hydrogen bond acceptor to the W1 water. To accommodate this difference would require a rotation of the W1 water and a change of some of its interactions with the conserved tyrosine or the other conserved water molecules ([Figure 4](#)), but it is not possible to see the details from the electron density. We speculate that the requirement for an uncommon water

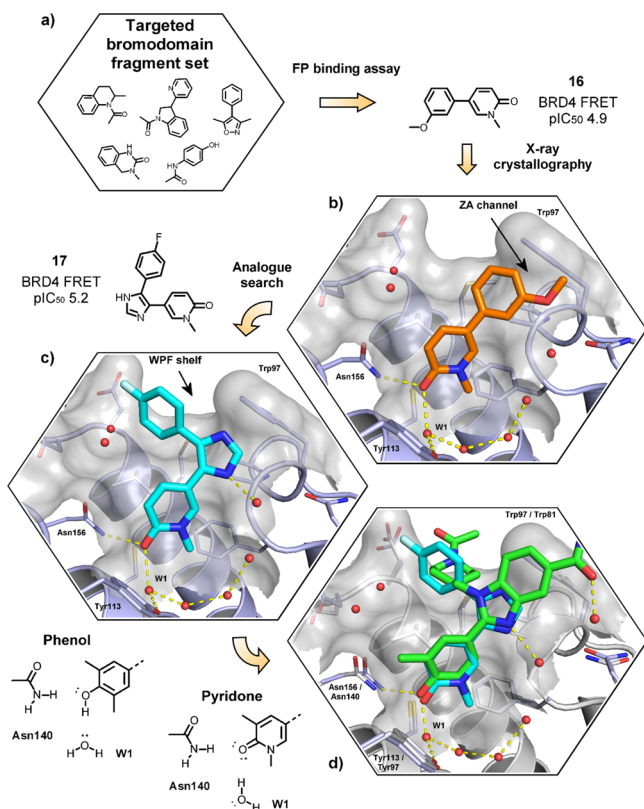


**Figure 4.** (a) Identification of pyridones as KAC-mimetics from a fragment-based screen.<sup>59</sup> (b) X-ray crystal structure of *N*-methyl pyridone fragment **16** (carbon = orange) in BRD2 BD1 (PDB 6TQ1). (c) X-ray crystal structure of *N*-methyl pyridone imidazole **17** (carbon = cyan) in BRD2 BD1 (PDB 6TQ2). (d) Superposition of X-ray crystal structures of *N*-methyl pyridone imidazole **17** (carbon = cyan) in BRD2 BD1 (PDB 6TQ2) and 2,6-dimethylphenol **10** (carbon = green) in BRD4 BD1 (PDB 6TPX).

orientation to bind the phenols may explain their lower ligand efficiency relative to the pyridone. Regardless of this, the close overlay between the crystal structures of these series suggested that we should attempt a hybridization approach. It is worth noting that other pyridone-containing BET inhibitors have been reported since this work was carried out.<sup>62–66</sup>

Preparation of hybrid 1,3-dimethylpyridone **19a** and close analogues was carried out according to Scheme 3, and biological results are shown in Table 3. Pleasingly, BRD4 activity for 1,3-dimethylpyridone **19a** was higher than that for 2,6-dimethylphenol **15g**, and lipophilicity was lowered by ~10-fold which resulted in a higher LLE. The requirement for two

**Table 3.** BRD4 Activities and PFI Values of Benzimidazole 2-Position Analogues **19a–d**

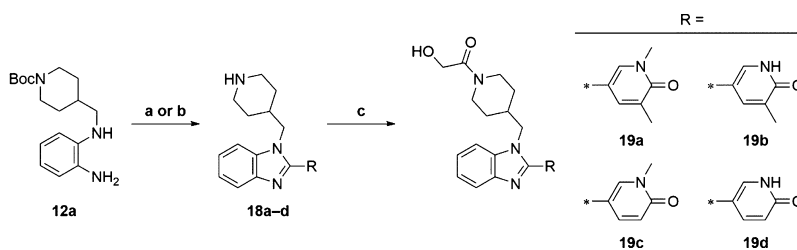
Compound	R	BRD4 FRET pIC <sub>50</sub> <sup>a</sup>	PFI	LE	LLE
<b>15g</b>		6.2	5.9	0.29	2.6
<b>19a</b>		6.6	4.8	0.31	5.0
<b>19b</b>		5.8	4.7	0.28	4.7
<b>19c</b>		5.1	4.4	0.25	4.0
<b>19d</b>		<4.3 <sup>b</sup>	4.1	-	-

<sup>a</sup>Expressed as the mean from at least two test occasions. <sup>b</sup>A pIC<sub>50</sub> value of <4.8 was determined on one test occasion out of four and was excluded from the reported mean value.

methyl substituents was established by testing mono C3-methyl **19b** and mono N1-methyl **19c** and both lowered activity relative to dimethyl **19a** but to different extents. Removal of both methyl groups to give NH pyridone **19d** resulted in the loss of measurable activity.

Notwithstanding the encouraging biochemical and physicochemical data for 1,3-dimethylpyridone **19a**, the BRD4 activity and MCP-1 WB potency (pIC<sub>50</sub> = 5.8) were still below our target levels. We therefore sought to replace the benzimidazole N1-substituent with a more potent group. SARs established during off-DNA ELT chemistry (data not shown) indicated that lipophilic substituents were preferred at this position, and this was consistent with binding to the nonpolar residues which comprise the WPF shelf (see Figure 3). The reduction in lipophilicity afforded by replacing the dimethylphenol KAC mimetic with the dimethylpyridone allowed investigation of a substituent lacking a polar amide group while maintaining the overall physicochemical properties in a

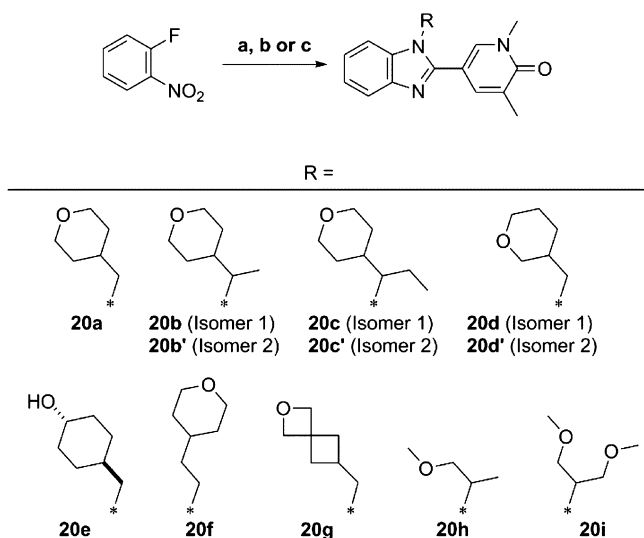
**Scheme 3.** Synthesis of Benzimidazole 2-Position Analogues **19a–d**<sup>a</sup>



<sup>a</sup>Reagents and conditions: for compounds **18a**, **18b**, and **18d**: (a) (i) RCHO, Na<sub>2</sub>S<sub>2</sub>O<sub>5</sub>, DMF, 100 °C; (ii) HCl in MeOH, rt; for compound **18c**: (b) RCO<sub>2</sub>H, PPA, 180 °C; (c) 2-hydroxyacetic acid, EDC-HCl, HOBt, DIPEA, DCM, rt.

desirable space. This led us to prepare 4-methylene tetrahydropyran (THP) **20a** (Scheme 4) which exhibited

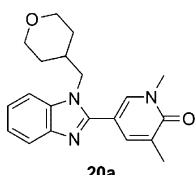
**Scheme 4. Synthesis of Dimethylpyridone Benzimidazole N1 Analogues 20a–i<sup>a</sup>**



<sup>a</sup>Reagents and conditions: (a) amine, DIPEA, DMSO or NMP or 2-MeTHF, microwave, 110–125 °C; (b) (i) 1,5-dimethyl-6-oxo-1,6-dihydropyridine-3-carbaldehyde, Na<sub>2</sub>S<sub>2</sub>O<sub>4</sub>, EtOH/H<sub>2</sub>O (2:1), 100 °C; (ii) for compound **20e**: TFA, DCM, rt; (c) (i) H<sub>2</sub>, Pd/C, EtOH, rt; (ii) Oxone, DMF/H<sub>2</sub>O (30:1), rt.

<100 nM activity at BRD4 and possessed favorable physicochemical properties (Table 4). These characteristics

**Table 4. Structure of 4-Methylene THP **20a** and Initial Profile**



BRD4 FRET pIC <sub>50</sub> <sup>a</sup>	7.1
WB pIC <sub>50</sub> <sup>a</sup> IL-6/MCP-1	6.7/6.6
BAZ2A FRET pIC <sub>50</sub> <sup>b</sup>	6.5
ChromLogD <sub>7.4</sub> /PFI	2.7/5.7
LE/LLE	0.39/4.8
FaSSIF (μg/mL)	>1000

<sup>a</sup>Expressed as the mean from at least four test occasions. <sup>b</sup>Expressed as the mean from two test occasions.

contributed to effective suppression of the proinflammatory cytokines IL-6 and MCP-1 in LPS-stimulated human WB and high solubility in FaSSIF (determined using a crystalline solid form).

Having identified an attractive lead compound, we carried out more comprehensive profiling to identify and understand any issues to guide the medicinal chemistry strategy. Accordingly, we screened 4-methylene THP **20a** against a panel of eight representative BCPs (see the Supporting Information) and found that it bound to bromodomain adjacent to zinc finger domain 2A (BAZ2A) with notable affinity (Table 4). BAZ2A has been identified as the large subunit of the nucleolar remodeling complex and plays a role in chromosome stability, and it is known to silence some rRNA genes and can delay proliferative growth when knocked down in cells.<sup>67</sup> It was unknown how this profile could translate to humans, so we set the goal to overcome this off-target activity during lead optimization. We also conducted PK profiling on 4-methylene THP **20a** to benchmark the pyridone benzimidazole series. Initially, compound stability in microsome and hepatocyte preparations was assessed and highlighted differences between species with rats displaying higher turnover than both humans and dogs (Table 5). Comparison of these data with observed in vivo clearance following iv administration demonstrated a good correlation. The high clearance observed in rats required improvement to ensure adequate systemic exposure following oral administration for preliminary toxicology studies.

At this stage, the human efficacious dose of 4-methylene THP **20a** was predicted using the single species scaling approach<sup>68,69</sup> (correcting for differences in the fraction unbound) in conjunction with the MCP-1 WB activity. A target coverage of IC<sub>50</sub> over a 24 h dosing period was selected at this stage of our investigations for sufficient engagement of the mechanism, and the predicted once-daily human doses based on this were >2 and 1.4 g from rats and dogs, respectively (see the Supporting Information for details and assumptions). These predicted high human doses were a result of the moderate WB MCP-1 activity combined with a predicted short half-life. With an aim to have a dose <100 mg, these contributing factors became a focus for our future optimization efforts.

During profiling lead benzimidazole **20a**, we obtained a 1.8 Å resolution X-ray crystal structure in BRD4 BD1, and this revealed an identical binding mode to that of hit benzimidazole **10** with direct overlay of the 1,3-dimethylpyridone and 2,6-dimethylphenol moieties (Figure 5a). This structure also provided a basis to interrogate the observed binding to BAZ2A through superposition of an apo structure of BAZ2A<sup>70</sup> (Figure 5b). This showed several differences most notably in the C-helices where Met149 in BRD4 BD1 is replaced by Ala1882 in

**Table 5. In Vitro and in Vivo PK Data of 4-Methylene THP **20a****

species	IVC (mL/min/g)		<i>f</i> <sub>ub</sub>	CL <sub>b</sub> (mL/min/kg)	CL <sub>u</sub> (mL/min/kg)	<i>V</i> <sub>dss</sub> (L/kg)	<i>T</i> <sub>1/2, iv</sub> (h)	<i>F</i> (%)	human predicted QD dose (mg)
	Mics	Heps							
rat <sup>a</sup>	3.2	17	0.55	82	149	1.4	0.2		>2000
dog <sup>b,c</sup>	<0.37	<1.3	0.47	8	17	1.4	2.3	97	1400
human	0.83	<0.87	0.40						

<sup>a</sup>iv dose (1.0 mg/kg): 1 h infusion in DMSO (2%, v/v) and Kleptose HPB (10%, w/v) in saline (0.9% w/v). <sup>b</sup>iv dose (0.5 mg/kg): 1 h infusion in DMSO (2%, v/v) and Kleptose HPB (10%, w/v) in saline (0.9% w/v). <sup>c</sup>po dose (1.0 mg/kg): a suspension of solid of unknown form in 1% (w/v) methylcellulose (400 cps) (aq).

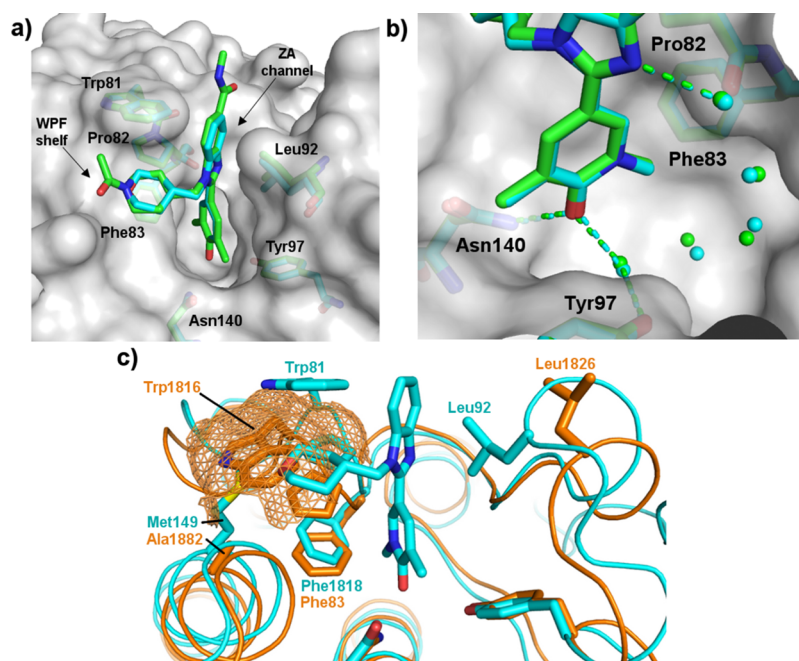


**Figure 5.** (a) Superposition of X-ray crystal structures of 1,3-dimethylpyridone **20a** (carbon = cyan, PDB 6TPY) and 2,6-dimethylphenol **10** in BRD4 BD1 (carbon = green, PDB 6TPX). A surface was applied to the protein of PDB 6TPX. (b) View at the base of the binding pocket from superposition of 1,3-dimethylpyridone **20a** (carbon, water molecules [spheres], and selected hydrogen bonds [dashed lines] = cyan PDB 6TPY) and 2,6-dimethylphenol **10** (carbon, water molecules [spheres], and selected hydrogen bonds [dashed lines] = green, PDB 6TPX) X-ray crystal structures in BRD4 BD1. A surface was applied to the protein of PDB 6TPX. (c) Superposition of the X-ray crystal structure of 1,3-dimethylpyridone **20a** in BRD4 BD1 (carbon = cyan, PDB 6TPY) with an apo structure of BAZ2A<sup>70</sup> (carbon = orange, PDB 4LZ2). A wireframe surface has been applied to Trp1816 of BAZ2A.

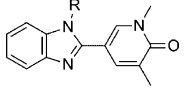
BAZ2A. The consequence of this difference is the collapse of the WPF motif (consisting of Trp1816-Pro1817-Phe1818) and a closed WPF-shelf in BAZ2A, whereas this region is fully open and accessible in the BET family. It was clear that this superposition did not provide an explanation for the observed BAZ2A activity for lead compound **20a** as the THP moiety would sterically clash with Trp1816 and preclude binding to this BCP. Another effect of the collapsed WPF motif in BAZ2A was the enlargement of the ZA channel relative to that in BRD4 BD1, and this was increased further by deletions in the ZA loop indicating that Leu1826 was unable to form a narrow junction equivalent to that caused by Leu92 in BRD4 BD1. We speculated that the enlarged ZA channel in BAZ2A permitted distortion of the dimethylphenol-benzimidazole dihedral angle from twisted ( $42^\circ$ ) in BRD4 BD1 to a more coplanar conformation in BAZ2A and that branching off the methylene group attached to the benzimidazole N1 position would restrict this conformational freedom, thereby increasing selectivity over BAZ2A.

Using this structural insight, we investigated branching on the methylene group and other modifications to the 4-methylene THP and counter-screened for their BAZ2A activities (Scheme 4 and Table 6). An additional consideration during this exploration was to limit significant increases in lipophilicity.

Incorporation of a methyl branch on the methylene gave the enantiomeric pair **20b** and **20b'** which was obtained upon chiral chromatographic separation of the racemic mixture. In terms of BRD4 FRET activity, a clear preference for stereoisomer **20b'** was observed, but BAZ2A activity was not significantly affected when compared to unbranched methylene **20a**. However, further extension of the branching substituent

did reduce BAZ2A activity with ethyl enantiomers **20c** and **20c'** exhibiting preferential binding to BRD4 by >125- and 40-fold, respectively. Strikingly, the 3-methylene THP enantiomers **20d** and **20d'** reduced BAZ2A activity by several orders of magnitude compared to 4-methylene THP **20a** with the latter enantiomer displaying particularly high BRD4 activity resulting in ~3000-fold selectivity. Other simple modifications to the 4-methylene THP group, such as moving the ether oxygen to an exocyclic position to give 4-methylene cyclohexylalcohol **20e** and homologating the methylene to give ethylene **20f**, lowered BAZ2A activity while maintaining BRD4 potency. The spirocyclic oxetane **20g**, a motif used as a replacement for 6-membered cyclic systems,<sup>71,72</sup> also increased selectivity over BAZ2A and, additionally, lowered microsomal clearance (rat and human = 0.99 and <0.40 mL/min/g, respectively) while remaining liponeutral compared to THP **20a**. Acyclic substituents were also explored with racemic propyl methoxy **20h** demonstrating >100-fold selectivity over BAZ2A but only moderate BRD4 activity. Achiral dimethoxypropyl **20i** maintained a high level of BRD4 activity and was inactive at BAZ2A. Taken together, these data revealed the 4-methylene THP group to be a privileged motif for binding to BAZ2A and only minor modifications were required to dampen activity.

We further profiled dimethoxypropyl **20i** and found that WB potencies ( $pIC_{50}$  = 6.6 and 7.0 for IL-6 and MCP-1 analytes, respectively) were commensurate with high BRD4 FRET activity. In addition, high solubility was determined in FaSSIF media (>1000  $\mu\text{g/mL}$ ) from a crystalline solid form. We also assessed the compound for stability in microsomes and hepatocytes and found that it was more stable in both rat and human preparations versus 4-methylene THP **20a** (Table

Table 6. BRD4 and BAZ2A Activities and ChromLogD<sub>7.4</sub> Values of Benzimidazole N1 Analogues 20a–i


Compound	R	pIC <sub>50</sub> <sup>a</sup>		Selectivity <sup>b</sup>	PFI
		BRD4 FRET	BAZ2A FRET		
20a		7.1	6.5	0.6	5.7
20b		5.6	4.2	1.4	6.1
	Isomer 1				
20b'		7.2	6.3	0.9	6.0
	Isomer 2				
20c		6.1	<4.0	>2.1	6.8
	Isomer 1				
20c'		6.8	5.2	1.6	6.4
	Isomer 2				
20d		7.5	4.6	2.9	6.0
	Isomer 1				
20d'		7.6	4.1 <sup>c</sup>	3.5	6.0
	Isomer 2				
20e		7.1	4.3	2.8	5.3
20f		7.3	4.4	2.9	6.2
20g		7.3	4.2	3.1	5.6
20h		6.5	4.4	2.1	6.1
20i		7.4	<4.0	>3.4	6.0

<sup>a</sup>Expressed as the mean from at least two test occasions. <sup>b</sup>Calculated as BRD4 FRET pIC<sub>50</sub> – BAZ2A pIC<sub>50</sub>. <sup>c</sup>pIC<sub>50</sub> values of <4.0 were determined on two test occasions out of four and were excluded from the reported mean value.

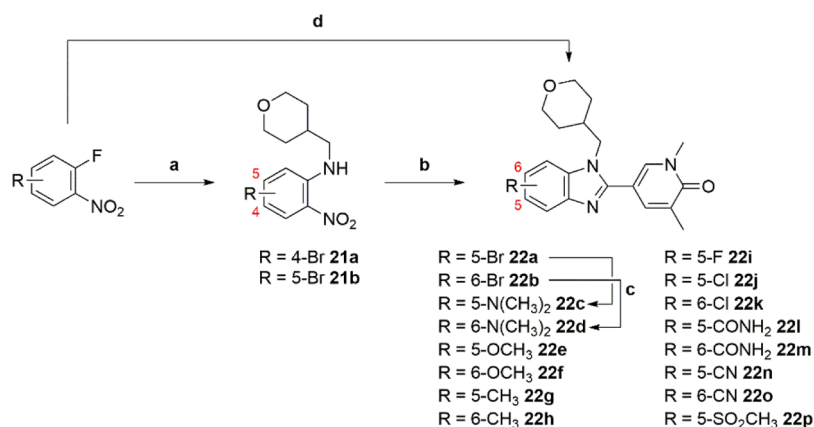
7). This improvement was noteworthy, given the slight increase in lipophilicity incurred upon replacement of the 4-methylene THP with the dimethoxypropyl and, therefore, represented an alternative strategy for improving the stability

of this cyclic ether compared to reducing the ring size.<sup>73</sup> A subsequent in vivo rat PK study revealed moderate clearance and a longer half-life relative to 4-methylene THP 20a. The clearance, and unbound clearance, of dimethoxypropyl 20i in

Table 7. In Vitro and in Vivo PK Data of Dimethoxypropyl 20i

species	IVC (mL/min/g)		$f_{ub}$	$CL_b$ (mL/min/kg)	$CL_u$ (mL/min/kg)	$V_{dss}$ (L/kg)	$T_{1/2, iv}$ (h)	$F$ (%)	human predicted QD dose (mg)
	Mics	Heps							
rat <sup>a,b</sup>	<0.46	1.1	0.59	37	63	2.1	3.2	46	1600
dog <sup>c,d</sup>	<0.37	<1.3	0.57	5	9	0.8	1.7	46	470
human	<0.40	<0.87	0.37						

<sup>a</sup>iv dose (1.5 mg/kg): 1 h infusion in DMSO (2%, v/v) and Kleptose HPB (10%, w/v) in saline (0.9% w/v). <sup>b</sup>po dose (3 mg/kg): a suspension of crystalline solid in 1% (w/v) methylcellulose (400 cps) (aq). <sup>c</sup>iv dose (0.5 mg/kg): 1 h infusion in DMSO (2%, v/v) and Kleptose HPB (10%, w/v) in saline (0.9% w/v). <sup>d</sup>po dose (1.0 mg/kg): a suspension of crystalline solid in 1% (w/v) methylcellulose (400 cps) (aq).

Scheme 5. Synthesis of Dimethylpyridone Benzimidazole 5- and 6-Position Analogues 22a–p<sup>a</sup>

<sup>a</sup>Reagents and conditions: for compounds **21a** and **21b**: (a) 4-substituted 1-fluoro-2-nitrobenzene or 4-substituted 4-bromo-2-fluoro-1-nitrobenzene, (tetrahydro-2H-pyran-4-yl)methanamine, DIPEA, 2-MeTHF, 80 °C; for compounds **22a** and **22b**: (b) 1,5-dimethyl-6-oxo-1,6-dihydropyridine-3-carbaldehyde, Na<sub>2</sub>S<sub>2</sub>O<sub>4</sub>, EtOH/H<sub>2</sub>O (2.5:1), 90 or 80 °C; (c) HN(CH<sub>3</sub>)<sub>2</sub>, Pd<sub>2</sub>(dba)<sub>3</sub> (2 mol %), JohnPhos (13 mol %), NaO<sup>t</sup>Bu, toluene or 1,4-dioxane, microwave, 90 °C; for compounds **22e–22p**: (d) (i) substituted 1-fluoro-2-nitrobenzene, (tetrahydro-2H-pyran-4-yl)methanamine, DIPEA, 2-MeTHF, microwave, 110 °C; (ii) 1,5-dimethyl-6-oxo-1,6-dihydropyridine-3-carbaldehyde, Na<sub>2</sub>S<sub>2</sub>O<sub>4</sub>, EtOH/H<sub>2</sub>O (2:1), 100 °C.

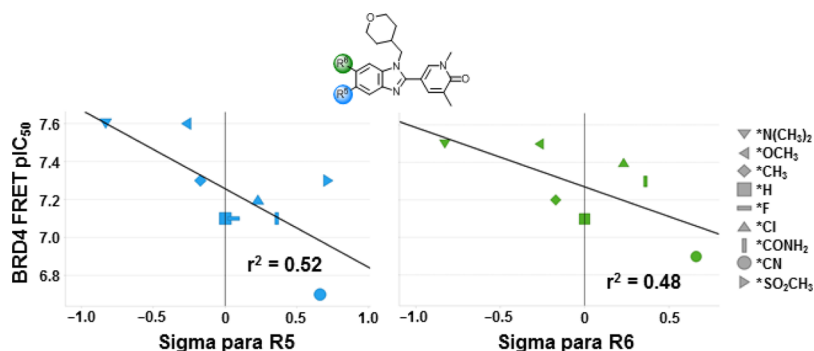


Figure 6. Plots of BRD4 FRET mean activities vs sigma para values for substituents at the 5-position (left) and 6-position (right).

dogs was slightly lower than that observed with 4-methylene THP **20a**, but a lower  $V_{dss}$  was determined resulting in a shorter  $T_{1/2}$ . These PK data, combined with the WB MCP-1 activity, were used to calculate the predicted once-daily human doses of 1.6 g and 470 mg from rat and dog data, respectively. Although the predicted doses were lower than those for 4-methylene THP **20a**, a further lowering of the projected dose was required to meet our target criterion of <100 mg.

In parallel with investigations at the benzimidazole N1-position, we pursued explorations at the 5- and 6-positions aiming to lower the predicted human dose versus lead compound **20a** based on a dual approach. First, an increase in potency was predicted by substituting these positions based on the crystal structure of 4-methylene THP **20a** in BRD4

BD1 (see Figure 5a). Here, the phenyl ring of the benzimidazole formed an edge-to-face interaction with Trp81, and we therefore hypothesized that increasing electron density in the ring would improve this interaction and lead to increased activity; it was also noted that the interaction to water through the benzimidazole N3 nitrogen could be modified through such electronic effects. Second, reports of unsubstituted benzimidazole rings being metabolically vulnerable<sup>74,75</sup> led us to block the 5- and 6-positions with appropriate substituents to lower the clearance and increase systemic exposure and the half-life.

We sought to test the first hypothesis by preparing analogues where the 5- and 6-positions were substituted with both electron-donating and electron-withdrawing groups. Synthesis

of these compounds was carried out using the established  $S_NAr$ -cyclization sequence, which, in the case of the dimethylamine target compounds **22c** and **22d**, required subsequent C–N cross-coupling of the Br-substituted benzimidazoles **22a** and **22b**, respectively (Scheme 5).

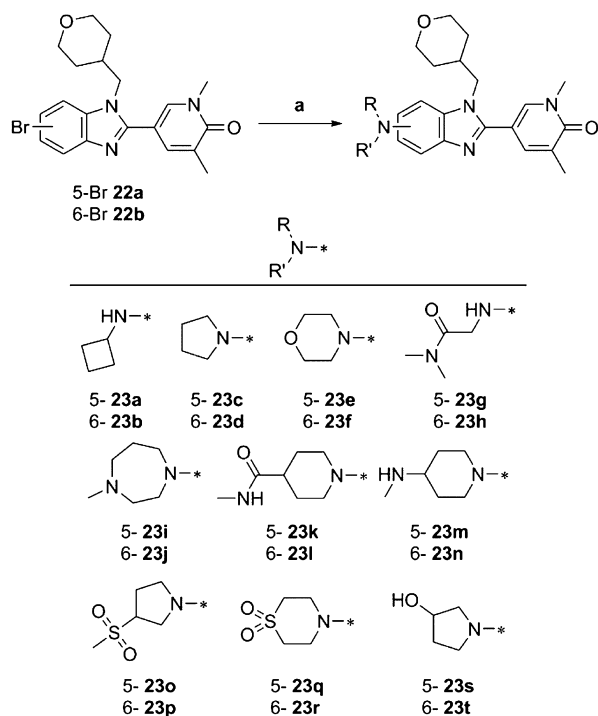
BRD4 FRET data were obtained for these compounds, and the activities were plotted against sigma para values<sup>76</sup> (Figure 6). A general correlation for increased electron density with increased potency was observed for both the 5- and 6-positions ( $r^2$  values of 0.52 and 0.48, respectively) which supported our hypothesis of improving the benzimidazole-Trp81 edge-to-face and/or the N3-water interaction(s).

As outlined previously, we were also interested to examine the effects upon metabolic stability by incorporating these substituents on the benzimidazole ring. Toward this end, potent dimethylamino 5-substituted benzimidazole **22c** was assessed in microsome preparations and levels of turnover were below the lower limit of quantification in all species (see the Supporting Information). This result was noteworthy, given the similar lipophilicities for 5-dimethylamine **22c** and unsubstituted benzimidazole **20a** (ChromLog $D_{7.4}$  = 2.9 and 2.7, respectively), and corroborated our strategy of blocking potential sites of metabolism (see Table 5 for microsome clearance data).

Based on the encouraging activities for the dimethylamines **22c** and **22d** and the low microsome clearance for the former 5-substituted congener, we prepared further amines at both the 5- and 6-positions to determine the preferred site of substitution for activity (Scheme 6).

We considered all matched molecular pairs (MMPs) of *N*-substituents at both the 5- and 6-positions and found that the

**Scheme 6. Synthesis of Dimethylpyridone Benzimidazole 5- and 6-Position Amine Analogues 23a–23t<sup>a</sup>**



<sup>a</sup>Reagents and conditions: (a) (i) NHRR', Pd<sub>2</sub>(dba)<sub>3</sub> (2 mol %), DavePhos (5 mol %), NaO<sup>t</sup>Bu, toluene or 1,4-dioxane, 80 °C; for compounds **23m** and **23n**: (ii) 4 M HCl in 1,4-dioxane, rt.

5-position was preferred for activity in most cases (Figure 7). This observation also held true for the WB activity where the 5-position substituents were more potent in 10 out of the 11 MMPs. Furthermore, most 5-substituents increased BRD4 FRET and MCP-1 WB activity relative to 5-dimethylamine **22c**. The 5-morpholine **23e** was particularly potent in both the biochemical and MCP-1 WB assays (pIC<sub>50</sub> = 8.0 and 7.9, respectively) and warranted further profiling. As expected, this 4-methylene THP-containing compound exhibited BAZ2A activity (pIC<sub>50</sub> = 6.7) corresponding to only 20-fold selectivity for BRD4. Nonetheless, we sought to confirm the earlier observation that substitution at the 5-position improved metabolic stability compared to unsubstituted benzimidazole **20a**. Similar to 5-dimethylamine **22c**, no detectable turnover of 5-morpholine **23e** was measured in human microsomes (see the Supporting Information). These latter data, combined with the low measured lipophilicity (ChromLog $D_{7.4}$  = 2.3) and high FaSSiF solubility (>1000 μg/mL, from amorphous solid), demonstrated the morpholine to be a favorable substituent at the 5-position.

Having made improvements at both the benzimidazole N1- and 5-positions independently, we sought to combine the favored substituents into one molecule predicting that it would display high BRD4 and low BAZ2A activity, while possessing favorable PK and physicochemical properties for testing the mechanism in vivo. Gratifyingly, our hypothesis was correct and the profile of the resulting compound **24** (I-BET469) (Table 8) is now discussed.

First, dimethylpyridone benzimidazole **24** displayed high BRD4 FRET and WB activities which exceeded our target levels. Activity at BRD4 in a cellular environment was also assessed for this compound using NanoBRET technology.<sup>77</sup> Here, HEK293 cells expressing a nanoluciferase-BRD4 fusion protein were incubated with dimethylpyridone benzimidazole **24** and a bromosporine tracer. Displacement of the tracer was monitored over 2 h resulting in a cellular pK<sub>d</sub> of 8.3, a value greater than that determined for I-BET151 (pK<sub>d</sub> = 7.8). The kinetics of binding were also measured and revealed a marginally slower *k*<sub>off</sub> for dimethylpyridone benzimidazole **24** relative to I-BET151 (see the Supporting Information). With regard to BCP selectivity, benzimidazole **24** was >5000-fold selective over BAZ2A because of the inclusion of the N1-dimethoxypropyl substituent. Screening in a panel of BCPs revealed the overall high selectivity for the BET family (see the Supporting Information); K<sub>d</sub> values of 37 and 49 nM were measured for CREBBP and EP300, respectively but were ≥25-fold higher than that measured for BRD4 BD1 and did not preclude further investigation of the compound.

A 1.3 Å resolution X-ray crystal structure of dimethylpyridone benzimidazole **24** in BRD4 BD1 was obtained (Figure 8) and showed the ligand bound in a comparable manner to the previous 4-methylene THP benzimidazole **20a**. Clear differences with dimethoxypropyl benzimidazole **24**, however, were that the branched N1-substituent simultaneously contacted the WPF-shelf and residues of the ZA loop (Leu92 and Leu94) on the opposing side of the binding pocket, and the morpholine 5-substituent was directed out of the ZA channel toward the solvent.

The PFI value of dimethylpyridone benzimidazole **24** (5.6) was within our desired criteria and therefore presented a low risk toward compound-related attrition. At this stage, we were keen to determine FaSSiF solubility from a crystalline form to better understand its pharmaceutical properties and potential

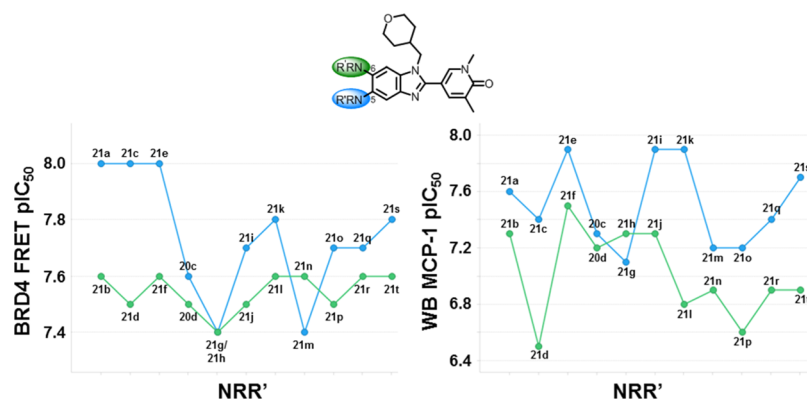


**Figure 7.** Plots of MMP activities for 5-position (blue) and 6-position (green) substituents. BRD4 FRET data (left) and MCP-1 WB data (right).

**Table 8.** Profile of Dimethylpyridone Benzimidazole 24

BRD4 FRET $pIC_{50}$ <sup>a</sup>	7.9
WB $pIC_{50}$ <sup>a</sup> IL-6/MCP-1	7.7/7.6
Cell BRET $pK_d$ <sup>a</sup>	8.3
BAZ2A FRET $pIC_{50}$ <sup>b</sup>	4.2
ChromLog $D_{7.4}$ /PFI	2.6/5.6
LE/LLE	0.35/6.4

<sup>a</sup>Expressed as the mean from at least four test occasions. <sup>b</sup> $pIC_{50}$  values of <4.0 were determined on four test occasions out of 10 and were excluded from the reported mean value.

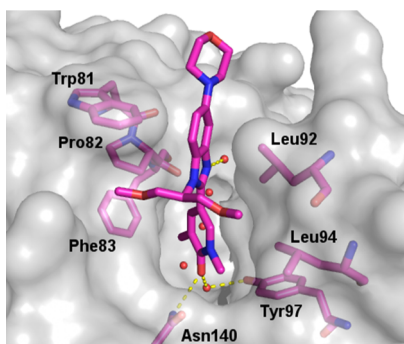
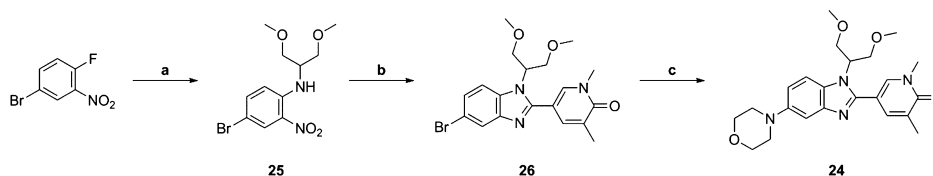


**Figure 8.** X-ray crystal structure of dimethylpyridone benzimidazole 24 in BRD4 BD1 (carbon = magenta, PDB 6TPZ). Water molecules at the base of the binding pocket are shown as red spheres, and selected hydrogen bonds are shown as yellow dashed lines.

**Scheme 7.** Synthesis of Dimethylpyridone Benzimidazole 24<sup>a</sup>



<sup>a</sup>Reagents and conditions: (a) 1,3-dimethoxypropan-2-amine,  $K_2CO_3$ , MeCN, 80 °C, 97%; (b) 1,5-dimethyl-6-oxo-1,6-dihydropyridine-3-carbaldehyde,  $Na_2S_2O_4$ , EtOH/ $H_2O$  (4:1), 90 °C, 56%; (c) morpholine,  $Pd_2(dba)_3$  (2 mol %), DavePhos (5 mol %),  $NaO^tBu$ , 2-MeTHF, 80 °C, 59%.

for development. We also required further quantities of the compound for in vivo studies, so synthesis of the crystalline material was carried out on a >220 mmol scale (Scheme 7).

Nucleophilic substitution of 4-bromo-1-fluoro-2-nitrobenzene with commercially available 1,3-dimethoxypropan-2-amine afforded *ortho*-nitroaniline 25 and was followed by ring formation to give benzimidazole 26. Palladium-catalyzed C–N cross-coupling of bromobenzimidazole 26 with morpholine followed by recrystallization from EtOAc delivered 50 g of the amination product 24. The solid state was confirmed as crystalline via X-ray powder diffraction (see the Supporting Information) and subsequent solubility measurements using this material revealed solubility >1000  $\mu g/mL$  in FaSSIF and >820  $\mu g/mL$  in other physiological media and aqueous buffers (see the Supporting Information). With no detectable turnover in rat, dog, and human microsomal and hepatocyte preparations, the crystalline material was dosed in a crossover rat PK study at 1, 3, and 30 mg/kg (Table 9). Following oral administration, the dose-normalized  $AUC_{0-\infty}$  values for each dose group were equivalent (53 and 52 min·kg/L for the 3 and 30 mg groups, respectively), indicating a linear dose-exposure relationship and because of the low clearance and high oral absorption, oral bioavailabilities were high (ca. 94% following administration at 3 and 30 mg/kg). Additionally, PK parameters were determined in the dog and demonstrated low clearance and high oral bioavailability. Single species scaling of the rat and dog PK parameters predicted human doses within our target of <100 mg (27 and 8 mg, respectively) for 24 h coverage of the WB MCP-1  $IC_{50}$ . With the low predicted human dose indicating low developability risk and wider biological profiling demonstrating minimal off-target activity (see the Supporting Information), we progressed dimethylpyridone benzimidazole 24 into further studies.

Table 9. In Vitro and in Vivo PK Data of Dimethylpyridone Benzimidazole 24

species	IVC (mL/min/g)			po dose (mg/kg)	AUC <sub>0-∞</sub> (ng·h/mL)	CL <sub>b</sub> (mL/min/kg)	CL <sub>u</sub> (mL/min/kg)	V <sub>dss</sub> (L/kg)	T <sub>1/2</sub> iv (h)	F (%)	human predicted QD dose (mg)
	Mics	Heps	f <sub>ub</sub>								
mouse	<0.48	<1.0	0.72	3.0	3618						
rat <sup>a,b</sup>	<0.46	<0.80	0.69	3.0	2614	17	24	2.3	3.8	94	27
				30.0	26973					93	
dog <sup>c,d</sup>	<0.37	<1.3	0.50	1.5	12503	2	4	0.9	5.3	101	8
human	<0.40	<0.87	0.72								

<sup>a</sup>iv dose (1.0 mg/kg): 1 h infusion in DMSO (2%, v/v) and Kleptose HPB (10%, w/v) in saline (0.9% w/v). <sup>b</sup>po dose: a suspension of crystalline solid in 1% (w/v) methylcellulose (400 cps) (aq). <sup>c</sup>iv dose (0.5 mg/kg): 1 h infusion in DMSO (2%, v/v) and Kleptose HPB (10%, w/v) in saline (0.9% w/v). <sup>d</sup>po dose: a suspension of solid of unknown form in 1% (w/v) methylcellulose (400 cps) (aq).

Having established potent binding and functional activity in vitro, we next wanted to demonstrate engagement of the BET mechanism in vivo. An investigation by Tarakhovskiy et al. was the first to establish the link between BET inhibition and inflammation.<sup>21</sup> These researchers treated LPS-stimulated bone marrow-derived macrophages with I-BET762 and observed suppressed expression of proinflammatory genes including IL-6. Epigenetic profiling provided further insight into the mechanism with the promoter of IL-6 displaying reduced BET recruitment in the presence of I-BET762. Furthermore, experiments in vivo demonstrated that inhibition of BET in a mouse model of endotoxic shock attenuated release of IL-6. We therefore sought to use IL-6 as a biomarker in LPS-challenged mice to establish the suitability of dimethylpyridone benzimidazole 24 to engage the BET mechanism in vivo. After confirming that adequate exposure would be achieved following oral dosing to the male CD-1 mouse (Table 9), dimethylpyridone benzimidazole 24 was administered orally at three different concentrations (1, 3, and 10 mg/kg) 30 min prior to LPS challenge and samples were taken at regular intervals for PKPD analysis over the following 5 h. Immunoassay of mouse IL-6 revealed suppression of cytokine levels in line with increasing unbound exposure over the duration of the study (Figure 9).

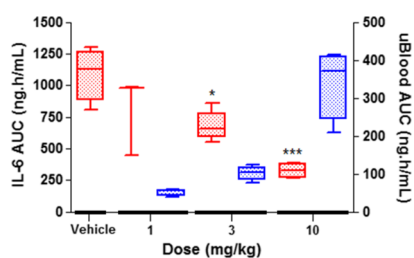


Figure 9. IL-6 (red) and unbound dimethylpyridone benzimidazole 24 (blue) AUC concentrations in the acute LPS model of inflammation. Statistical differences in %inhibition of IL-6 AUC levels were determined as  $p < 0.05$  (\*) and  $p < 0.001$  (\*\*\*)

Having confirmed BET-mediated effects in an acute in vivo model, we next investigated dimethylpyridone benzimidazole 24 in a chronic immune-mediated model more relevant to human immune disease. The ability of BET inhibitors to interfere with the immune response through dampened T cell and B cell activation has previously been established.<sup>78,79</sup> We therefore utilized a T cell-dependent immunization model wherein male CD-1 mice were challenged with the 2,4,6-trinitrophenyl keyhole limpet hemocyanin (TNP-KLH)

antigen, and IgG1 levels were measured following QD or once every other day (QOD) oral administration of dimethylpyridone benzimidazole 24 for 14 days. Greater inhibition of IgG1 levels relative to the vehicle on day 14 was achieved in the 3 mg/kg QD versus the 0.3 mg/kg QD dose group (20 and 65%, respectively) which was in accordance with the higher average free drug concentrations ( $C_{av}$ ) (Figure 10). Additionally, similar suppression of IgG1 levels compared

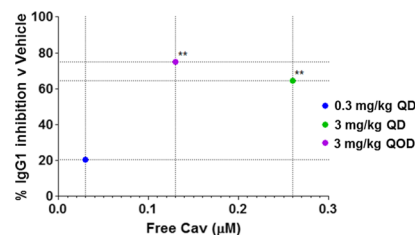


Figure 10. Mean %inhibition of IgG1 (relative to the vehicle) at day 14 vs free average drug concentration. Statistical differences in % inhibition of IgG1 were determined as  $p < 0.01$  (\*\*).

to the vehicle was observed with the 3 mg/kg QOD regimen versus QD (75 and 65%, respectively). The manifestation of auto-antigen presentation to T cells, and consequent auto-antibody production, fundamentally underlies auto-immune disease. Therefore, the demonstration that BET inhibition can attenuate antibody production in T cell-dependent immunization may allow such an approach to be used for clinical benefit in these conditions.

Taken together, these experiments demonstrate that dimethylpyridone benzimidazole 24 possesses suitable properties to engage the BET mechanism in vivo and elicit potent immunomodulatory effects. Moreover, the potency and oral PK properties of this molecule provide the flexibility to model different dosing regimens and levels of mechanism engagement to refine human dose predictions for different disease indications. Overall, the data presented here make this BET inhibitor a potential candidate for assessment in humans.

## CONCLUSIONS

We have described the discovery of a hit 3,5-dimethylphenol benzimidazole series using ELT for an oral BET inhibitor program. An X-ray crystal structure revealed the dimethylphenol moiety to be the KAc mimetic. Hybridization of this with an *N*-methylpyridone fragment-derived series led to increased potency and lowered lipophilicity. A compound containing this KAc mimetic was selected as a lead because of its high potency, encouraging physicochemical properties, and excellent PK

profile in dogs, but it exhibited off-target BCP activity and high clearance in the rat leading to a high predicted human dose. As part of lead optimization efforts, structural information guided an exploration at the benzimidazole N1-position and minor modifications to the 4-methylene THP substituent were sufficient to abolish BAZ2A activity. In parallel with these investigations, substituents were included at the 5- and 6-positions and electron-donating groups were found to increase activity while also improving metabolic stability. Combination of the optimized N1-dimethoxypropyl and 5-morpholine groups resulted in dimethylpyridone benzimidazole **24**, a compound possessing high BRD4 and WB activity, and favorable physicochemical properties. This 3,5-dimethylpyridone benzimidazole is devoid of BAZ2A activity and possesses PK properties leading to predicted human doses of <30 mg and thereby minimizes risk associated with compound-related attrition. Finally, engagement of the BET mechanism and immunomodulatory effects were demonstrated in vivo confirming dimethylpyridone benzimidazole **24** as a candidate-quality molecule.

## EXPERIMENTAL SECTION

**Chemistry Methods and Characterization for Compounds 8–26.** All commercial chemicals and solvents used were of reagent grade and used without further purification. Hydrophobic frit cartridges by ISOLUTE, which contain a frit selectively permeable to organic solutions, were used for separation of organic phases from aqueous phases under gravity. ISOLUTE aminopropyl cartridges were used for scavenging SPE protocols. ISOLUTE C18 cartridges were used for SPE workup of palladium-catalyzed amination reactions. Column chromatography was carried out either using manual or automated flash chromatography systems including a Biotage SP4 using SNAP silica cartridges or a CombiFlash using RediSep silica cartridges. Preparative high-performance liquid chromatography (HPLC) and mass-directed autopreparative HPLC (MDAP) purification were conducted using a Waters ZQ MS using alternate-scan positive and negative electrospray using either of the following two LC methods: method A: Either a SunFire C18 column (100 mm × 19 mm, 5 μm packing diameter) at a 20 mL/min flow rate or a SunFire C18 column (150 mm × 30 mm, 5 μm packing diameter) at a 40 mL/min flow rate. Gradient elution was carried out at ambient temperature, with the mobile phases as (A) water containing 0.1% (v/v) formic acid and (B) acetonitrile containing 0.1% (v/v) formic acid. The UV detection was a summed signal from wavelengths of 210 to 350 nm. Method B: either an Xbridge C18 column (100 mm × 19 mm, 5 μm packing diameter) at a 20 mL/min flow rate or an Xbridge C18 column (150 mm × 30 mm, 5 μm packing diameter) at a 40 mL/min flow rate. Gradient elution was carried out at ambient temperature, with the mobile phases as (A) 10 mM ammonium bicarbonate in water solution, adjusted to pH 10 with 0.88 ammonia solution, and (B) acetonitrile. The UV detection was a summed signal from wavelengths of 210 to 350 nm. Microwave irradiation was carried out using either an Anton Paar Multiwave Pro or a Biotage I60 system. Melting points were measured using a Buchi M-565 automatic melting point apparatus. IR spectra were obtained on a PerkinElmer Spectrum 2 spectrometer. <sup>1</sup>H NMR spectra were recorded on either a Bruker AV-400 spectrometer at 400 MHz or a Bruker AV-600 spectrometer at 600 MHz or Varian VNMR400 at 400 MHz. <sup>13</sup>C NMR spectra were recorded on a Bruker AV-600 spectrometer at 150 MHz. NMR spectra were acquired at 293 K, and chemical shifts (δ) are reported in parts per million (ppm) relative to CHCl<sub>3</sub> (δ 7.26), dimethyl sulfoxide (DMSO; δ 2.50), and MeOH (δ 3.31). Coupling constants (J) are expressed in hertz (Hz) to the nearest 0.5 Hz. HRMS were recorded on a Micromass Q-ToF Ultima hybrid quadrupole time-of-flight mass spectrometer after liquid chromatography separation using an Agilent 1100 Liquid Chromatograph equipped with a Phenomenex Luna C18 reversed phase column (100

mm × 2.1 mm, 3 μm packing diameter). Elution was carried out at 35 °C with the mobile phases as (A) 0.1% formic acid in water and (B) 0.1% formic acid in acetonitrile using a gradient starting at 5% B, increasing linearly to 100% B over 6 min, and remaining at 100% B for 2.5 min. The flow rate was 0.5 mL/min. The purity of all biologically tested compounds was ≥95% as determined by LC–MS UV traces except for compound **19b** (93% purity). The specific LC–MS UV method used for purity determination is noted for each compound and is from any of the following: method A: Waters ZQ Acquity UPLC system equipped with an CSH C18 column (50 mm × 2.1 mm, 1.7 μm packing diameter). Elution was carried out at 40 °C with the mobile phases as (A) 10 mM ammonium bicarbonate in water solution, adjusted to pH 10 with 0.88 ammonia solution, and (B) acetonitrile using a gradient starting at 3% B, increasing linearly to 95% B over 1.5 min, and remaining at 95% B for 0.4 min. The flow rate was 1 mL/min. The UV detection was a summed signal from wavelengths of 210–350 nm. MS analysis was carried out using alternate-scan positive and negative electrospray. Method B: Kinetex C8 column (30 mm × 2.1 mm, 1.7 μm packing diameter). Elution was carried out at rt with the mobile phases as (A) 0.1% formic acid in water and (B) 0.1% formic acid in acetonitrile using a gradient starting at 5% B, increasing linearly to 95% B over 2.75 min, and remaining at 95% B for 0.25 min. The flow rate was 0.65 mL/min. The UV detection was a summed signal from wavelengths of 210–400 nm. MS analysis was carried out using alternate-scan positive and negative electrospray. Method C: Shimadzu 2010 Mass Spectrometer equipped with an Xtimate C18 column (30 mm × 2.1 mm, 3 μm packing diameter). Elution was carried out at 50 °C with the mobile phases as (A) 0.04% trifluoroacetic acid (TFA) in water and (B) 0.02% TFA in acetonitrile using a gradient starting at 0% B, increasing linearly to 60% B over 0.90 min, and remaining at 60% B for 0.60 min. The flow rate was 1.2 mL/min. The UV detection was performed at 220 nm. MS analysis was carried out using positive electrospray. Method D: as method C but using a gradient starting at 10% B, increasing linearly to 80% B over 0.90 min, and remaining at 80% B for 0.60 min. Method E: as method C but using a gradient starting at 0% B, increasing linearly to 30% B over 0.90 min, and remaining at 30% B for 0.60 min. Method F: the Waters ZQ Acquity UPLC system equipped with an CSH C18 column (50 mm × 2.1 mm, 1.7 μm packing diameter). Elution was carried out at 40 °C with the mobile phases as (A) 0.1% formic acid in water and (B) 0.1% formic acid in acetonitrile using a gradient starting at 3% B, increasing linearly to 95% B over 1.5 min, and remaining at 95% B for 0.4 min. The flow rate was 1 mL/min. The UV detection was a summed signal from wavelengths of 210 to 350 nm. MS analysis was carried out using alternate-scan positive and negative electrospray.

**2-(4-Hydroxy-3,5-dimethylphenyl)-N-methyl-1-(piperidin-4-ylmethyl)-1H-benzod[*j*]imidazole-5-carboxamide Trifluoroacetic Acid Salt (**8**).** To a solution of 4-fluoro-N-methyl-3-nitrobenzamide (19.8 mg, 0.10 mmol) in EtOH (2 mL) were added *tert*-butyl 4-(aminomethyl)piperidine-1-carboxylate (21.4 mg, 0.10 mmol) and diisopropylethylamine (DIPEA; 52 μL, 0.30 μmol). The reaction mixture was heated at 80 °C overnight, cooled to rt, and concentrated to dryness. The resulting crude was dissolved in EtOH (2 mL), and 4-hydroxy-3,5-dimethylbenzaldehyde (30.0 mg, 0.20 mmol) was added followed by Na<sub>2</sub>S<sub>2</sub>O<sub>4</sub> (104 mg, 0.60 mmol) in water (0.5 mL). The reaction mixture was stirred in a sealed tube at 80 °C for 18 h, cooled to rt, and concentrated to a small volume. The residue was diluted with EtOAc (2 mL), and the organic layer was washed with saturated aqueous NaHCO<sub>3</sub> (2 mL). The layers were separated, and the aqueous layer was extracted with EtOAc (2 × 2 mL). The organics were combined, dried over Na<sub>2</sub>SO<sub>4</sub>, filtered, and concentrated to dryness to give crude *tert*-butyl 4-((2-(4-hydroxy-3,5-dimethylphenyl)-5-(methylcarbamoyl)-1H-benzo[*d*]imidazol-1-yl)methyl)piperidine-1-carboxylate. This was treated with 50% TFA in dichloromethane (DCM; 1 mL) for 3 h at rt and then concentrated to dryness. The crude was purified directly by preparative HPLC (SunFire C8 OBD Prep Column [30 mm × 50 mm, 5 μm], 40 mL/min, water/MeCN containing 0.1% TFA, UV detection at 220 nm) to give the title compound (20 mg, 0.05 mmol, 38% yield). <sup>1</sup>H NMR

(400 MHz, DMSO- $d_6$ ):  $\delta$  9.10 (br s, 1 H), 8.55 (br s, 1 H), 8.19 (s, 1 H), 8.03 (br s, 1 H), 7.89 (m, 2 H), 7.44 (s, 2 H), 4.40 (d, 2 H,  $J$  = 7.0 Hz), 3.17–3.10 (m, 2 H), 2.82 (d, 3 H,  $J$  = 4.5 Hz), 2.75–2.65 (m, 2 H), 2.27 (s, 6 H), 2.06 (br s, 1 H), 1.54–1.45 (m, 2 H), 1.20–1.05 (m, 2 H); LC–MS (method B)  $m/z$ : 393 [(M + H)<sup>+</sup>];  $R_t$ : 0.78 min; 95% purity.

**1-((1-Benzoylpiperidin-4-yl)methyl)-2-(4-hydroxy-3,5-dimethylphenyl)-N-methyl-1H-benzodimidazole-5-carboxamide Trifluoroacetic Acid Salt (9)**. To a solution of benzoic acid (12.2 mg, 0.10 mmol) in dimethylformamide (DMF; 0.5 mL) were added 1-[[bis(dimethylamino)methylene]-1H-1,2,3-triazolo[4,5-*b*]pyridinium 3-oxide hexafluorophosphate (HATU; 38.0 mg, 0.10 mmol) and DIPEA (52  $\mu$ L, 0.30 mmol). The reaction mixture was stirred at rt for 5 min and added to a solution of 2-(4-hydroxy-3,5-dimethylphenyl)-N-methyl-1-(piperidin-4-ylmethyl)-1H-benzodimidazole-5-carboxamide trifluoroacetic acid salt **8** (20 mg, 0.38 mmol) in DMF (0.5 mL). The reaction mixture was stirred at rt overnight and diluted with EtOAc (2 mL). The organic layer was washed with saturated aqueous NaHCO<sub>3</sub> (2 mL), and the layers were separated. The aqueous layer was extracted with EtOAc (2  $\times$  2 mL), and the organics were combined, dried over Na<sub>2</sub>SO<sub>4</sub>, and filtered. The filtrate was concentrated to dryness, and the crude material was purified by preparative HPLC (SunFire C8 OBD Prep Column [30 mm  $\times$  50 mm, 5  $\mu$ m], 40 mL/min, water/MeCN containing 0.1% TFA, UV detection at 220 nm) to give the title compound (13 mg, 0.03 mmol, 53% yield). <sup>1</sup>H NMR (400 MHz, DMSO- $d_6$ ):  $\delta$  9.14 (br s, 1 H), 8.60–8.50 (m, 1 H), 8.16 (s, 1 H), 8.01–7.89 (m, 2 H), 7.46 (s, 2 H), 7.42–7.36 (m, 3 H), 7.31–7.25 (m, 2 H), 4.41 (m, 2 H), 4.37–4.21 (m, 2 H), 3.53–3.32 (m, 2 H), 2.8 (d, 3 H,  $J$  = 4.5 Hz), 2.27 (s, 6 H), 2.06–1.93 (m, 1 H), 1.42–1.30 (m, 2 H), 1.11–0.96 (m, 2 H); LC–MS (method B)  $m/z$ : 497 [(M + H)<sup>+</sup>];  $R_t$ : 1.30 min; 95% purity.

**1-((1-Acetylpiperidin-4-yl)methyl)-2-(4-hydroxy-3,5-dimethylphenyl)-N-methyl-1H-benzodimidazole-5-carboxamide Trifluoroacetic Acid Salt (10)**. To a solution of 2-(4-hydroxy-3,5-dimethylphenyl)-N-methyl-1-(piperidin-4-ylmethyl)-1H-benzodimidazole-5-carboxamide trifluoroacetic acid salt **8** (20 mg, 0.38 mmol) in a mixture of tetrahydrofuran (THF; 0.5 mL) and MeCN (0.5 mL) were added pyridine (40  $\mu$ L, 0.50 mmol) and acetic anhydride (28  $\mu$ L, 0.30 mmol) at 0 °C. The reaction mixture was stirred at rt overnight and concentrated to dryness. The crude was partitioned between EtOAc (1 mL) and aqueous NaHCO<sub>3</sub> (1 mL), and the layers were separated. The aqueous layer was extracted with EtOAc (2  $\times$  1 mL), the organics combined, dried over Na<sub>2</sub>SO<sub>4</sub>, filtered, and concentrated. The material was dissolved in a mixture of THF (2 mL)/MeOH (0.5 mL) and treated with 2 M LiOH (0.15 mL) for 3 h. The reaction mixture was concentrated to dryness, and the crude material was purified by preparative HPLC (SunFire C8 OBD Prep Column [30 mm  $\times$  50 mm, 5  $\mu$ m], 40 mL/min, water/MeCN containing 0.1% TFA, UV detection at 220 nm) to give the title compound (16 mg, 0.29 mmol, 78% yield). <sup>1</sup>H NMR (400 MHz, DMSO- $d_6$ ):  $\delta$  9.15 (br s, 1 H), 8.61–8.56 (m, 1 H), 8.18 (s, 1 H), 7.97 (d, 1 H,  $J$  = 8.0 Hz), 7.93 (d, 1 H,  $J$  = 8.0 Hz), 7.47 (s, 2 H), 4.45–4.35 (m, 2 H), 4.22–4.13 (m, 1 H), 3.70–3.60 (m, 1H), 2.82 (d, 3 H,  $J$  = 4.5 Hz), 2.39–2.25 (m, 2 H), 2.27 (s, 6 H), 2.00–1.92 (m, 1 H), 1.45–1.35 (m, 1 H), 1.32–1.22 (m, 1 H), 1.10–0.95 (m, 1 H), 0.89–0.75 (m, 1 H); LC–MS (method F)  $m/z$ : 435 [(M + H)<sup>+</sup>];  $R_t$ : 0.52 min; 100% purity.

**tert-Butyl 4-(((2-Nitrophenyl)amino)methyl)piperidine-1-carboxylate (11a)**. A mixture of 1-fluoro-2-nitrobenzene (40 g, 283 mmol), *tert*-butyl 4-(aminomethyl)piperidine-1-carboxylate (72.9 g, 340 mmol), and K<sub>2</sub>CO<sub>3</sub> (78 g, 567 mmol) in MeCN (1500 mL) was stirred at 80 °C overnight. The reaction mixture was washed with 10% aqueous citric acid, saturated aqueous NaHCO<sub>3</sub>, and brine ( $\times$ 3). The organic layer was dried with Na<sub>2</sub>SO<sub>4</sub> and concentrated to give the crude material. The residue was purified by column chromatography on silica gel eluting with petroleum ether/EtOAc (10/1 to 3:1, v/v) to give the title compound as a crude yellow solid (117 g, 337 mmol). LC–MS (method C)  $m/z$ : 280 [(M – ‘Bu)<sup>+</sup>];  $R_t$ : 1.49 min; 97% purity.

**tert-Butyl 4-(((2-Nitrophenyl)amino)piperidine-1-carboxylate (11b)**. A mixture of 1-fluoro-2-nitrobenzene (5 g, 35.4 mmol), K<sub>2</sub>CO<sub>3</sub> (9.79 g, 70.9 mmol) and *tert*-butyl 4-aminopiperidine-1-carboxylate (8.52 g, 42.5 mmol) in MeCN (354 mL) was stirred at 110 °C overnight. To the reaction mixture was added EtOAc and washed with 10% aqueous citric acid, saturated aqueous NaHCO<sub>3</sub>, and brine ( $\times$ 3). The organic was dried with Na<sub>2</sub>SO<sub>4</sub> and concentrated to give the crude material. The residue was purified by column chromatography on silica gel eluting with petroleum ether/EtOAc (10:1 to 3:1) to give the title compound as a yellow solid (11.5 g, 34.2 mmol, 97% yield). LC–MS (method C)  $m/z$ : 266 [(M – ‘Bu)<sup>+</sup>], 344 [(M + Na)<sup>+</sup>];  $R_t$ : 1.47 min; 96% purity.

**tert-Butyl 3-(((2-Nitrophenyl)amino)methyl)azetidide-1-carboxylate (11c)**. To a solution of 1-fluoro-2-nitrobenzene (5 g, 35.4 mmol) in MeCN (200 mL) were added *tert*-butyl 3-(aminomethyl)azetidide-1-carboxylate (7.92 g, 42.5 mmol) and K<sub>2</sub>CO<sub>3</sub> (9.79 g, 70.9 mmol). The reaction mixture was stirred at 80 °C overnight. The mixture was filtered, and the filtrate was concentrated in vacuo to give a residue which was diluted with EtOAc (200 mL). The solution was washed with brine (3  $\times$  50 mL), dried over Na<sub>2</sub>SO<sub>4</sub>, filtered, and concentrated in vacuo. The crude product was purified by flash column chromatography eluting with 100% EtOAc in petroleum ether to give the title compound as a bright yellow solid (11.04 g, 34.8 mmol, 98% yield). LC–MS (method D)  $m/z$ : 252 [(M – ‘Bu)<sup>+</sup>], 330 [(M + Na)<sup>+</sup>];  $R_t$ : 1.10 min; 97% purity.

**tert-Butyl 3-(((2-Nitrophenyl)amino)methyl)pyrrolidine-1-carboxylate (11d)**. A mixture of 1-fluoro-2-nitrobenzene (3 g, 21.2 mmol), K<sub>2</sub>CO<sub>3</sub> (5.88 g, 42.5 mmol), and *tert*-butyl 3-(aminomethyl)pyrrolidine-1-carboxylate (5.11 g, 25.5 mmol) in MeCN (213 mL) was stirred at 110 °C overnight. To the reaction mixture was added EtOAc, and this was washed with 10% aqueous citric acid, saturated aqueous NaHCO<sub>3</sub>, and brine ( $\times$ 3). The organic layer was dried with Na<sub>2</sub>SO<sub>4</sub> and concentrated to give the crude material. The residue was purified by column chromatography on silica gel eluting with petroleum ether/EtOAc (10:1 to 3:1) to give the title compound as a yellow solid (6.8 g, 21.0 mmol, 99% yield). LC–MS (method D)  $m/z$ : 266 [(M – ‘Bu)<sup>+</sup>], 344 [(M + Na)<sup>+</sup>];  $R_t$ : 1.17 min; 99% purity.

**tert-Butyl (trans-4-(((2-Nitrophenyl)amino)methyl)cyclohexyl)carbamate (11e)**. To 1-fluoro-2-nitrobenzene (2.6 g, 18.4 mmol) in MeCN (113 mL) were added *tert*-butyl (trans-4-(aminomethyl)cyclohexyl)carbamate (5.05 g, 22.1 mmol) and K<sub>2</sub>CO<sub>3</sub> (2.55 g, 18.4 mmol). The reaction mixture was stirred at 100 °C. After cooling to rt, the reaction mixture was filtered on a pad of Celite. The solvent was washed twice with saturated aqueous NaHCO<sub>3</sub> and water and then dried over Na<sub>2</sub>SO<sub>4</sub> and concentrated in vacuo to give the crude product as a yellow gum. This was purified by column chromatography on silica gel eluting with petroleum ether/EtOAc (5:1 to 4:1) to give the title compound as a yellow gum (5.93 g, 17.0 mmol, 92% yield). LC–MS (method C)  $m/z$ : 294 [(M – ‘Bu)<sup>+</sup>];  $R_t$ : 1.49 min; 100% purity.

**tert-Butyl (cis-4-(((2-Nitrophenyl)amino)methyl)cyclohexyl)carbamate (11f)**. A mixture of 1-fluoro-2-nitrobenzene (1.54 g, 10.9 mmol), *tert*-butyl (cis-4-(aminomethyl)cyclohexyl)carbamate (2.99 g, 13.1 mmol), and K<sub>2</sub>CO<sub>3</sub> (3.02 g, 21.8 mmol) in MeCN (72.8 mL) was stirred at 100 °C overnight. The reaction mixture was filtered and evaporated in vacuo to dryness and purified by column chromatography on silica gel eluting with petroleum ether/EtOAc (5:1 to 1:1) to give the title compound as a yellow solid (3.8 g, 10.9 mmol, 100% yield). LC–MS (method D)  $m/z$ : 294 [(M – ‘Bu)<sup>+</sup>];  $R_t$ : 1.22 min; 100% purity.

**tert-Butyl 4-(((2-Aminophenyl)amino)methyl)piperidine-1-carboxylate (12a)**. A solution of *tert*-butyl 4-(((2-nitrophenyl)amino)methyl)piperidine-1-carboxylate **11a** (50 g, 149 mmol) and Pd/C (1 g, 0.940 mmol) in DMF (300 mL) was stirred at 30 °C overnight under 1 atm of hydrogen. The reaction mixture was filtered through a pad of Celite and was washed with EtOAc (3  $\times$  45 mL) and brine. The combined organics was concentrated to give the title compound as a dark brown solid (43 g, 140 mmol, 94% yield). LC–MS (method C)  $m/z$ : 206 [(M + H)<sup>+</sup>];  $R_t$ : 1.13 min; 99% purity.

**tert-Butyl 4-((2-Aminophenyl)amino)piperidine-1-carboxylate (12b).** A solution of *tert*-butyl 4-((2-nitrophenyl)amino)piperidine-1-carboxylate **11b** (11.5 g, 35.8 mmol) and palladium (1.15 g, 1.08 mmol) in DMF (300 mL) was stirred at 30 °C overnight under 1 atm of hydrogen. The reaction mixture was filtered through a pad of Celite and was washed with EtOAc (3 × 45 mL) and brine. The combined organics was concentrated to give the title compound as a dark brown solid (10.4 g, 33.7 mmol, 94% yield). LC–MS (method C) *m/z*: 236 [(M – ‘Bu)<sup>+</sup>], 292 [(M + H)<sup>+</sup>]; *R*<sub>t</sub>: 1.05 min; 94% purity.

**tert-Butyl 3-(((2-Aminophenyl)amino)methyl)azetidene-1-carboxylate (12c).** A solution of *tert*-butyl 3-(((2-nitrophenyl)amino)methyl)azetidene-1-carboxylate **11c** (11.04 g, 34.8 mmol) in DMF (300 mL) was treated with Pd/C (1.0 g, 9.40 mmol). The reaction mixture was hydrogenated under 30 psi pressure at 30 °C overnight. The mixture was filtered through a pad of Celite. The solution was diluted with EtOAc (500 mL), washed with water and brine, dried over Na<sub>2</sub>SO<sub>4</sub>, filtered, and concentrated in vacuo to give the title compound as a yellow solid (8.89 g, 31.7 mmol, 91% yield). LC–MS (method C) *m/z*: 178 [(M – ‘Bu)<sup>+</sup>]; *R*<sub>t</sub>: 0.83 min; 89% purity.

**tert-Butyl 3-(((2-Aminophenyl)amino)methyl)pyrrolidine-1-carboxylate (12d).** A solution of *tert*-butyl 3-(((2-nitrophenyl)amino)methyl)pyrrolidine-1-carboxylate **11d** (6.8 g, 21.2 mmol) and palladium (0.72 g, 0.68 mmol) in DMF (300 mL) was stirred at 30 °C overnight under 1 atm of hydrogen. The reaction mixture was filtered through a pad of Celite and was washed with EtOAc (3 × 45 mL) and brine. The combined organic extracts were concentrated to give the title compound as a dark brown solid (6.3 g, 20.9 mmol, 99% yield). LC–MS (method C) *m/z*: 192 [(M – ‘Bu)<sup>+</sup>]; *R*<sub>t</sub>: 1.06 min; 97% purity.

**tert-Butyl (cis-4-(((2-Nitrophenyl)amino)methyl)cyclohexyl)carbamate (12f).** *tert*-Butyl (cis-4-(((2-nitrophenyl)amino)methyl)cyclohexyl)carbamate **11f** (3.8 g, 10.9 mmol) was hydrogenated utilizing Pd/C (0.231 g, 2.18 mmol) under 30 psi pressure in DMF (150 mL) overnight. The reaction mixture was filtered and evaporated in vacuo to dryness to give the title compound (3.32 g, 10.2 mmol, 93% yield). LC–MS (method D) *m/z*: 320 [(M + H)<sup>+</sup>]; *R*<sub>t</sub>: 0.89 min; 91% purity.

**tert-Butyl 4-((2-(4-Hydroxy-3,5-dimethylphenyl)-1H-benzo[d]imidazol-1-yl)methyl)piperidine-1-carboxylate (13a).** To a mixture of *tert*-butyl 4-(((2-aminophenyl)amino)methyl)piperidine-1-carboxylate **12a** (423 mg, 1.385 mmol) and 4-hydroxy-3,5-dimethylbenzaldehyde (208 mg, 1.39 mmol) in DMF (3 mL) was added Na<sub>2</sub>S<sub>2</sub>O<sub>5</sub> (342 mg, 1.80 mmol). The reaction mixture was stirred at 100 °C overnight. The mixture was cooled and filtered. The mixture was diluted with EtOAc (30 mL), washed with brine (3 × 10 mL), dried over Na<sub>2</sub>SO<sub>4</sub>, filtered, and concentrated. The residue was purified on silica gel eluting with 0–3% MeOH in DCM to give the title compound as a yellow solid (469 mg, 1.07 mmol, 77% yield). LC–MS (method C) *m/z*: 436 [(M + H)<sup>+</sup>]; *R*<sub>t</sub>: 0.97 min; 99% purity.

**tert-Butyl 4-((2-(4-Hydroxy-3,5-dimethylphenyl)-1H-benzo[d]imidazol-1-yl)piperidine-1-carboxylate (13b).** A solution of *tert*-butyl 4-(((2-aminophenyl)amino)piperidine-1-carboxylate **12b** (10.4 g, 35.7 mmol), 4-hydroxy-3,5-dimethylbenzaldehyde (5.36 g, 35.7 mmol), and Na<sub>2</sub>S<sub>2</sub>O<sub>5</sub> (8.82 g, 46.4 mmol) in DMF (357 mL) was stirred at 100 °C under nitrogen overnight. To the mixture was added EtOAc (50 mL) which was then washed with brine (×3). The organic layer was dried over Na<sub>2</sub>SO<sub>4</sub>. The crude was purified by column chromatography on silica gel eluting with petroleum ether/EtOAc (20:1 to 3:1) to give the title compound as a pale solid (10.6 g, 24.8 mmol, 70% yield). LC–MS (method C) *m/z*: 422 [(M + H)<sup>+</sup>]; *R*<sub>t</sub>: 1.17 min; 99% purity.

**tert-Butyl 3-((2-(4-Hydroxy-3,5-dimethylphenyl)-1H-benzo[d]imidazol-1-yl)methyl)azetidene-1-carboxylate (13c).** To a solution of *tert*-butyl 3-(((2-aminophenyl)amino)methyl)azetidene-1-carboxylate **12c** (8.89 g, 32.1 mmol) and 4-hydroxy-3,5-dimethylbenzaldehyde (4.81 g, 32.1 mmol) in DMF (80 mL) was added Na<sub>2</sub>S<sub>2</sub>O<sub>5</sub> (7.92 g, 41.7 mmol). The reaction mixture was stirred at 100 °C overnight. The mixture was filtered, and the solid was washed with DCM (300 mL). The filtrate was washed with water (3 × 100 mL) and brine (3 × 50 mL), dried over Na<sub>2</sub>SO<sub>4</sub>, filtered, and concentrated in vacuo to

give a residue which was purified on silica gel eluting with 1–2% MeOH in DCM to give the title compound as a yellow solid (5.27 g, 12.3 mmol, 38% yield). LC–MS (method C) *m/z*: 408 [(M + H)<sup>+</sup>]; *R*<sub>t</sub>: 1.10 min; 95% purity.

**tert-Butyl 3-((2-(4-Hydroxy-3,5-dimethylphenyl)-1H-benzo[d]imidazol-1-yl)methyl)pyrrolidine-1-carboxylate (13d).** A solution of *tert*-butyl 3-(((2-aminophenyl)amino)methyl)pyrrolidine-1-carboxylate **12d** (6.3 g, 21.6 mmol), 4-hydroxy-3,5-dimethylbenzaldehyde (3.08 g, 20.5 mmol), and Na<sub>2</sub>S<sub>2</sub>O<sub>5</sub> (5.34 g, 28.1 mmol) in DMF (216 mL) was stirred at 100 °C under nitrogen overnight. The mixture was added to EtOAc (50 mL), and this was washed with brine (×3). The organic layer was dried over Na<sub>2</sub>SO<sub>4</sub>. The crude was purified by column chromatography on silica gel eluting with petroleum ether/EtOAc (20:1 to 3:1) to give the title compound as a pale solid (6.6 g, 15.3 mmol, 71% yield). LC–MS (method C) *m/z*: 422 [(M + H)<sup>+</sup>]; *R*<sub>t</sub>: 1.15 min; 97% purity.

**tert-Butyl (trans-4-((2-(4-Hydroxy-3,5-dimethylphenyl)-1H-benzo[d]imidazole-1-yl)methyl)cyclohexyl)carbamate (13e).** Step b: *tert*-Butyl (trans-4-(((2-nitrophenyl)amino)methyl)cyclohexyl)carbamate **11e** (5.93 g, 17.0 mmol) was hydrogenated utilizing Pd/C (0.59 g, 5.54 mmol) under 30 psi pressure in DMF (150 mL) at 30 °C overnight. After cooling to rt, the reaction mixture was filtered and washed with EtOAc (25 mL). The solution was concentrated in vacuo to give the crude *tert*-butyl (trans-4-(((2-aminophenyl)amino)methyl)cyclohexyl)carbamate **12e** which was used for the next step directly without purification. Step c: to crude *tert*-butyl (trans-4-(((2-aminophenyl)amino)methyl)cyclohexyl)carbamate **12e** (5.3 g, 16.6 mmol) in DMF (150 mL) were added 4-hydroxy-3,5-dimethylbenzaldehyde (2.49 g, 16.6 mmol) and Na<sub>2</sub>S<sub>2</sub>O<sub>5</sub> (3.78 g, 19.9 mmol). The reaction mixture was stirred under nitrogen at 100 °C overnight. Water was added to the reaction mixture, and the aqueous layer was extracted with DCM (2 × 100 mL). The combined organic layers were washed with brine and water and then dried over Na<sub>2</sub>SO<sub>4</sub>. The crude product was chromatographed on silica gel eluting with petroleum ether/EtOAc (3:1, 2:1, 1:1) to give the title compound as a pale white solid (7 g, 15.4 mmol, 93% overall yield). LC–MS (method C) *m/z*: 450 [(M + H)<sup>+</sup>]; *R*<sub>t</sub>: 1.18 min; 100% purity.

**tert-Butyl (cis-4-((2-(4-Hydroxy-3,5-dimethylphenyl)-1H-benzo[d]imidazol-1-yl)methyl)cyclohexyl)carbamate (13f).** A mixture of *tert*-butyl (cis-4-(((2-nitrophenyl)amino)methyl)cyclohexyl)carbamate **12f** (3.48 g, 10.9 mmol), 4-hydroxy-3,5-dimethylbenzaldehyde (1.72 g, 11.4 mmol), and Na<sub>2</sub>S<sub>2</sub>O<sub>5</sub> (2.69 g, 14.1 mmol) in DMF (150 mL) was stirred under nitrogen at 100 °C overnight. The reaction mixture was treated with brine, and the organic layer was washed with brine (×2) and then dried over Na<sub>2</sub>SO<sub>4</sub> and concentrated in vacuo to give the crude which was purified by column chromatography on silica gel eluting with petroleum ether/EtOAc (3:1 to 1:1) to give the title compound as a white solid (4.1 g, 9.1 mmol, 83% yield). LC–MS (method C) *m/z*: 450 [(M + H)<sup>+</sup>]; *R*<sub>t</sub>: 1.19 min; 99% purity.

**2,6-Dimethyl-4-(1-(piperidin-4-ylmethyl)-1H-benzo[d]imidazole-2-yl)phenol Dihydrochloride (14a).** A solution of *tert*-butyl 4-((2-(4-hydroxy-3,5-dimethylphenyl)-1H-benzo[d]imidazol-1-yl)methyl)piperidine-1-carboxylate **13a** (200 mg, 0.46 mmol) in DCM (2 mL) was charged with 4 M HCl in MeOH (2 mL, 8.00 mmol). The reaction was stirred at 50 °C for 1 h. The solvent was removed under high vacuum to give the title compound as a yellow solid (186 mg, 0.46 mmol, 99% yield). LC–MS (method C) *m/z*: 336 [(M + H)<sup>+</sup>]; *R*<sub>t</sub>: 0.82 min; 100% purity.

**2,6-Dimethyl-4-(1-(piperidin-4-yl)-1H-benzo[d]imidazole-2-yl)phenol Dihydrochloride (14b).** A solution of *tert*-butyl 4-((2-(4-hydroxy-3,5-dimethylphenyl)-1H-benzo[d]imidazol-1-yl)piperidine-1-carboxylate **13b** (3.6 g, 8.54 mmol) and 4 M HCl in MeOH (80 mL, 320 mmol) was stirred at rt for 1 h. The solvent was removed, and the residue was washed with EtOAc (3 × 5 mL) and evaporated to give the title compound as a yellow solid (3 g, 7.61 mmol, 89% yield). <sup>1</sup>H NMR (300 MHz, DMSO-*d*<sub>6</sub>): δ 9.89–9.71 (m, 1 H), 9.41 (br s, 1 H), 9.03 (d, *J* = 9.0 Hz, 1 H), 8.63–8.55 (m, 1 H), 7.88–7.79 (m, 1 H), 7.63–7.53 (m, 2 H), 7.40 (s, 2 H), 4.94–4.78 (m, 1 H), 3.12 (q, *J* = 11.0 Hz, 2 H), 2.93 (q, *J* = 11.0 Hz, 2 H), 2.30 (s, 6 H),

2.21 (d,  $J = 11.0$  Hz, 2 H), two piperidine proton signals obscured by DMSO; LC-MS (method C)  $m/z$ : 322 [(M + H)<sup>+</sup>];  $R_t$ : 0.80 min; 100% purity.

**4-(1-(Azetidin-3-ylmethyl)-1H-benzo[d]imidazol-2-yl)-2,6-dimethylphenol Dihydrochloride (14c).** Batch 1: a solution of *tert*-butyl 3-((2-(4-hydroxy-3,5-dimethylphenyl)-1H-benzo[d]imidazol-1-yl)methyl)azetidine-1-carboxylate **13c** (1.0 g, 2.454 mmol) in 4 M HCl in MeOH (20 mL, 80 mmol) was stirred at 45 °C for 1 h. The solvent was removed in vacuo to give the crude product. Batch 2: a solution of *tert*-butyl 3-((2-(4-hydroxy-3,5-dimethylphenyl)-1H-benzo[d]imidazol-1-yl)methyl)azetidine-1-carboxylate **13c** (5.27 g, 12.93 mmol) in 4 M HCl in MeOH (100 mL, 400 mmol) was stirred at 45 °C for 1 h. The solvent was removed in vacuo to give the crude product. Both batches were combined and washed with 5% MeOH in DCM to afford the title compound as a pink solid (5.1 g, 12.2 mmol, 79% yield). LC-MS (method E)  $m/z$ : 308 [(M + H)<sup>+</sup>];  $R_t$ : 0.81 min; 91% purity.

**2,6-Dimethyl-4-(1-(pyrrolidin-3-ylmethyl)-1H-benzo[d]imidazole-2-yl)phenol Dihydrochloride (14d).** A solution of *tert*-butyl 3-((2-(4-hydroxy-3,5-dimethylphenyl)-1H-benzo[d]imidazol-1-yl)methyl)pyrrolidine-1-carboxylate **13d** (1 g, 2.37 mmol) and 4 M HCl in MeOH (20 mL, 80 mmol) was stirred at rt for 1 h. The solvent was removed, and the residue was washed with EtOAc (3 × 5 mL) and evaporated to give the title compound as a brown solid (0.87 g, 2.21 mmol, 93% yield). <sup>1</sup>H NMR (300 MHz, MeOH-*d*<sub>4</sub>): δ 8.16–8.09 (m, 1 H), 7.88–7.81 (m, 1 H), 7.75–7.64 (m, 2 H), 7.57 (s, 2 H), 4.85 (d,  $J = 6.5$  Hz, 2 H), 3.43–3.34 (m, 1 H), 3.28–3.20 (m, 1 H), 3.20–3.08 (m, 1 H), 3.00–2.81 (m, 2 H), 2.37 (s, 6 H), 2.00 (d,  $J = 4.5$  Hz, 1 H), 1.68–1.51 (m, 1 H); LC-MS (method C)  $m/z$ : 322 [(M + H)<sup>+</sup>];  $R_t$ : 0.79 min; 100% purity.

**4-(1-(trans-4-Aminocyclohexyl)methyl)-1H-benzo[d]imidazol-2-yl)-2,6-dimethylphenol Dihydrochloride (14e).** A suspension of *tert*-butyl (*trans*-4-((2-(4-hydroxy-3,5-dimethylphenyl)-1H-benzo[d]imidazol-1-yl)methyl)cyclohexyl)carbamate **13e** (1 g, 2.22 mmol) in 4 M HCl in MeOH (20 mL, 80 mmol) and MeOH (20 mL) was stirred at rt for 3 h. The reaction mixture was evaporated in vacuo to give the title compound as a yellow gum (0.7 g, 1.66 mmol, 75% yield). <sup>1</sup>H NMR (400 MHz, MeOH-*d*<sub>4</sub>): δ 8.05–8.00 (m, 1 H), 7.85–7.80 (m, 1 H), 7.71–7.66 (m, 2 H), 7.52 (s, 2 H), 4.54 (d,  $J = 7.5$  Hz, 2 H), 3.04–2.94 (m, 1 H), 2.36 (s, 6 H), 1.96 (d,  $J = 13.0$  Hz, 2 H), 1.93–1.86 (m, 1 H), 1.65 (d,  $J = 13.0$  Hz, 2 H), 1.26 (q,  $J = 13.0$  Hz, 2 H), 1.06 (q,  $J = 13.0$  Hz, 2 H); LC-MS (method C)  $m/z$ : 350 [(M + H)<sup>+</sup>];  $R_t$ : 0.84 min; 99% purity.

**4-(1-(cis-4-Aminocyclohexyl)methyl)-1H-benzo[d]imidazol-2-yl)-2,6-dimethylphenol Dihydrochloride (14f).** A mixture of *tert*-butyl (*cis*-4-((2-(4-hydroxy-3,5-dimethylphenyl)-1H-benzo[d]imidazol-1-yl)methyl)cyclohexyl)carbamate **13f** (1 g, 2.22 mmol) and 4 M HCl in MeOH (20 mL, 80 mmol) in MeOH (10 mL) was stirred at rt overnight. The reaction mixture was evaporated in vacuo to give the title compound as a pale green solid (0.73 g, 1.71 mmol, 77% yield). <sup>1</sup>H NMR (400 MHz, MeOH-*d*<sub>4</sub>): δ 8.09–8.00 (m, 1 H), 7.86–7.80 (m, 1 H), 7.72–7.63 (m, 2 H), 7.55 (s, 2 H), 4.64 (d,  $J = 7.5$  Hz, 2 H), 3.29–3.26 (m, 1 H), 2.37 (s, 6 H), 2.15–2.04 (m, 1 H), 1.74–1.58 (m, 4 H), 1.56–1.45 (m, 2 H), 1.43–1.30 (m, 2 H); LC-MS (method C)  $m/z$ : 350 [(M + H)<sup>+</sup>];  $R_t$ : 0.83 min; 99% purity.

**1-(4-((2-(4-Hydroxy-3,5-dimethylphenyl)-1H-benzo[d]imidazol-1-yl)methyl)piperidin-1-yl)ethanone Hydrochloride (15a).** To a suspension of 2,6-dimethyl-4-(1-(piperidin-4-ylmethyl)-1H-benzo[d]imidazol-2-yl)phenol dihydrochloride **14a** (30 mg, 0.073 mmol) in DCM (0.5 mL) was added NEt<sub>3</sub> (0.041 mL, 0.29 mmol), and then, the mixture was stirred at rt for 5 min. To the solution were added AcOH (5.3 mg, 0.09 mmol) and (benzotriazol-1-yloxy)tris(dimethylamino)phosphonium hexafluorophosphate (BOP, 48.7 mg, 0.11 mmol), and then, the mixture was stirred at 30 °C for 3 h. The mixture was concentrated in vacuo to give a residue which was purified by preparative HPLC to give the title compound as a colorless gum (26 mg, 0.06 mmol, 43% yield). <sup>1</sup>H NMR (400 MHz, MeOH-*d*<sub>4</sub>): δ 8.03–8.00 (m, 1 H), 7.83–7.80 (m, 1 H), 7.71–7.65 (m, 2 H), 7.52 (s, 2 H), 4.57 (dd,  $J = 7.0, 3.0$  Hz, 2 H), 4.41 (d,  $J = 13.5$  Hz, 1 H), 3.84 (d,  $J = 14.0$  Hz, 1 H), 3.00–2.93 (m, 1 H), 2.48–

2.42 (m, 1 H), 2.36 (s, 6 H), 2.20–2.14 (m, 1 H), 2.02 (s, 3 H), 1.61 (d,  $J = 13.5$  Hz, 1 H), 1.50 (d,  $J = 13.0$  Hz, 1 H), 1.22–1.11 (m, 1 H), 1.06–0.96 (m, 1 H); LC-MS (method A)  $m/z$ : 378 [(M + H)<sup>+</sup>];  $R_t$ : 0.88 min; 98% purity.

**1-(4-((2-(4-Hydroxy-3,5-dimethylphenyl)-1H-benzo[d]imidazol-1-yl)piperidin-1-yl)ethanone (15b).** A mixture of 2,6-dimethyl-4-(1-(piperidin-4-yl)-1H-benzo[d]imidazol-2-yl)phenol dihydrochloride **14b** (79 mg, 200 μmol), NEt<sub>3</sub> (24.29 mg, 240 μmol), BOP (133 mg, 300 μmol), and AcOH (48.0 mg, 800 μmol) in DCM (2 mL) was stirred at rt overnight. The reaction mixture was purified by preparative HPLC to give the title compound as a pale white gum (14 mg, 0.37 mmol, 19% yield). <sup>1</sup>H NMR (400 MHz, MeOH-*d*<sub>4</sub>): δ 7.74–7.66 (m, 2 H), 7.32–7.30 (m, 2 H), 7.25 (s, 2 H), 4.12 (d,  $J = 14.0$  Hz, 1 H), 3.24–3.15 (m, 2 H), 2.70–2.42 (m, 3 H), 2.32 (s, 6 H), 2.98 (s, 3 H), 2.01 (br s, 2 H), 1.33–1.30 (m, 1 H); LC-MS (method A)  $m/z$ : 364 [(M + H)<sup>+</sup>];  $R_t$ : 0.83 min; 100% purity.

**1-(3-((2-(4-Hydroxy-3,5-dimethylphenyl)-1H-benzo[d]imidazol-1-yl)methyl)azetidin-1-yl)ethanone (15c).** A mixture of 4-(1-(azetidin-3-ylmethyl)-1H-benzo[d]imidazol-2-yl)-2,6-dimethylphenol **14c** (61.5 mg, 0.20 mmol), AcOH (14.4 mg, 0.24 mmol), BOP (133 mg, 0.30 mmol), and NEt<sub>3</sub> (81 mg, 0.80 mmol) in DCM (2 mL) was stirred at 25 °C for 20 h. The reaction mixture was filtered and evaporated in vacuo to dryness and purified by preparative HPLC to give the title compound as a yellow gum (30 mg, 0.09 mmol, 43% yield). <sup>1</sup>H NMR (400 MHz, MeOH-*d*<sub>4</sub>): δ 7.69–7.66 (m, 2 H), 7.40–7.32 (m, 4 H), 4.70 (d,  $J = 7.5$  Hz, 2 H), 4.11 (t,  $J = 8.5$  Hz, 1 H), 3.88 (t,  $J = 9.0$  Hz, 1 H), 3.73 (dd,  $J = 9.0, 5.5$  Hz, 1 H), 3.54 (dd,  $J = 10.0, 5.5$  Hz, 1 H), 3.08–3.01 (m, 1 H), 2.34 (s, 6 H), 1.73 (s, 3 H); LC-MS (method A)  $m/z$ : 350 [(M + H)<sup>+</sup>];  $R_t$ : 0.78 min; 98% purity.

**1-(3-((2-(4-Hydroxy-3,5-dimethylphenyl)-1H-benzo[d]imidazol-1-yl)methyl)pyrrolidin-1-yl)ethanone (15d).** A mixture of 2,6-dimethyl-4-(1-(pyrrolidin-3-ylmethyl)-1H-benzo[d]imidazol-2-yl)phenol dihydrochloride **14d** (80 mg, 0.20 mmol), AcOH (14.6 mg, 0.24 mmol), BOP (135 mg, 0.30 mmol), and NEt<sub>3</sub> (82 mg, 0.81 mmol) in DCM (2 mL) was stirred at rt under nitrogen overnight. The reaction mixture was evaporated in vacuo, and the crude was purified by preparative HPLC to give the title compound as a pale white gum (46 mg, 0.12 mmol, 61% yield). <sup>1</sup>H NMR (400 MHz, MeOH-*d*<sub>4</sub>): δ 7.70–7.61 (m, 2 H), 7.38–7.29 (m, 4 H), 4.47 (dd,  $J = 12.0, 8.0$  Hz, 2 H), 3.30–3.24 (m, 3 H), 3.02–2.98 (m, 1 H), 2.78–2.67 (m, 1 H), 2.33 (s, 6 H), 1.91–1.83 (m, 4 H), 1.63–1.61 (m, 1 H); LC-MS (method A)  $m/z$ : 364 [(M + H)<sup>+</sup>];  $R_t$ : 0.81 min; 100% purity.

***N*-(trans-4-((2-(4-hydroxy-3,5-dimethylphenyl)-1H-benzo[d]imidazol-1-yl)methyl)cyclohexyl)acetamide (15e).** A mixture of 4-(1-((*trans*-4-aminocyclohexyl)methyl)-1H-benzo[d]imidazol-2-yl)-2,6-dimethylphenol dihydrochloride **14e** (80 mg, 0.19 mmol), AcOH (13.7 mg, 0.23 mmol), BOP (126 mg, 0.28 mmol), and NEt<sub>3</sub> (77 mg, 0.76 mmol) in DCM (2 mL) was stirred at rt under nitrogen overnight. The reaction mixture was evaporated in vacuo to give the crude, which was purified by preparative HPLC to give the title compound as a pale white gum (28 mg, 0.070 mmol, 37% yield). <sup>1</sup>H NMR (400 MHz, MeOH-*d*<sub>4</sub>): δ 7.67–7.65 (m, 1 H), 7.60–7.58 (m, 1 H), 7.36–7.28 (m, 4 H), 4.28 (d,  $J = 7.5$  Hz, 2 H), 3.51–3.43 (m, 1 H), 2.89 (d,  $J = 2.0$  Hz, 1 H), 2.33 (s, 6 H), 1.86 (s, 3 H), 1.81–1.73 (m, 3 H), 1.47–1.43 (m, 2 H), 1.08–0.90 (m, 4 H); LC-MS (method F)  $m/z$ : 392 [(M + H)<sup>+</sup>];  $R_t$ : 0.55 min; 100% purity.

***N*-(cis-4-((2-(4-Hydroxy-3,5-dimethylphenyl)-1H-benzo[d]imidazol-1-yl)methyl)cyclohexyl)acetamide (15f).** A mixture of 4-(1-((*cis*-4-aminocyclohexyl)methyl)-1H-benzo[d]imidazol-2-yl)-2,6-dimethylphenol dihydrochloride **14f** (69.9 mg, 0.20 mmol), AcOH (14.4 mg, 0.24 mmol), BOP (133 mg, 0.30 mmol), and NEt<sub>3</sub> (81 mg, 0.80 mmol) in DCM (1 mL) was stirred at rt over the weekend. The reaction mixture was evaporated in vacuo to give the crude product which was purified by preparative HPLC to give the title compound (19 mg, 0.47 mmol, 24% yield). <sup>1</sup>H NMR (400 MHz, MeOH-*d*<sub>4</sub>): δ 7.68–7.65 (m, 1 H), 7.60 (d,  $J = 7.0$  Hz, 1 H), 7.36–7.29 (m, 4 H), 4.34 (d,  $J = 7.5$  Hz, 2 H), 3.80 (br s, 1 H), 2.33 (s, 6 H), 1.97–1.91

(m, 4 H), 1.50–1.30 (m, 6 H), 1.22–1.18 (m, 2 H); LCMS (method F) *m/z*: 392 [(M + H)<sup>+</sup>]; *R*<sub>t</sub>: 0.55 min; 100% purity.

**2-Hydroxy-1-(4-((2-(4-hydroxy-3,5-dimethylphenyl)-1H-benzo[d]imidazol-1-yl)methyl)piperidin-1-yl)ethanone (15g).** A mixture of 2,6-dimethyl-4-(1-(piperidin-4-ylmethyl)-1H-benzo[d]imidazol-2-yl)phenol hydrochloride **14a** (60 mg, 0.16 mmol), 2-hydroxyacetic acid (18.4 mg, 0.24 mmol), BOP (107 mg, 0.24 mmol), and NEt<sub>3</sub> (0.09 mL, 0.65 mmol) in DCM (1 mL) under nitrogen was stirred at rt overnight. The crude was purified by preparative thin-layer chromatography (TLC) (DCM/MeOH 20:1) to give the title compound as a pale white gum (24 mg, 0.06 mmol, 36% yield). <sup>1</sup>H NMR (400 MHz, MeOH-*d*<sub>4</sub>): δ 7.68–7.60 (m, 2 H), 7.36–7.27 (m, 4 H), 4.37–4.31 (m, 3 H), 4.13 (d, *J* = 3.5 Hz, 2 H), 3.63–3.57 (m, 1 H), 2.88–2.78 (m, 1 H), 2.55–2.46 (m, 1 H), 2.32 (s, 6 H), 2.13–2.01 (m, 1H), 1.45–1.39 (m, 2 H), 1.13–0.92 (m, 2 H); LC–MS (method C) *m/z*: 394 [(M + H)<sup>+</sup>]; *R*<sub>t</sub>: 0.94 min; 97% purity.

**1,3-Dimethyl-5-(1-(piperidin-4-ylmethyl)-1H-benzo[d]imidazol-2-yl)pyridin-2(1H)-one Dihydrochloride (18a).** Step a (i): a solution of *tert*-butyl 4-(((2-aminophenyl)amino)methyl)piperidine-1-carboxylate **12a** (2.1 g, 6.9 mmol), 1,5-dimethyl-6-oxo-1,6-dihydropyridine-3-carbaldehyde (1.14 g, 7.6 mmol), and Na<sub>2</sub>S<sub>2</sub>O<sub>5</sub> (1.70 g, 8.9 mmol) in DMF (50 mL) was stirred at 100 °C under nitrogen for 6 h. EtOAc (30 mL) was added to the mixture which was washed with brine (×3). The organic layer was dried over Na<sub>2</sub>SO<sub>4</sub> and concentrated in vacuo to give *tert*-butyl 4-((2-(1,5-dimethyl-6-oxo-1,6-dihydropyridin-3-yl)-1H-benzo[d]imidazol-1-yl)methyl)piperidine-1-carboxylate as a brown oil (2.86 g, 6.4 mmol, 92% yield). LC–MS (method C) *m/z*: 437 [(M + H)<sup>+</sup>]; *R*<sub>t</sub>: 1.15 min; 97% purity. Step a (ii): a mixture of *tert*-butyl 4-((2-(1,5-dimethyl-6-oxo-1,6-dihydropyridin-3-yl)-1H-benzo[d]imidazol-1-yl)methyl)piperidine-1-carboxylate (2.8 g, 6.4 mmol) and 4 M HCl in MeOH (15 mL, 60.0 mmol) in MeOH (15 mL) was stirred at 25 °C for 2 h. The solvent was removed in vacuo to give the title compound as a pale solid (2.44 g, 5.9 mmol, 93% yield). LC–MS (method E) *m/z*: 337 [(M + H)<sup>+</sup>]; *R*<sub>t</sub>: 0.84 min; 100% purity.

**3-Methyl-5-(1-(piperidin-4-ylmethyl)-1H-benzo[d]imidazol-2-yl)pyridin-2(1H)-one Dihydrochloride (18b).** Step a (i): to a solution of *tert*-butyl 4-(((2-aminophenyl)amino)methyl)piperidine-1-carboxylate **12a** (1.03 g, 3.4 mmol) and 5-methyl-6-oxo-1,6-dihydropyridine-3-carbaldehyde (640 mg, 3.36 mmol) in DMF (10 mL) was added Na<sub>2</sub>S<sub>2</sub>O<sub>5</sub> (830 mg, 4.37 mmol). The reaction mixture was stirred at 100 °C overnight. The mixture was filtered, and the solid was washed with EtOAc (30 mL). The filtrate was washed with water (3 × 10 mL) and brine (3 × 10 mL), dried over Na<sub>2</sub>SO<sub>4</sub>, filtered, and concentrated in vacuo to give the residue which was purified on silica gel eluting with 1–4% MeOH in DCM to give *tert*-butyl 4-((2-(5-methyl-6-oxo-1,6-dihydropyridin-3-yl)-1H-benzo[d]imidazol-1-yl)methyl)piperidine-1-carboxylate as a brown solid (1.17 g, 2.1 mmol, 63% yield). LC–MS (method C) *m/z*: 423 [(M + H)<sup>+</sup>]; *R*<sub>t</sub>: 1.13 min; 76% purity. Step a (ii): a solution of *tert*-butyl 4-((2-(5-methyl-6-oxo-1,6-dihydropyridin-3-yl)-1H-benzo[d]imidazol-1-yl)methyl)piperidine-1-carboxylate (1.17 g, 2.1 mmol) in 4 M HCl in MeOH (30 mL, 120 mmol) was stirred at rt for 2 h. The solvent was removed in vacuo to give the title compound as a gray solid (1.04 g, 2.1 mmol, 100% yield). LC–MS (method C) *m/z*: 323 [(M + H)<sup>+</sup>]; *R*<sub>t</sub>: 0.52 min; 80% purity.

**1-Methyl-5-(1-(piperidin-4-ylmethyl)-1H-benzo[d]imidazol-2-yl)pyridin-2(1H)-one (18c).** Step b: a solution of *tert*-butyl 4-(((2-aminophenyl)amino)methyl)piperidine-1-carboxylate **12a** (1.8 g, 5.9 mmol) and 1-methyl-6-oxo-1,6-dihydropyridine-3-carboxylic acid (0.99 g, 6.48 mmol) in polyphosphoric acid (PPA) (15 g) was stirred at 180 °C under a nitrogen atmosphere for 2 h. The reaction was quenched by saturated aqueous NaHCO<sub>3</sub> and purified by preparative HPLC to give the title compound as a pale solid (1.2 g, 1.9 mmol). LC–MS (method E) *m/z*: 323 [(M + H)<sup>+</sup>]; *R*<sub>t</sub>: 0.74 min; 59% purity.

**5-(1-(Piperidin-4-ylmethyl)-1H-benzo[d]imidazol-2-yl)pyridin-2(1H)-one Dihydrochloride (18d).** Step a (i): a mixture of *tert*-butyl 4-(((2-aminophenyl)amino)methyl)piperidine-1-carboxylate **12a** (1.24 g, 4.06 mmol), 6-oxo-1,6-dihydropyridine-3-carbaldehyde

(500 mg, 4.06 mmol), and Na<sub>2</sub>S<sub>2</sub>O<sub>5</sub> (1.16 g, 6.1 mmol) in DMF (20 mL) was stirred at 100 °C overnight. The reaction mixture was treated with water and extracted with DCM. The organic layer was washed with saturated aqueous NaHCO<sub>3</sub> solution (×2) and water and then dried over Na<sub>2</sub>SO<sub>4</sub> and concentrated in vacuo to give *tert*-butyl 4-((2-(6-oxo-1,6-dihydropyridin-3-yl)-1H-benzo[d]imidazol-1-yl)methyl)piperidine-1-carboxylate as a pale yellow solid (1.44 g, 3.5 mmol, 86% yield). LC–MS (method C) *m/z*: 409 [(M + H)<sup>+</sup>]; *R*<sub>t</sub>: 1.06 min; 99% purity. Step a (ii): a mixture of *tert*-butyl 4-((2-(6-oxo-1,6-dihydropyridin-3-yl)-1H-benzo[d]imidazol-1-yl)methyl)piperidine-1-carboxylate (1.44 g, 3.53 mmol) and 6 M HCl in MeOH (30 mL) was stirred at rt overnight. The reaction mixture was evaporated in vacuo to give the title compound as a white solid (1.3 g, 3.4 mmol, 96% yield). LC–MS (method C) *m/z*: 309 [(M + H)<sup>+</sup>]; *R*<sub>t</sub>: 0.28 min; 99% purity.

**5-(1-((1-(2-Hydroxyacetyl)piperidin-4-yl)methyl)-1H-benzo[d]imidazol-2-yl)-1,3-dimethylpyridin-2(1H)-one (19a).** A mixture of 1,3-dimethyl-5-(1-(piperidin-4-ylmethyl)-1H-benzo[d]imidazol-2-yl)pyridin-2(1H)-one dihydrochloride **18a** (2.44 g, 6.0 mmol), 2-hydroxyacetic acid (0.97 g, 12.8 mmol), DIPEA (3.31 g, 25.6 mmol), 1H-benzo[d][1,2,3]triazol-1-ol (HOBt, 1.08 g, 7.0 mmol), and *N*<sup>1</sup>-((ethylimino)methylene)-*N*<sup>3</sup>,*N*<sup>3</sup>-dimethylpropane-1,3-diamine (EDC)·HCl (1.35 g, 7.0 mmol) in DCM (60 mL) was stirred at 25 °C overnight. The reaction mixture was purified by column chromatography on silica gel eluting with DCM/MeOH (200:1 to 50:1). This was further purified by preparative HPLC to give the title compound as a pale solid (240 mg, 0.58 mmol, 10% yield). <sup>1</sup>H NMR (300 MHz, MeOH-*d*<sub>4</sub>): δ 8.03 (d, *J* = 2.0 Hz, 1 H), 7.76–7.71 (m, 1 H), 7.67 (d, *J* = 7.5 Hz, 1 H), 7.63 (d, *J* = 7.5 Hz, 1 H), 7.39–7.28 (m, 2 H), 4.40 (d, *J* = 12.5 Hz, 1 H), 4.30 (d, *J* = 7.5 Hz, 2 H), 4.23–4.07 (m, 2 H), 3.68 (s, 3 H), 3.63 (d, *J* = 12.5 Hz, 1 H), 2.85 (t, *J* = 12.5 Hz, 1 H), 2.51 (t, *J* = 12.5 Hz, 1 H), 2.22 (s, 3 H), 2.18–2.04 (m, 1 H), 1.45 (d, *J* = 12.5 Hz, 2 H), 1.25–0.99 (m, 2 H); LC–MS (method C) *m/z*: 395 [(M + H)<sup>+</sup>]; *R*<sub>t</sub>: 0.87 min; 95% purity.

**5-(1-((1-(2-Hydroxyacetyl)piperidin-4-yl)methyl)-1H-benzo[d]imidazol-2-yl)-3-methylpyridin-2(1H)-one (19b).** A mixture of 3-methyl-5-(1-(piperidin-4-ylmethyl)-1H-benzo[d]imidazol-2-yl)pyridin-2(1H)-one **18b** (600 mg, 1.49 mmol) in DCM (10 mL) was treated with DIPEA (962 mg, 7.44 mmol), 2-hydroxyacetic acid (226 mg, 2.98 mmol), HOBt (274 mg, 1.79 mmol), and EDC·HCl (571 mg, 2.98 mmol) and then stirred at rt under a nitrogen atmosphere overnight. The mixture was concentrated in vacuo to give the residue which was purified by preparative TLC (MeOH/DCM = 1:15) to give the impure material. This was repurified by preparative HPLC and dried under high vacuum to give the title compound as a white solid (126 mg, 0.31 mmol, 21% yield). <sup>1</sup>H NMR (400 MHz, MeOH-*d*<sub>4</sub>): δ 8.14 (d, *J* = 2.0 Hz, 1 H), 8.09–8.02 (m, 1 H), 7.88–7.81 (m, 2 H), 7.74–7.66 (m, 2 H), 4.52 (d, *J* = 5.5 Hz, 2 H), 4.45 (d, *J* = 12.5 Hz, 1 H), 4.26–4.13 (m, 2 H), 3.69 (d, *J* = 12.5 Hz, 1 H), 2.93 (t, *J* = 12.5 Hz, 1 H), 2.57 (t, *J* = 12.5 Hz, 1 H), 2.28–2.23 (m, 1 H), 2.22 (s, 3 H), 1.61 (t, *J* = 15.0 Hz, 2 H), 1.34–1.10 (m, 2 H); LC–MS (method C) *m/z*: 381 [(M + H)<sup>+</sup>]; *R*<sub>t</sub>: 0.84 min; 93% purity.

**5-(1-((1-(2-Hydroxyacetyl)piperidin-4-yl)methyl)-1H-benzo[d]imidazol-2-yl)-1-methylpyridin-2(1H)-one (19c).** A mixture of 1-methyl-5-(1-(piperidin-4-ylmethyl)-1H-benzo[d]imidazol-2-yl)pyridin-2(1H)-one **18c** (500 mg, 1.55 mmol), 2-hydroxyacetic acid (236 mg, 3.10 mmol), DIPEA (10.5 mL, 7.8 mmol), HOBt (285 mg, 1.86 mmol), and EDC·HCl (595 mg, 3.10 mmol) in DCM (10 mL) was stirred at rt overnight. The reaction mixture was filtered, evaporated in vacuo to dryness, and purified by preparative TLC (DCM/MeOH = 20:1) to give the title compound (62 mg, 0.16 mmol, 10% yield). <sup>1</sup>H NMR (400 MHz, DMSO-*d*<sub>6</sub>): δ 8.27 (d, *J* = 2.5 Hz, 1 H), 7.84 (dd, *J* = 9.5, 2.5 Hz, 1 H), 7.68 (d, *J* = 7.5 Hz, 1 H), 7.64 (d, *J* = 7.5 Hz, 1 H), 7.30–7.20 (m, 2 H), 6.54 (d, *J* = 9.5 Hz, 1 H), 4.38 (t, *J* = 5.0 Hz, 1 H), 4.32–4.18 (m, 3 H), 4.07–3.93 (m, 2 H), 3.63–3.51 (m, 4 H), 2.78 (t, *J* = 12.5 Hz, 1 H), 2.44 (t, *J* = 12.5 Hz, 1 H), 2.06–1.93 (m, 1 H), 1.34 (t, *J* = 12.0 Hz, 2 H), 1.11 (q, *J* = 12.0 Hz, 1 H), 0.97 (q, *J* = 12.0 Hz, 1 H); LC–MS (method F) *m/z*: 381 [(M + H)<sup>+</sup>]; *R*<sub>t</sub>: 0.42 min; 100% purity.

5-(1-((1-(2-Hydroxyacetyl)piperidin-4-yl)methyl)-1H-benzo[d]imidazol-2-yl)pyridin-2(1H)-one (19d). A mixture of 5-(1-(piperidin-4-ylmethyl)-1H-benzo[d]imidazol-2-yl)pyridin-2(1H)-one dihydrochloride 18d (500 mg, 1.31 mmol), DIPEA (847 mg, 6.56 mmol), HOBT (241 mg, 1.57 mmol), EDC-HCl (503 mg, 2.62 mmol), and 2-hydroxyacetic acid (199 mg, 2.62 mmol) in DCM (10 mL) was stirred at rt overnight. The reaction mixture was purified by preparative HPLC and then purified twice further by preparative TLC (DCM/MeOH = 20:1) to give the title compound as a yellow solid (56 mg, 0.15 mmol, 12% yield). <sup>1</sup>H NMR (400 MHz, DMSO-*d*<sub>6</sub>): δ 7.90–7.82 (m, 2 H), 7.66 (d, *J* = 7.5 Hz, 1 H), 7.63 (d, *J* = 7.5 Hz, 1 H), 7.29–7.19 (m, 2 H), 6.49 (d, *J* = 9.5 Hz, 1 H), 4.39 (t, *J* = 5.0 Hz, 1 H), 4.31–4.14 (m, 3 H), 4.08–3.92 (m, 2 H), 3.58 (d, *J* = 12.5 Hz, 1 H), 2.79 (t, *J* = 12.5 Hz, 1 H), 2.44 (t, *J* = 12.5 Hz, 1 H), 2.06–1.92 (m, 1 H), 1.36 (t, *J* = 12.5 Hz, 2 H), 1.11 (q, *J* = 12.0 Hz, 1 H), 0.97 (q, *J* = 12.0 Hz, 1 H), NH not resolved; LC-MS (method F) *m/z*: 367 [(M + H)<sup>+</sup>]; *R*<sub>f</sub>: 0.40 min; 97% purity.

1,3-Dimethyl-5-(1-((tetrahydro-2H-pyran-4-yl)methyl)-1H-benzod[imidazol-2-yl)pyridin-2(1H)-one (20a). Step a: batch 1: (tetrahydro-2H-pyran-4-yl)methanamine (0.26 mL, 2.13 mmol) was added to a solution of 1-fluoro-2-nitrobenzene (0.11 mL, 1.06 mmol) and DIPEA (0.56 mL, 3.19 mmol) in NMP (1 mL) at rt in a microwave vial. The vial was sealed and heated in a microwave at 120 °C for 30 min. Once cooled, the reaction mixture was diluted with EtOAc (5 mL) and the organic layer was extracted with water (4 × 5 mL). The aqueous phase was then back extracted with EtOAc (4 × 5 mL). The combined organic layers were dried over a hydrophobic frit before being concentrated in vacuo to give an orange oil (~70 mg). Batch 2: (tetrahydro-2H-pyran-4-yl)methanamine (3.5 mL, 28.3 mmol) was added to a solution of 1-fluoro-2-nitrobenzene (1.5 mL, 14.1 mmol) and DIPEA (5.0 mL, 28.3 mmol) in NMP (10 mL) at rt in a microwave vial. The vial was sealed and heated in a microwave at 120 °C for 30 min. Once cooled the reaction mixture was diluted with EtOAc (50 mL) and the organic layer extracted with water (4 × 50 mL). The aqueous phase was then back extracted with EtOAc (4 × 50 mL). The combined organic layers were dried over a hydrophobic frit before being concentrated in vacuo to give an orange oil. Both batches were combined, loaded in DCM, and purified with a CombiFlash RF+ 40 g silica cartridge using a gradient of 0–15% EtOAc in cyclohexane over 10 column volumes and then held at 15% for further 10 column volumes. The relevant fractions were combined and concentrated in vacuo to give 2-nitro-*N*-((tetrahydro-2H-pyran-4-yl)methyl)aniline as an orange oil (2.3 g, 9.6 mmol, 63% yield). <sup>1</sup>H NMR (400 MHz, CDCl<sub>3</sub>): δ 8.18 (dd, *J* = 8.5, 1.5 Hz, 1 H), 8.21–8.12 (m, 1 H), 7.45 (ddd, *J* = 8.5, 7.0, 1.5 Hz, 1 H), 6.85 (dd, *J* = 8.5, 1.5 Hz, 1 H), 6.66 (ddd, *J* = 8.5, 7.0, 1.5 Hz, 1 H), 4.03 (dd, *J* = 11.5, 4.0 Hz, 2 H), 3.43 (ddd, *J* = 12.0, 11.5, 2.0 Hz, 2 H), 3.22 (dd, *J* = 6.5, 5.5 Hz, 2 H), 2.02–1.90 (m, 1 H), 1.76 (ddd, *J* = 12.0, 4.0, 2.0 Hz, 2 H), 1.49–1.38 (m, 2 H); LC-MS (method A) *m/z*: 237 [(M + H)<sup>+</sup>]; *R*<sub>f</sub>: 1.07 min; 96% purity. Step b (i): batch 1: to a mixture of 2-nitro-*N*-((tetrahydro-2H-pyran-4-yl)methyl)aniline (1.5 g, 6.4 mmol), 1,5-dimethyl-6-oxo-1,6-dihydropyridine-3-carbaldehyde (0.96 g, 6.35 mmol) and Na<sub>2</sub>S<sub>2</sub>O<sub>4</sub> (2.0 g, 11.4 mmol) in EtOH (2 mL) and water (1 mL) were added in a sealed tube and stirred at 100 °C for 16 h. The reaction mixture was diluted with water (100 mL) and extracted with EtOAc (3 × 100 mL). The organic layer was washed with brine (250 mL), separated, dried over anhydrous Na<sub>2</sub>SO<sub>4</sub>, and concentrated under reduced pressure. The crude material was purified by column chromatography using silica gel 100–200 mesh, eluting with EtOAc and then 2% MeOH in DCM. The collected fractions were concentrated under reduced pressure to afford batch 1 (560 mg). Batch 2: to a mixture of 2-nitro-*N*-((tetrahydro-2H-pyran-4-yl)methyl)aniline (1.5 g, 6.4 mmol), 1,5-dimethyl-6-oxo-1,6-dihydropyridine-3-carbaldehyde (0.96 g, 6.4 mmol), and Na<sub>2</sub>S<sub>2</sub>O<sub>4</sub> (2.0 g, 11.4 mmol) in EtOH (2 mL) and water (1 mL) were added in a sealed tube and stirred at 100 °C for 16 h. The reaction mixture was diluted with water (100 mL) and extracted with EtOAc (3 × 100 mL). The organic layer was washed with brine (250 mL), separated, dried over anhydrous Na<sub>2</sub>SO<sub>4</sub>, and concentrated under reduced pressure. The crude material was purified by column chromatography

using silica gel 100–200 mesh, eluting with EtOAc and then 5% MeOH in DCM. The collected fractions were concentrated under reduced pressure. The material was purified by column chromatography using silica gel 230–400 mesh, eluting with 2% MeOH in DCM. The collected fractions were concentrated under reduced pressure. The material was washed with Et<sub>2</sub>O (2 × 10 mL), decanted, and dried under reduced pressure to afford batch 2 (900 mg). Both batches were combined and purified by flash chromatography (column: Grace; silica 40 mm; 24 g cartridge). Pure fractions were collected and concentrated under reduced pressure to afford the title compound as a white solid (1.2 g, 3.6 mmol, 28% combined yield). mp 158 °C; IR (solid)  $\nu$  (cm<sup>-1</sup>): 2918, 2840, 1654, 1619, 1459, 1091; <sup>1</sup>H NMR (600 MHz, DMSO-*d*<sub>6</sub>): δ 8.13 (s, 1 H), 7.74 (s, 1 H), 7.68 (d, *J* = 7.5 Hz, 1 H), 7.62 (d, *J* = 7.5 Hz, 1 H), 7.26 (t, *J* = 7.5 Hz, 1 H), 7.21 (t, *J* = 7.5 Hz, 1 H), 4.28 (d, *J* = 7.0 Hz, 2 H), 3.72 (dd, *J* = 11.5, 3.5 Hz, 2 H), 3.56 (s, 3 H), 3.11 (td, *J* = 11.5, 2.0 Hz, 2 H), 2.11 (s, 3 H), 1.96 (ddd, *J* = 11.0, 7.0, 4.0 Hz, 1 H), 1.24–1.12 (m, 4 H); <sup>13</sup>C NMR (150 MHz, DMSO-*d*<sub>6</sub>): δ 162.3, 150.9, 142.8, 138.8, 137.2, 136.5, 128.3, 122.7, 122.3, 119.3, 111.6, 108.8, 66.8 (2C), 49.8, 37.9 (2C), 35.6, 30.4, 17.4; LC-MS (method F) *m/z*: 338 [(M + H)<sup>+</sup>]; *R*<sub>f</sub>: 0.52 min; 100% purity. HRMS: [(M + H)<sup>+</sup>] calcd for C<sub>20</sub>H<sub>24</sub>N<sub>3</sub>O<sub>2</sub>, 338.1869; found, 338.1868.

1,3-Dimethyl-5-(1-(1-(tetrahydro-2H-pyran-4-yl)ethyl)-1H-benzod[imidazole-2-yl)pyridin-2(1H)-one (20b and 20b'). Step a: 1-fluoro-2-nitrobenzene (0.11 mL, 1.04 mmol), 1-(tetrahydro-2H-pyran-4-yl)ethanamine hydrochloride (250 mg, 1.51 mmol), and DIPEA (0.8 mL, 4.58 mmol) were suspended in DMSO (1 mL) within a sealed vessel and heated in a microwave for 20 min at 120 °C. The reaction mixture was allowed to cool to rt. The reaction vessel was sealed and heated within a microwave for a further 20 min at 120 °C. The reaction mixture was allowed to cool to rt. The solvent was removed under a stream of nitrogen, and the residue was taken up into EtOAc (10 mL), diluted with water (10 mL), and extracted with EtOAc (3 × 10 mL). The combined organic extracts were dried over a hydrophobic frit, and the filtrate was purified by normal phase column chromatography on an 80 g silica column and eluted with 0–70% cyclohexane in EtOAc over 10 column volumes. The desired fractions were combined, and the solvent was removed in vacuo to give a yellow oil which was dried in a vacuum oven overnight to yield crude racemic 2-nitro-*N*-(1-(tetrahydro-2H-pyran-4-yl)ethyl)aniline (378 mg, 1.51 mmol). <sup>1</sup>H NMR (400 MHz, CDCl<sub>3</sub>): δ 8.18 (dd, *J* = 8.5, 1.5 Hz, 1 H), 8.12 (d, *J* = 8.0 Hz, 1 H), 7.42 (ddd, *J* = 8.5, 7.0, 1.5 Hz, 1 H), 6.86 (d, *J* = 8.5 Hz, 1 H), 6.62 (ddd, *J* = 8.5, 7.0, 1.5 Hz, 1 H), 4.07–4.00 (m, 2 H), 3.63–3.52 (m, 1 H), 3.44–3.35 (m, 2 H), 1.83–1.73 (m, 2 H), 1.70–1.63 (m, 1 H), 1.55–1.39 (m, 2 H), 1.27 (d, *J* = 6.5 Hz, 3 H); LC-MS (method A) *m/z*: 251 [(M + H)<sup>+</sup>]; *R*<sub>f</sub>: 1.17 min; 100% purity. Step c (i): racemic 2-nitro-*N*-(1-(tetrahydro-2H-pyran-4-yl)ethyl)aniline (142 mg, 0.567 mmol) was dissolved in EtOH (10 mL) and added to 5% Pd/C (15 mg, 0.007 mmol). The reaction mixture was stirred at rt under an atmosphere of hydrogen for 6 h. The reaction mixture was filtered over Celite and washed with EtOH (30 mL). The solvent was removed in vacuo to give racemic *N*<sup>1</sup>-(1-(tetrahydro-2H-pyran-4-yl)ethyl)benzene-1,2-diamine as a purple gum (125 mg, 0.57 mmol, 100% yield). <sup>1</sup>H NMR (400 MHz, DMSO-*d*<sub>6</sub>): δ 6.53 (dd, *J* = 7.5, 1.5 Hz, 1 H), 6.47 (td, *J* = 7.5, 1.5 Hz, 1 H), 6.42 (dd, *J* = 7.5, 1.5 Hz, 1 H), 6.36 (td, *J* = 7.5, 1.5 Hz, 1 H), 4.46 (s, 2 H), 3.99 (d, *J* = 8.5 Hz, 1 H), 3.91–3.84 (m, 2 H), 3.29–3.19 (m, 3 H), 1.74 (d, *J* = 13.0 Hz, 1 H), 1.71–1.61 (m, 1 H), 1.58 (d, *J* = 13.0 Hz, 1 H), 1.31 (td, *J* = 13.0, 4.5 Hz, 1 H), 1.25 (td, *J* = 13.0, 4.5 Hz, 1 H), 1.06 (d, *J* = 6.5 Hz, 3 H); LC-MS (method A) *m/z*: 221 [(M + H)<sup>+</sup>]; *R*<sub>f</sub>: 0.93 min; 91% purity. Step c (ii): batch 1: racemic *N*<sup>1</sup>-(1-(tetrahydro-2H-pyran-4-yl)ethyl)benzene-1,2-diamine (60 mg, 0.27 mmol) and 1,5-dimethyl-6-oxo-1,6-dihydropyridine-3-carbaldehyde (45 mg, 0.30 mmol) were dissolved in DMF (1.5 mL) and water (0.05 mL). Potassium peroxydisulfate (109 mg, 0.18 mmol) was added, and the reaction mixture was evacuated and purged with nitrogen (×3) and left to stir for 18 h at rt under an atmosphere of nitrogen. The reaction mixture was diluted with DCM (30 mL) and washed with water (30 mL). The aqueous phase was extracted with DCM (3 × 30 mL), and the organic layers were

combined and dried over a hydrophobic frit. The solvent was removed in vacuo, and the residue was dissolved in 1:1 DMSO/MeOH (0.6 mL) and purified by MDAP (method B). The solvent was evaporated in vacuo to give batch 1 racemic 1,3-dimethyl-5-(1-(1-(tetrahydro-2H-pyran-4-yl)ethyl)-1H-benzo[d]imidazol-2-yl)pyridin-2(1H)-one as a brown solid (66 mg). Batch 2: racemic N<sup>1</sup>-(1-(tetrahydro-2H-pyran-4-yl)ethyl)benzene-1,2-diamine (65 mg, 0.30 mmol) and 1,5-dimethyl-6-oxo-1,6-dihydropyridine-3-carbaldehyde (45 mg, 0.30 mmol) were dissolved in DMF (1.5 mL) and water (0.05 mL). Potassium peroxydisulfate (118 mg, 0.19 mmol) was added, and the reaction mixture was stirred for 5 h at rt under an atmosphere of nitrogen. The reaction mixture was diluted with water (30 mL). The aqueous phase was extracted with DCM (4 × 30 mL), and the organic layers were combined and dried over a hydrophobic frit. The solvent was removed in vacuo, and the residue was dissolved in 1:1 DMSO/MeOH (0.6 mL) and purified by MDAP (method B). The solvent was evaporated in vacuo to give batch 2 racemic 1,3-dimethyl-5-(1-(1-(tetrahydro-2H-pyran-4-yl)ethyl)-1H-benzo[d]imidazole-2-yl)pyridin-2(1H)-one as a brown solid (56 mg). The two batches (batch 1, 36 mg and batch 2, 50 mg) were combined and dissolved in EtOH (2 mL). Two injections were made onto a Chiralpak AD-H column (250 mm × 30 mm). An isocratic system of 30% EtOH in heptane with a flow rate of 25 mL/min was used at rt. The UV detection was performed at 215 nm. The appropriate fractions were combined and evaporated in vacuo to give the title compounds. Isomer 1 **20b** (28 mg, 0.08 mmol, 14% combined yield). >99% ee determined by HPLC analysis on a Chiralpak AD-H (250 mm × 4.6 mm) column. Peak elution at R<sub>t</sub>: 8.88 min. An isocratic system of 30% EtOH in heptane with a flow rate of 1 mL/min was used at rt. The UV detection was performed at 215 nm; <sup>1</sup>H NMR (400 MHz, CDCl<sub>3</sub>): δ 7.78 (dd, J = 7.0, 2.0 Hz, 1 H), 7.66 (d, J = 2.0 Hz, 1 H), 7.57 (dd, J = 7.0, 2.0 Hz, 1 H), 7.36–7.33 (m, 1 H), 7.31 (td, J = 7.0, 2.0 Hz, 1 H), 7.27 (td, J = 7.0, 2.0 Hz, 1 H), 4.15 (dq, J = 10.5, 7.0 Hz, 1 H), 4.03 (dd, J = 11.5, 4.0 Hz, 1 H), 3.75 (dd, J = 11.5, 4.0 Hz, 1 H), 3.66 (s, 3 H), 3.39 (td, J = 11.5, 2.0 Hz, 1 H), 3.13 (td, J = 11.5, 2.0 Hz, 1 H), 2.41 (tdt, J = 11.5, 10.5, 4.0 Hz, 1 H), 2.25 (s, 3 H), 1.85 (ddd, J = 13.0, 4.0, 2.0 Hz, 1 H), 1.75 (d, J = 7.0 Hz, 3 H), 1.35 (dtd, J = 13.0, 11.5, 4.0 Hz, 1 H), 0.98 (dtd, J = 13.0, 11.5, 4.0 Hz, 1 H), 0.70 (ddd, J = 13.0, 4.0, 2.0 Hz, 1 H); LC–MS (method A) m/z: 352 [(M + H)<sup>+</sup>]; R<sub>t</sub>: 0.87 min; 100% purity. Isomer 2 **20b'** (28 mg, 0.08 mmol, 14% combined yield). 99% ee determined by HPLC analysis on a Chiralpak AD-H (250 mm × 4.6 mm) column. Peak elution at R<sub>t</sub>: 10.83 min. An isocratic system of 30% EtOH in heptane with a flow rate of 1 mL/min was used at rt. The UV detection was performed at 215 nm; <sup>1</sup>H NMR (400 MHz, CDCl<sub>3</sub>): δ 7.78 (dd, J = 7.0, 2.0 Hz, 1 H), 7.66 (d, J = 2.0 Hz, 1 H), 7.57 (dd, J = 7.0, 2.0 Hz, 1 H), 7.36–7.33 (m, 1 H), 7.31 (td, J = 7.0, 2.0 Hz, 1 H), 7.28 (td, J = 7.0, 2.0 Hz, 2 H), 4.15 (dq, J = 10.5, 7.0 Hz, 1 H), 4.03 (dd, J = 11.5, 4.0 Hz, 1 H), 3.75 (dd, J = 11.5, 4.0 Hz, 1 H), 3.66 (s, 3 H), 3.39 (td, J = 11.5, 2.0 Hz, 1 H), 3.13 (td, J = 11.5, 2.0 Hz, 1 H), 2.41 (tdt, J = 11.5, 10.5, 4.0 Hz, 1 H), 2.25 (s, 3 H), 1.85 (ddd, J = 13.0, 4.0, 2.0 Hz, 1 H), 1.75 (d, J = 7.0 Hz, 3 H), 1.35 (dtd, J = 13.0, 11.5, 4.0 Hz, 2 H), 0.98 (dtd, J = 13.0, 11.5, 4.0 Hz, 1 H), 0.70 (ddd, J = 13.0, 4.0, 2.0 Hz, 1 H); LC–MS (method A) m/z: 352 [(M + H)<sup>+</sup>]; R<sub>t</sub>: 0.87 min; 100% purity.

**1,3-Dimethyl-5-(1-(1-(tetrahydro-2H-pyran-4-yl)propyl)-1H-benzod[imidazole-2-yl]pyridin-2(1H)-one (20c and 20c')**. Step a: 1-fluoro-2-nitrobenzene (0.11 mL, 1.04 mmol), DIPEA (0.22 mL, 1.26 mmol), and 1-(tetrahydro-2H-pyran-4-yl)propan-1-amine (179 mg, 1.25 mmol) were suspended in NMP (1 mL) within a sealed vial and heated in a microwave at 125 °C for 1 h. The mixture was allowed to reach rt and then diluted with water (40 mL) and extracted with EtOAc (5 × 40 mL). The organic layers were combined and dried over a hydrophobic frit, and the solvent was removed in vacuo. The residue was taken up into DCM (5 mL) and purified by normal phase column chromatography on a 40 g silica column and eluting with 0–100% EtOAc in cyclohexane over 10 column volumes. The desired fractions were combined, and the solvent was removed in vacuo to give 2-nitro-N-(1-(tetrahydro-2H-pyran-4-yl)propyl)aniline as an orange gum (265 mg, 1.00 mmol, 96% yield). <sup>1</sup>H NMR (400

MHz, CDCl<sub>3</sub>): δ 8.18 (dd, J = 8.5, 1.5 Hz, 1 H), 8.12 (d, J = 8.5 Hz, 1 H), 7.40 (ddd, J = 8.5, 7.0, 1.5 Hz, 1 H), 6.88 (d, J = 8.5 Hz, 1 H), 6.61 (ddd, J = 8.5, 7.0, 1.5 Hz, 1 H), 4.01 (dd, J = 11.5, 4.5 Hz, 2 H), 3.50–3.43 (m, 1 H), 3.42–3.34 (m, 2 H), 1.88–1.74 (m, 2 H), 1.74–1.67 (m, 1 H), 1.65–1.58 (m, 1 H), 1.56–1.40 (m, 3 H), 0.96 (t, J = 7.5 Hz, 3 H); LC–MS (method A) m/z: 263 [(M + H)<sup>+</sup>]; R<sub>t</sub>: 1.24 min; 99% purity. Step b (i): 2-Nitro-N-(1-(tetrahydro-2H-pyran-4-yl)propyl)aniline (265 mg, 1.00 mmol), Na<sub>2</sub>S<sub>2</sub>O<sub>4</sub> (524 mg, 3.01 mmol), and 1,5-dimethyl-6-oxo-1,6-dihydropyridine-3-carbaldehyde (212 mg, 1.40 mmol) were suspended in EtOH (1.5 mL) and water (0.75 mL) within a sealed vessel and heated in a microwave at 100 °C for 65 min. The reaction mixture was allowed to cool to rt. The reaction mixture was diluted with saturated aqueous NaHCO<sub>3</sub> (30 mL). The aqueous phase was extracted with DCM (4 × 30 mL), and the organic extracts were combined and dried over a hydrophobic frit. The solvent was removed in vacuo, and the residue was taken up into DCM (5 mL) and purified by normal phase column chromatography on a 40 g silica cartridge eluting with 0–100% EtOAc in cyclohexane over 10 column volumes followed by 100% EtOAc over 10 column volumes and MeOH over 10 column volumes. The desired fractions were combined, and the solvent was removed in vacuo to give racemic 1,3-dimethyl-5-(1-(1-(tetrahydro-2H-pyran-4-yl)propyl)-1H-benzod[imidazole-2-yl]pyridin-2(1H)-one (330 mg). Racemate (324 mg) was dissolved in EtOH (3 mL). Three injections were made onto a Chiralcel OD-H column (250 mm × 30 mm). An isocratic system of 10% EtOH in heptane with a flow rate of 30 mL/min was used at rt. The UV detection was performed at 215 nm. The appropriate fractions were combined and evaporated in vacuo. Mixed fractions were reprocessed using the same conditions to give the title compounds. Isomer 1 **20c** (170 mg, 0.47 mmol, 47% yield). >99% ee determined by HPLC analysis on a Chiralcel OD-H (250 mm × 4.6 mm) column. Peak elution at R<sub>t</sub>: 26.02 min. An isocratic system of 10% EtOH in heptane with a flow rate of 1 mL/min was used at rt. The UV detection was performed at 215 nm; <sup>1</sup>H NMR (400 MHz, CDCl<sub>3</sub>): δ 7.79 (dd, J = 7.5, 1.5 Hz, 1 H), 7.61 (d, J = 1.5 Hz, 1 H), 7.56 (d, J = 7.5 Hz, 1 H), 7.43 (s, 1 H), 7.31 (td, J = 7.5, 1.5 Hz, 1 H), 7.29–7.25 (m, 1 H), 4.05 (dd, J = 11.5, 4.0 Hz, 1 H), 3.97 (td, J = 11.0, 4.0 Hz, 1 H), 3.82 (dd, J = 11.5, 4.0 Hz, 1 H), 3.65 (s, 3 H), 3.41 (td, J = 11.5, 2.0 Hz, 1 H), 3.19 (td, J = 11.5, 2.0 Hz, 1 H), 2.48–2.34 (m, 1 H), 2.25 (s, 3 H), 2.29–2.16 (m, 1 H), 2.13–2.02 (m, 1 H), 1.87 (ddd, J = 13.0, 4.0, 2.0 Hz, 1 H), 1.39 (dtd, J = 13.0, 11.5, 4.0 Hz, 1 H), 1.14 (dtd, J = 13.0, 11.5, 4.0 Hz, 1 H), 0.93–0.86 (m, 1 H), 0.77 (t, J = 7.5 Hz, 3 H); LC–MS (method F) m/z: 366 [(M + H)<sup>+</sup>]; R<sub>t</sub>: 0.66 min; 100% purity. Isomer 2 **20c'** (151 mg, 0.41 mmol, 41% yield). 99% ee determined by HPLC analysis on a Chiralcel OD-H (250 mm × 4.6 mm) column. Peak elution at R<sub>t</sub>: 30.83 min. An isocratic system of 10% EtOH in heptane with a flow rate of 1 mL/min was used at rt. The UV detection was performed at 215 nm; <sup>1</sup>H NMR (400 MHz, CDCl<sub>3</sub>): δ 7.79 (dd, J = 7.5, 1.5 Hz, 1 H), 7.61 (d, J = 1.5 Hz, 1 H), 7.56 (d, J = 7.5 Hz, 1 H), 7.43 (s, 1 H), 7.29–7.25 (m, 1 H), 7.31 (td, J = 7.5, 1.5 Hz, 1 H), 4.05 (dd, J = 11.5, 4.0 Hz, 1 H), 3.97 (td, J = 11.0, 4.0 Hz, 1 H), 3.82 (dd, J = 11.5, 4.0 Hz, 1 H), 3.65 (s, 3 H), 3.41 (td, J = 11.5, 2.0 Hz, 1 H), 3.19 (td, J = 11.5, 2.0 Hz, 1 H), 2.48–2.34 (m, 1 H), 2.25 (s, 3 H), 2.29–2.16 (m, 1 H), 2.13–2.02 (m, 1 H), 1.87 (ddd, J = 13.0, 4.0, 2.0 Hz, 1 H), 1.39 (dtd, J = 13.0, 11.5, 4.0 Hz, 1 H), 1.14 (dtd, J = 13.0, 11.5, 4.0 Hz, 1 H), 0.93–0.86 (m, 1 H), 0.77 (t, J = 7.5 Hz, 3 H); LC–MS (method F) m/z: 366 [(M + H)<sup>+</sup>]; R<sub>t</sub>: 0.66 min; 100% purity.

**1,3-Dimethyl-5-(1-(1-(tetrahydro-2H-pyran-3-yl)methyl)-1H-benzod[imidazole-2-yl]pyridin-2(1H)-one (20d and 20d')**. Step a: 1-fluoro-2-nitrobenzene (0.11 mL, 1.042 mmol), DIPEA (0.40 mL, 2.292 mmol), and (tetrahydro-2H-pyran-3-yl)methanamine (144 mg, 1.25 mmol) were suspended in NMP (1 mL) within a sealed vial and heated in a microwave at 125 °C for 1 h. The reaction mixture was allowed to reach rt and then diluted with water (40 mL) and extracted with EtOAc (5 × 40 mL). The organic layers were combined and dried over a hydrophobic frit, and the solvent was removed in vacuo. The residue was taken up into DCM (5 mL) and purified by normal phase column chromatography on a 40 g silica column and eluted with 0–100% EtOAc in cyclohexane over 10 column volumes. The

desired fractions were combined, the solvent was removed in vacuo, and the residue was dried in a vacuum oven overnight to give 2-nitro-*N*-((tetrahydro-2*H*-pyran-3-yl)methyl)aniline as an orange gum (201 mg, 0.85 mmol, 82% yield). <sup>1</sup>H NMR (400 MHz, CDCl<sub>3</sub>): δ 8.19 (dd, *J* = 8.5, 1.5 Hz, 1 H), 8.15–8.05 (m, 1 H), 7.45 (ddd, *J* = 8.5, 7.0, 1.5 Hz, 1 H), 6.85 (dd, *J* = 8.5, 1.5 Hz, 1 H), 6.66 (ddd, *J* = 8.5, 7.0, 1.5 Hz, 1 H), 3.96 (ddd, *J* = 11.0, 4.0, 1.5 Hz, 1 H), 3.86 (dt, *J* = 11.0, 4.0 Hz, 1 H), 3.51 (ddd, *J* = 11.0, 9.0, 4.0 Hz, 1 H), 3.34 (dd, *J* = 11.0, 9.0 Hz, 1 H), 3.31–3.17 (m, 2 H), 2.10–1.95 (m, 2 H), 1.76–1.59 (m, 2 H), 1.48–1.37 (m, 1 H); LC–MS (method A): no mass ion observed; *R*<sub>t</sub>: 1.12 min; 98% purity. Step b (i): 2-nitro-*N*-((tetrahydro-2*H*-pyran-3-yl)methyl)aniline (201 mg, 0.85 mmol), Na<sub>2</sub>S<sub>2</sub>O<sub>4</sub> (444 mg, 2.55 mmol), and 1,5-dimethyl-6-oxo-1,6-dihydropyridine-3-carbaldehyde (180 mg, 1.19 mmol) were suspended in EtOH (1.5 mL) and water (0.75 mL) within a sealed vessel and heated in a microwave at 100 °C for 65 min. The reaction mixture was allowed to cool to rt. The reaction mixture was diluted with water (30 mL). The aqueous phase was extracted with DCM (4 × 30 mL), and the organic layers were combined and dried over a hydrophobic frit. The solvent was removed in vacuo, and the residue was dissolved in 1:1 DMSO/MeOH (0.6 mL) and purified by MDAP (method B). The solvent was evaporated in vacuo to give racemic 1,3-dimethyl-5-(1-((tetrahydro-2*H*-pyran-3-yl)methyl)-1*H*-benzo[*d*]imidazole-2-yl)pyridin-2(1*H*)-one (148 mg). Racemate (144 mg) was dissolved in EtOH (2 mL). Two injections were made onto a Chiralpak AD-H column (250 mm × 30 mm). An isocratic system of 40% EtOH (containing 0.2% isopropylamine) in heptane (containing 0.2% isopropylamine) with a flow rate of 30 mL/min was used at rt. The UV detection was performed at 215 nm. The appropriate fractions were combined and evaporated in vacuo to give the title compounds. Isomer 1 **20d** (68 mg, 0.20 mmol, 24% yield). >99% ee determined by HPLC analysis on a Chiralpak AD-H (250 mm × 4.6 mm) column. Peak elution at *R*<sub>t</sub>: 11.23 min. An isocratic system of 50% EtOH (containing 0.2% isopropylamine) in heptane with a flow rate of 1 mL/min was used at rt. The UV detection was performed at 215 nm; <sup>1</sup>H NMR (400 MHz, CDCl<sub>3</sub>): δ 7.81 (d, *J* = 2.0 Hz, 1 H), 7.79–7.76 (m, 1 H), 7.58–7.56 (m, 1 H), 7.42–7.37 (m, 1 H), 7.34–7.29 (m, 2 H), 4.28 (dd, *J* = 14.5, 8.5 Hz, 1 H), 4.13 (dd, *J* = 14.5, 7.0 Hz, 1 H), 3.76–3.69 (m, 1 H), 3.66 (s, 3 H), 3.62–3.48 (m, 2 H), 3.25 (dd, *J* = 11.5, 7.5 Hz, 1 H), 2.26 (s, 3 H), 2.25–2.18 (m, 1 H), 1.76–1.67 (m, 1 H), 1.67–1.59 (m, 1 H), 1.55–1.45 (m, 1 H), 1.37–1.27 (m, 1 H); LC–MS (method A) *m/z*: 338 [(*M* + *H*)<sup>+</sup>]; *R*<sub>t</sub>: 0.85 min; 100% purity. Isomer 2 **20d'** (74 mg, 0.22 mmol, 26% yield). >99% ee determined by HPLC analysis on a Chiralpak AD-H (250 mm × 4.6 mm) column. Peak elution at *R*<sub>t</sub>: 17.57 min. An isocratic system of 50% EtOH (containing 0.2% isopropylamine) in heptane with a flow rate of 1 mL/min was used at rt. The UV detection was performed at 215 nm; <sup>1</sup>H NMR (400 MHz, CDCl<sub>3</sub>): δ 7.81 (d, *J* = 2.0 Hz, 1 H), 7.79–7.76 (m, 1 H), 7.58–7.56 (m, 1 H), 7.42–7.37 (m, 1 H), 7.34–7.28 (m, 2 H), 4.28 (dd, *J* = 14.5, 8.5 Hz, 1 H), 4.13 (dd, *J* = 14.5, 7.0 Hz, 1 H), 3.76–3.69 (m, 1 H), 3.66 (s, 3 H), 3.62–3.48 (m, 2 H), 3.25 (dd, *J* = 11.5, 7.5 Hz, 1 H), 2.26 (s, 3 H), 2.25–2.18 (m, 1 H), 1.76–1.67 (m, 1 H), 1.67–1.59 (m, 1 H), 1.55–1.45 (m, 1 H), 1.37–1.27 (m, 1 H); LC–MS (method A) *m/z*: 338 [(*M* + *H*)<sup>+</sup>]; *R*<sub>t</sub>: 0.85 min; 100% purity.

5-(1-((*trans*-4-Hydroxycyclohexyl)methyl)-1*H*-benzo[*d*]imidazole-2-yl)-1,3-dimethylpyridin-2(1*H*)-one (**20e**). Step a: to a solution of 1-fluoro-2-nitrobenzene (100 mg, 0.71 mmol) in 2-methyl tetrahydrofuran (2-MeTHF, 1 mL) were added (*trans*-4-(*tert*-butoxycyclohexyl)methanamine (158 mg, 0.85 mmol) and DIPEA (0.37 mL, 2.13 mmol). The reaction vessel was sealed and heated in a microwave at 110 °C for 20 min. The reaction was cooled and then heated to 110 °C for 20 min. The solvent was removed under a stream of nitrogen. Step b (i): to the dried material were added 1,5-dimethyl-6-oxo-1,6-dihydropyridine-3-carbaldehyde (118 mg, 0.78 mmol) and Na<sub>2</sub>S<sub>2</sub>O<sub>4</sub> (370 mg, 2.13 mmol) as a solution in EtOH (1.0 mL), followed by water (0.5 mL). The sealed vessel was heated at 100 °C for 6 h. The solvent was removed under a stream of nitrogen. The reaction mixture was partitioned between saturated aqueous NaHCO<sub>3</sub> (3 mL) and DCM (2 × 3 mL). The DCM was

removed under a stream of nitrogen, and the residue was purified by MDAP (method B). Step b (ii): to the dried material were added DCM (0.2 mL) and TFA (0.2 mL), and the solution was left for 2 h. The solvent was removed under a stream of nitrogen, and the residue was purified by MDAP (method B) to give the title compound (6 mg, 0.02 mmol, 2% overall yield). <sup>1</sup>H NMR (400 MHz, DMSO-*d*<sub>6</sub>): δ 8.11 (d, *J* = 2.5 Hz, 1 H), 7.74–7.71 (m, 1 H), 7.62 (dd, *J* = 7.5, 1.5 Hz, 1 H), 7.61 (dd, *J* = 7.0, 1.5 Hz, 1 H), 7.25 (ddd, *J* = 7.5, 7.0, 1.5 Hz, 1 H), 7.21 (ddd, *J* = 7.5, 7.0, 1.5 Hz, 1 H), 4.39 (d, *J* = 4.5 Hz, 1 H), 4.19 (d, *J* = 7.5 Hz, 2 H), 3.56 (s, 3 H), 3.29–3.21 (m, 1 H), 2.10 (s, 3 H), 1.75–1.58 (m, 3 H), 1.38–1.28 (m, 2 H), 1.00–0.85 (m, 4 H); LC–MS (method F) *m/z*: 352 [(*M* + *H*)<sup>+</sup>]; *R*<sub>t</sub>: 0.47 min; 96% purity.

1,3-Dimethyl-5-(1-(2-(tetrahydro-2*H*-pyran-4-yl)ethyl)-1*H*-benzo[*d*]imidazole-2-yl)pyridin-2(1*H*)-one (**20f**). Step a: to a solution of 1-fluoro-2-nitrobenzene (50 mg, 0.35 mmol) in 2-MeTHF (1 mL) were added 2-(tetrahydro-2*H*-pyran-4-yl)ethanamine (55 mg, 0.43 mmol) and DIPEA (0.19 mL, 1.06 mmol). The reaction vessel was sealed and heated in a microwave at 110 °C for 20 min. After cooling the reaction, further 2-(tetrahydro-2*H*-pyran-4-yl)ethanamine (55 mg, 0.43 mmol) was added and the vial was capped and heated to 120 °C for 20 min. The solvent was removed under a stream of nitrogen. Step b (i): to the dried material were added 1,5-dimethyl-6-oxo-1,6-dihydropyridine-3-carbaldehyde (58.9 mg, 0.39 mmol) and Na<sub>2</sub>S<sub>2</sub>O<sub>4</sub> (185 mg, 1.06 mmol) as a solution in EtOH (1.0 mL), followed by water (0.5 mL). The sealed vessel was heated to 100 °C for 18 h. The solvent was removed under a stream of nitrogen. The reaction mixture was partitioned between saturated aqueous NaHCO<sub>3</sub> (3 mL) and DCM (2 × 3 mL). The DCM was removed under a stream of nitrogen. The sample was dissolved in DMSO (1 mL) and purified by MDAP (method B). The solvent was evaporated under a stream of nitrogen to give the title compound (12 mg, 0.03 mmol, 9% overall yield). <sup>1</sup>H NMR (600 MHz, DMSO-*d*<sub>6</sub>): δ 8.11 (d, *J* = 2.5 Hz, 1 H), 7.73–7.71 (m, 1 H), 7.64–7.59 (m, 2 H), 7.27 (t, *J* = 7.5 Hz, 1 H), 7.22 (t, *J* = 7.5 Hz, 1 H), 4.32 (t, *J* = 7.5 Hz, 2 H), 3.77 (dd, *J* = 11.5, 3.0 Hz, 2 H), 3.56 (s, 3 H), 3.17 (td, *J* = 11.5, 2.0 Hz, 2 H), 2.11 (s, 3 H), 1.65 (q, *J* = 7.5 Hz, 2 H), 1.47 (dd, *J* = 11.5, 2.0 Hz, 2 H), 1.44–1.36 (m, 1 H), 1.16 (qd, *J* = 11.5, 4.5 Hz, 2 H); LC–MS (method F) *m/z*: 352 [(*M* + *H*)<sup>+</sup>]; *R*<sub>t</sub>: 0.55 min; 100% purity.

5-(1-(2-Oxaspiro[3.3]heptan-6-ylmethyl)-1*H*-benzo[*d*]imidazole-2-yl)-1,3-dimethylpyridin-2(1*H*)-one (**20g**). Step a: to a solution of 1-fluoro-2-nitrobenzene (100 mg, 0.71 mmol) in 2-MeTHF (1 mL) were added 2-oxaspiro[3.3]heptan-6-ylmethanamine (108 mg, 0.85 mmol) and DIPEA (0.37 mL, 2.13 mmol). The reaction vessel was sealed and heated in a microwave at 110 °C for 30 min. The solvent was removed under a stream of nitrogen. The residue was purified by MDAP (method B). Step b (i): to the dried material were added 1,5-dimethyl-6-oxo-1,6-dihydropyridine-3-carbaldehyde (118 mg, 0.78 mmol) and Na<sub>2</sub>S<sub>2</sub>O<sub>4</sub> (370 mg, 2.13 mmol) as a solution in EtOH (1.0 mL), followed by water (0.5 mL). The sealed vessel was heated to 100 °C for 4 h. The solvent was removed under a stream of nitrogen. The reaction mixture was partitioned between saturated aqueous NaHCO<sub>3</sub> (1.5 mL) and DCM (2 × 3 mL). The DCM was removed under a stream of nitrogen. The residue was dissolved in DMSO (1 mL) and purified by MDAP (method B) to give the title compound (10 mg, 0.03 mmol, 4% overall yield). <sup>1</sup>H NMR (600 MHz, DMSO-*d*<sub>6</sub>): δ 8.11 (s, 1 H), 7.72 (s, 1 H), 7.63 (d, *J* = 7.5 Hz, 1 H), 7.60 (d, *J* = 7.5 Hz, 1 H), 7.25 (t, *J* = 7.5 Hz, 1 H), 7.21 (t, *J* = 7.5 Hz, 1 H), 4.44 (s, 2 H), 4.34 (d, *J* = 7.5 Hz, 2 H), 4.32 (s, 2 H), 3.56 (s, 3 H), 2.41 (tt, *J* = 7.5 Hz, 1 H), 2.11 (s, 3 H), 2.09 (dd, *J* = 12.0, 7.5 Hz, 2 H), 1.81 (dd, *J* = 12.0, 7.5 Hz, 2 H); LC–MS (method F) *m/z*: 350 [(*M* + *H*)<sup>+</sup>]; *R*<sub>t</sub>: 0.56 min; 99% purity.

5-(1-(1-Methoxypropan-2-yl)-1*H*-benzo[*d*]imidazole-2-yl)-1,3-dimethylpyridin-2(1*H*)-one (**20h**). Step a: to a solution of 1-fluoro-2-nitrobenzene (100 mg, 0.71 mmol) in 2-MeTHF (1 mL) were added 1-methoxypropan-2-amine (1.42 mmol, 126 mg) and DIPEA (0.37 mL, 2.13 mmol). The reaction vessel was sealed and heated in a microwave at 110 °C for 20 min. The reaction was cooled and then heated to 120 °C for 20 min. The solvent was removed under a

stream of nitrogen. Step b (i): to the dried material were added 1,5-dimethyl-6-oxo-1,6-dihydropyridine-3-carbaldehyde (118 mg, 0.78 mmol) and  $\text{Na}_2\text{S}_2\text{O}_4$  (370 mg, 2.13 mmol) as a solution in EtOH (1.0 mL), followed by water (0.5 mL). The sealed vessel was heated to 100 °C for 18 h. The solvent was removed under a stream of nitrogen. The sample was dissolved in DMSO (1 mL) and purified by MDAP (method B) to give the title compound (66 mg, 0.21 mmol, 27% overall yield).  $^1\text{H}$  NMR (400 MHz,  $\text{DMSO}-d_6$ ):  $\delta$  8.02 (d,  $J$  = 2.5 Hz, 1 H), 7.79–7.74 (m, 1 H), 7.65–7.60 (m, 2 H), 7.24–7.19 (m, 2 H), 4.84–4.73 (m, 1 H), 4.02 (t,  $J$  = 10.0 Hz, 1 H), 3.68 (dd,  $J$  = 10.0, 4.5 Hz, 1 H), 3.55 (s, 3 H), 3.15 (s, 3 H), 2.10 (s, 3 H), 1.54 (d,  $J$  = 7.0 Hz, 3 H); LC–MS (method F)  $m/z$ : 312 [(M + H) $^+$ ];  $R_t$ : 0.53 min; 99% purity.

**5-(1-(1,3-Dimethoxypropan-2-yl)-1H-benzo[d]imidazole-2-yl)-1,3-dimethylpyridin-2(1H)-one (20i)**. Step a: a mixture of 1-fluoro-2-nitrobenzene (0.15 mL, 1.42 mmol), DIPEA (0.37 mL, 2.12 mmol), and 1,3-dimethoxypropan-2-amine (340 mg, 2.85 mmol) in a microwave vial was diluted with anhydrous NMP (2 mL). The vial was sealed and heated in a microwave at 125 °C for 30 min. The reaction mixture was diluted with water (5 mL) and extracted with EtOAc (3  $\times$  5 mL). The organic extracts were combined, washed with brine (15 mL), and dried through a hydrophobic frit. The solvent was removed in vacuo, and the residue was purified by MDAP (method B). The appropriate fractions were combined, and the solvent was removed by rotary evaporation. The remaining mixture was diluted with water (3 mL) and extracted with EtOAc (3  $\times$  3 mL). The organic extracts were combined and dried through a hydrophobic frit to give *N*-(1,3-dimethoxypropan-2-yl)-2-nitroaniline as an orange oil (275 mg, 1.15 mmol, 80% yield).  $^1\text{H}$  NMR (400 MHz,  $\text{CDCl}_3$ ):  $\delta$  8.34 (d,  $J$  = 7.0 Hz, 1 H), 8.18 (dd,  $J$  = 8.5, 1.5 Hz, 1 H), 7.43 (ddd,  $J$  = 8.5, 7.0, 1.5 Hz, 1 H), 6.96 (dd,  $J$  = 8.5, 1.0 Hz, 1 H), 6.65 (ddd,  $J$  = 8.5, 7.0, 1.0 Hz, 1 H), 3.94–3.84 (m, 1 H), 3.65–3.53 (m, 4 H), 3.42 (s, 6 H); LC–MS (method F)  $m/z$ : 241 [(M + H) $^+$ ];  $R_t$ : 1.07 min; 100% purity. Step b (i): to a mixture of 1,5-dimethyl-6-oxo-1,6-dihydropyridine-3-carbaldehyde (185 mg, 1.22 mmol) and  $\text{Na}_2\text{S}_2\text{O}_4$  (580 mg, 3.33 mmol) in a microwave vessel was added a solution of *N*-(1,3-dimethoxypropan-2-yl)-2-nitroaniline (267 mg, 1.11 mmol) in EtOH (2 mL) followed by water (1 mL). The vial was sealed and heated in a microwave at 100 °C for 65 min. The reaction mixture was diluted with water (3 mL) and extracted with EtOAc (2  $\times$  5 mL). The organic extracts were combined and passed through a hydrophobic frit, and the solvent was removed under vacuum. The residue was purified by MDAP (method B). The appropriate fractions were combined, and the solvent was removed by rotary evaporation to give the title compound as a white solid (129 mg, 0.38 mmol, 34% yield).  $^1\text{H}$  NMR (400 MHz,  $\text{DMSO}-d_6$ ):  $\delta$  8.05 (d,  $J$  = 2.5 Hz, 1 H), 7.82–7.77 (m, 1 H), 7.70–7.67 (m, 1 H), 7.65–7.60 (m, 1 H), 7.25–7.17 (m, 2 H), 4.84 (tt,  $J$  = 9.0, 4.5 Hz, 1 H), 4.02 (dd,  $J$  = 10.5, 9.0 Hz, 2 H), 3.77 (dd,  $J$  = 10.5, 4.5 Hz, 2 H), 3.54 (s, 3 H), 3.16 (s, 6 H), 2.09 (s, 3 H); LC–MS (method F)  $m/z$ : 342 [(M + H) $^+$ ];  $R_t$ : 0.60 min; 100% purity.

**4-Bromo-2-nitro-*N*-((tetrahydro-2H-pyran-4-yl)methyl)aniline (21a)**. 4-Bromo-1-fluoro-2-nitrobenzene (5 g, 22.7 mmol) was taken up in 2-MeTHF (50 mL). DIPEA (6.0 mL, 34.1 mmol) and (tetrahydro-2H-pyran-4-yl)methanamine (3.93 g, 34.1 mmol) were added, and the reaction mixture was heated to 80 °C. The reaction was cooled and diluted with EtOAc (100 mL) and then washed with water (100 mL) and brine (100 mL). The organic layer was dried with  $\text{Na}_2\text{SO}_4$ , filtered, and concentrated in vacuo to yield the title compound as an orange solid (7.15 g, 21.6 mmol, 95% yield).  $^1\text{H}$  NMR (400 MHz,  $\text{CDCl}_3$ ):  $\delta$  8.33 (d,  $J$  = 2.5 Hz, 1 H), 8.13 (t,  $J$  = 5.5 Hz, 1 H), 7.51 (dd,  $J$  = 9.0, 2.5 Hz, 1 H), 6.77 (d,  $J$  = 9.0 Hz, 1 H), 4.03 (dd,  $J$  = 11.5, 4.5 Hz, 2 H), 3.42 (td,  $J$  = 11.5, 2.0 Hz, 2 H), 3.21 (dd,  $J$  = 6.5, 5.5 Hz, 2 H), 1.95 (ttt,  $J$  = 11.5, 6.5, 3.5 Hz, 1 H), 1.75 (ddd,  $J$  = 13.0, 3.5, 2.0 Hz, 2 H), 1.43 (dtd,  $J$  = 13.0, 11.5, 4.5 Hz, 2 H); LC–MS (method A)  $m/z$ : not observed [(M + H) $^+$ ];  $R_t$ : 1.25 min; 90% purity.

**5-Bromo-2-nitro-*N*-((tetrahydro-2H-pyran-4-yl)methyl)aniline (21b)**. 4-Bromo-2-fluoro-1-nitrobenzene (10 g, 44.7 mmol) was dissolved in 2-MeTHF (100 mL), and (tetrahydro-2H-pyran-4-

yl)methanamine (5.47 mL, 44.7 mmol) and DIPEA (11.7 mL, 67.1 mmol) were added. The reaction mixture was heated at 80 °C for 2 h and then added to water (200 mL) and extracted with EtOAc (2  $\times$  200 mL). The combined organics were washed with water (200 mL) and brine (200 mL), dried, and evaporated in vacuo to give the title compound as a yellow solid (12.2 g, 38.7 mmol, 87% yield).  $^1\text{H}$  NMR (400 MHz,  $\text{CDCl}_3$ ):  $\delta$  8.14 (t,  $J$  = 5.5 Hz, 1 H), 8.04 (d,  $J$  = 9.0 Hz, 1 H), 7.02 (d,  $J$  = 2.0 Hz, 1 H), 6.77 (dd,  $J$  = 9.0, 2.0 Hz, 1 H), 4.04 (dd,  $J$  = 11.0, 4.5 Hz, 2 H), 3.44 (td,  $J$  = 11.5, 2.0 Hz, 2 H), 3.20 (dd,  $J$  = 6.5, 5.5 Hz, 2 H), 1.96 (ttt,  $J$  = 11.5, 6.5, 3.5 Hz, 1 H), 1.76 (ddd,  $J$  = 13.0, 3.5, 2.0 Hz, 2 H), 1.44 (dtd,  $J$  = 13.0, 11.5, 4.5 Hz, 2 H). LC–MS (method F)  $m/z$ : 315, 317 [(M + H) $^+$ ];  $R_t$ : 1.25 min; 100% purity.

**5-(5-Bromo-1-((tetrahydro-2H-pyran-4-yl)methyl)-1H-benzo[d]imidazol-2-yl)-1,3-dimethylpyridin-2(1H)-one (22a)**. 4-Bromo-2-nitro-*N*-((tetrahydro-2H-pyran-4-yl)methyl)aniline **21a** (15.6 g, 49.5 mmol) and 1,5-dimethyl-6-oxo-1,6-dihydropyridine-3-carbaldehyde (7.48 g, 49.5 mmol) were combined in EtOH (375 mL) and water (150 mL).  $\text{Na}_2\text{S}_2\text{O}_4$  (25.9 g, 148 mmol) was added and the mixture heated to 90 °C. The reaction was cooled and concentrated to remove the EtOH. The residue was partitioned between 10:1 DCM/ $^i$ PrOH (500 mL) and water (400 mL). The aqueous layer was re-extracted with 10:1 DCM/ $^i$ PrOH (500 mL), and the combined organics were dried with  $\text{Na}_2\text{SO}_4$ , filtered, and concentrated in vacuo to yield an orange oil. The crude product was applied to a 340 g silica cartridge in the minimum amount of DCM and eluted with 5% (3:1 EtOAc/EtOH) in cyclohexane for 2 column volumes, then 5–50% (3:1 EtOAc/EtOH) over 10 column volumes, and then held at 50% for 15 column volumes. The appropriate fractions were concentrated in vacuo to give the title compound as white foam (9.21 g, 21.0 mmol, 43% yield).  $^1\text{H}$  NMR (400 MHz,  $\text{CDCl}_3$ ):  $\delta$  7.87 (d,  $J$  = 1.5 Hz, 1 H), 7.73 (d,  $J$  = 2.5 Hz, 1 H), 7.48–7.45 (m, 1 H), 7.39 (dd,  $J$  = 8.5, 1.5 Hz, 1 H), 7.24 (d,  $J$  = 8.5 Hz, 1 H), 4.11 (d,  $J$  = 7.5 Hz, 2 H), 3.88 (dd,  $J$  = 11.5, 3.5 Hz, 2 H), 3.64 (s, 3 H), 3.22 (td,  $J$  = 11.5, 2.0 Hz, 2 H), 2.23 (s, 3 H), 2.11–1.95 (m, 1 H), 1.35–1.18 (m, 4 H); LC–MS (method A)  $m/z$ : 416, 418 [(M + H) $^+$ ];  $R_t$ : 0.96 min; 100% purity.

**5-(6-Bromo-1-((tetrahydro-2H-pyran-4-yl)methyl)-1H-benzo[d]imidazol-2-yl)-1,3-dimethylpyridin-2(1H)-one (22b)**. 5-Bromo-2-nitro-*N*-((tetrahydro-2H-pyran-4-yl)methyl)aniline **21b** (12.2 g, 38.7 mmol) and 1,5-dimethyl-6-oxo-1,6-dihydropyridine-3-carbaldehyde (6.4 g, 42.6 mmol) were combined in EtOH (200 mL) and water (100 mL), and the mixture was heated to 80 °C; then,  $\text{Na}_2\text{S}_2\text{O}_4$  (20.2 g, 116 mmol) was added, and the resulting suspension was heated for 18 h at 80 °C. The mixture was evaporated in vacuo to approximately half its original volume and then extracted with EtOAc (3  $\times$  100 mL), and the combined organics were dried and evaporated in vacuo to give colorless foam. This was dissolved in DCM (30 mL) and loaded onto a 340 g silica column and then eluted with 0–25% EtOH in EtOAc, and product-containing fractions evaporated in vacuo to give the title compound as a pale yellow solid (10.2 g, 24.5 mmol, 63% yield).  $^1\text{H}$  NMR (400 MHz,  $\text{CDCl}_3$ ):  $\delta$  7.73 (d,  $J$  = 2.5 Hz, 1 H), 7.62 (d,  $J$  = 8.5 Hz, 1 H), 7.54 (d,  $J$  = 1.5 Hz, 1 H), 7.49–7.46 (m, 1 H), 7.41 (dd,  $J$  = 8.5, 1.5 Hz, 1 H), 4.11 (d,  $J$  = 7.5 Hz, 2 H), 3.91 (dd,  $J$  = 11.5, 3.5 Hz, 2 H), 3.66 (s, 3 H), 3.27 (td,  $J$  = 11.5, 2.5 Hz, 2 H), 2.25 (s, 3 H), 2.15–2.04 (m, 1 H), 1.38–1.21 (m, 4 H); LC–MS (method F)  $m/z$ : 416, 418 [(M + H) $^+$ ];  $R_t$ : 0.85 min; 100% purity.

**5-(5-(Dimethylamino)-1-((tetrahydro-2H-pyran-4-yl)methyl)-1H-benzo[d]imidazol-2-yl)-1,3-dimethylpyridin-2(1H)-one (22c)**. A mixture of 5-(5-bromo-1-((tetrahydro-2H-pyran-4-yl)methyl)-1H-benzo[d]imidazol-2-yl)-1,3-dimethylpyridin-2(1H)-one **22a** (100 mg, 0.24 mmol), 2 M dimethylamine in THF (0.6 mL, 1.20 mmol),  $\text{Pd}_2(\text{dba})_3$  (9 mg, 0.01 mmol), JohnPhos (9 mg, 0.03 mmol), and  $\text{NaO}^t\text{Bu}$  (35 mg, 0.36 mmol) in toluene (2 mL) in a sealed microwave vial was purged with nitrogen and heated in a microwave at 90 °C for 20 min. The reaction mixture was filtered over Celite, and the pad was washed with EtOAc (20 mL). The solvent was removed in vacuo, and the residue was dissolved in 1:1 DMSO/MeOH (2 mL) and purified by MDAP (method A). The solvent was evaporated in vacuo, and the residue was dissolved in MeOH (0.5 mL). The solution was applied to a 0.5 g MeOH-preconditioned aminopropyl

cartridge which was then washed with MeOH (3 mL). The wash was evaporated under a stream of nitrogen, and the residue was dried in a high-vacuum oven to give the title compound as an off-white solid (48 mg, 0.13 mmol, 53% yield).  $^1\text{H NMR}$  (400 MHz,  $\text{CDCl}_3$ ):  $\delta$  7.72 (d,  $J = 2.5$  Hz, 1 H), 7.52–7.48 (m, 1 H), 7.25 (d,  $J = 9.0$  Hz, 1 H), 7.11 (d,  $J = 2.5$  Hz, 1 H), 6.92 (dd,  $J = 9.0, 2.5$  Hz, 1 H), 4.08 (d,  $J = 7.5$  Hz, 2 H), 3.90 (dd,  $J = 11.5, 4.0$  Hz, 2 H), 3.65 (s, 3 H), 3.24 (td,  $J = 11.5, 2.0$  Hz, 2 H), 2.99 (s, 6 H), 2.25 (s, 3 H), 2.09 (t,  $J = 11.5, 7.5, 3.5$  Hz, 1 H), 1.36 (ddd,  $J = 13.0, 3.5, 2.0$  Hz, 2 H), 1.27 (dtd,  $J = 13.0, 11.5, 4.0$  Hz, 2 H); LC–MS (method F)  $m/z$ : 381 [(M + H) $^+$ ];  $R_t$ : 0.48 min; 100% purity.

**5-(6-(Dimethylamino)-1-((tetrahydro-2H-pyran-4-yl)methyl)-1H-benzo[d]imidazol-2-yl)-1,3-dimethylpyridin-2(1H)-one (22d).** 5-(6-Bromo-1-((tetrahydro-2H-pyran-4-yl)methyl)-1H-benzo[d]imidazol-2-yl)-1,3-dimethylpyridin-2(1H)-one **22b** (50 mg, 0.12 mmol), JohnPhos (4.6 mg, 0.015 mmol), 2 M dimethylamine in THF (0.10 mL, 0.20 mmol), NaO $t$ Bu (23.1 mg, 0.24 mmol), and Pd $_2$ (dba) $_3$  (4.5 mg, 0.05 mmol) were suspended in 1,4-dioxane (1 mL). The reaction vessel was sealed and heated in a microwave at 90 °C for 20 min. The reaction mixture was allowed to cool to rt, and JohnPhos (4.6 mg, 0.015 mmol), Pd $_2$ (dba) $_3$  (4.5 mg, 0.005 mmol), and NaO $t$ Bu (23.1 mg, 0.24 mmol) were added to the reaction vessel. The reaction vessel was sealed and heated in a microwave at 90 °C for 20 min. The reaction was allowed to cool to rt, and the solution was loaded onto a 1 g C18 SPE cartridge (preconditioned with MeCN [3 mL]). The column was flushed with MeCN (3 mL), and the filtrate was evaporated under a stream of nitrogen. The sample was dissolved in DMSO (1 mL) and purified by MDAP (method B). The appropriate fractions were evaporated, and the sample was dissolved in DMSO (1 mL) and purified by MDAP (method A) to give the title compound (8.9 mg, 0.02 mmol, 19% yield).  $^1\text{H NMR}$  (400 MHz,  $\text{DMSO}-d_6$ ):  $\delta$  8.05 (d,  $J = 2.5$  Hz, 1 H), 7.72–7.68 (m, 1 H), 7.41 (d,  $J = 9.0$  Hz, 1 H), 6.83 (d,  $J = 2.5$  Hz, 1 H), 6.76 (dd,  $J = 9.0, 2.5$  Hz, 1 H), 4.20 (d,  $J = 7.5$  Hz, 2 H), 3.72 (dd,  $J = 11.5, 4.0$  Hz, 2 H), 3.55 (s, 3 H), 3.11 (td,  $J = 11.5, 2.5$  Hz, 2 H), 2.95 (s, 6 H), 2.10 (s, 3 H), 1.94 (ddd,  $J = 11.5, 7.5, 3.5$  Hz, 1 H), 1.28–1.10 (m, 4 H); LC–MS (method F)  $m/z$ : 381 [(M + H) $^+$ ];  $R_t$ : 0.50 min; 99% purity.

**General  $S_N\text{Ar}$ -Cyclization Method.** To a solution of the appropriately substituted 1-fluoro-2-nitrobenzene (83 mg, 0.52 mmol) in 2-MeTHF (0.5 mL) were added (tetrahydro-2H-pyran-4-yl)methanamine (50 mg, 0.43 mmol) and DIPEA (0.23 mL, 1.30 mmol). The reaction vessel was sealed and heated in a microwave at 110 °C for 20 min. The solvent was removed under a stream of nitrogen. To the dried material were added 1,5-dimethyl-6-oxo-1,6-dihydropyridine-3-carbaldehyde (72 mg, 0.48 mmol) and Na $_2$ S $_2$ O $_4$  (227 mg, 1.30 mmol) as a solution in EtOH (1.0 mL), followed by water (0.5 mL). The sealed vessels were heated at 100 °C for 18 h. The solvent was removed under a stream of nitrogen. The reaction mixture was partitioned between saturated aqueous NaHCO $_3$  (3 mL) and DCM (2  $\times$  3 mL). The DCM extracts were evaporated under a stream of nitrogen. The residue was dissolved in DMSO (1 mL) and purified by MDAP (method B). The solvent was removed under a stream of nitrogen to give the compounds **22e–22p**.

**5-(5-Methoxy-1-((tetrahydro-2H-pyran-4-yl)methyl)-1H-benzo[d]imidazol-2-yl)-1,3-dimethylpyridin-2(1H)-one (22e).** 7 mg, 0.02 mmol, 4% yield.  $^1\text{H NMR}$  (600 MHz,  $\text{DMSO}-d_6$ ):  $\delta$  8.09 (s, 1 H), 7.72 (s, 1 H), 7.56 (d,  $J = 8.5$  Hz, 1 H), 7.13 (d,  $J = 2.0$  Hz, 1 H), 6.88 (dd,  $J = 8.5, 2.0$  Hz, 1 H), 4.23 (d,  $J = 7.5$  Hz, 2 H), 3.79 (s, 3 H), 3.71 (d,  $J = 11.5$  Hz, 2 H), 3.55 (s, 3 H), 3.10 (t,  $J = 11.5$  Hz, 2 H), 2.10 (s, 3 H), 1.94 (t,  $J = 11.5, 7.5, 3.5$  Hz, 1 H), 1.20 (d,  $J = 11.5$  Hz, 2 H), 1.13 (qd,  $J = 11.5, 3.5$  Hz, 2 H). LC–MS (method F)  $m/z$ : 368 [(M + H) $^+$ ];  $R_t$ : 0.51 min; 96% purity.

**5-(6-Methoxy-1-((tetrahydro-2H-pyran-4-yl)methyl)-1H-benzo[d]imidazol-2-yl)-1,3-dimethylpyridin-2(1H)-one (22f).** 8 mg, 0.02 mmol, 4% yield.  $^1\text{H NMR}$  (600 MHz,  $\text{DMSO}-d_6$ ):  $\delta$  8.08 (s, 1 H), 7.71 (s, 1 H), 7.48 (d,  $J = 8.5$  Hz, 1 H), 7.22 (s, 1 H), 6.83 (dd,  $J = 8.5, 2.0$  Hz, 1 H), 4.24 (d,  $J = 7.5$  Hz, 2 H), 3.83 (s, 3 H), 3.71 (d,  $J = 11.5$  Hz, 2 H), 3.55 (s, 3 H), 3.11 (t,  $J = 11.5$  Hz, 2 H), 2.10 (s, 3 H), 1.93 (t,  $J = 11.5, 7.5, 3.5$  Hz, 1 H), 1.20 (d,  $J = 11.5$  Hz, 2 H), 1.19–

1.11 (m, 2 H). LC–MS (method F)  $m/z$ : 368 [(M + H) $^+$ ];  $R_t$ : 0.53 min; 96% purity.

**1,3-Dimethyl-5-(5-methyl-1-((tetrahydro-2H-pyran-4-yl)methyl)-1H-benzo[d]imidazol-2-yl)pyridin-2(1H)-one (22g).** 11 mg, 0.03 mmol, 7% yield.  $^1\text{H NMR}$  (600 MHz,  $\text{DMSO}-d_6$ ):  $\delta$  8.11 (s, 1 H), 7.72 (s, 1 H), 7.55 (d,  $J = 8.0$  Hz, 1 H), 7.40 (s, 1 H), 7.08 (d,  $J = 8.0$  Hz, 1 H), 4.24 (d,  $J = 7.5$  Hz, 2 H), 3.71 (dd,  $J = 11.5, 3.5$  Hz, 2 H), 3.55 (s, 3 H), 3.10 (t,  $J = 11.5$  Hz, 2 H), 2.41 (s, 3 H), 2.10 (s, 3 H), 1.94 (t,  $J = 11.5, 7.5, 3.5$  Hz, 1 H), 1.19 (dd,  $J = 11.5$  Hz, 2 H), 1.13 (qd,  $J = 11.5, 3.5$  Hz, 2 H). LC–MS (method F)  $m/z$ : 352 [(M + H) $^+$ ];  $R_t$ : 0.54 min; 100% purity.

**1,3-Dimethyl-5-(6-methyl-1-((tetrahydro-2H-pyran-4-yl)methyl)-1H-benzo[d]imidazol-2-yl)pyridin-2(1H)-one (22h).** 11 mg, 0.03 mmol, 6% yield.  $^1\text{H NMR}$  (600 MHz,  $\text{DMSO}-d_6$ ):  $\delta$  8.10 (s, 1 H), 7.72 (s, 1 H), 7.48 (d,  $J = 8.5$  Hz, 1 H), 7.47 (s, 1 H), 7.03 (d,  $J = 8.5$  Hz, 1 H), 4.23 (d,  $J = 7.5$  Hz, 2 H), 3.71 (dd,  $J = 11.5, 3.5$  Hz, 2 H), 3.55 (s, 3 H), 3.11 (t,  $J = 11.5$  Hz, 2 H), 2.46 (s, 3 H), 2.10 (s, 3 H), 1.95 (t,  $J = 11.5, 7.5, 3.5$  Hz, 1 H), 1.21 (dd,  $J = 11.5$  Hz, 2 H), 1.14 (qd,  $J = 11.5, 3.5$  Hz, 2 H). LC–MS (method F)  $m/z$ : 352 [(M + H) $^+$ ];  $R_t$ : 0.55 min; 100% purity.

**5-(5-Fluoro-1-((tetrahydro-2H-pyran-4-yl)methyl)-1H-benzo[d]imidazole-2-yl)-1,3-dimethylpyridin-2(1H)-one (22i).** 15 mg, 0.04 mmol, 9% yield.  $^1\text{H NMR}$  (600 MHz,  $\text{DMSO}-d_6$ ):  $\delta$  8.14 (s, 1 H), 7.74 (s, 1 H), 7.72 (dd,  $J = 8.5, 4.5$  Hz, 1 H), 7.41 (dd,  $J = 9.5, 2.0$  Hz, 1 H), 7.13 (ddd,  $J = 9.5, 8.5, 2.0$  Hz, 1 H), 4.29 (d,  $J = 7.5$  Hz, 2 H), 3.71 (dd,  $J = 11.5, 3.5$  Hz, 2 H), 3.56 (s, 3 H), 3.11 (t,  $J = 11.5$  Hz, 2 H), 2.10 (s, 3 H), 1.95 (t,  $J = 11.5, 7.5, 3.5$  Hz, 1 H), 1.20 (dd,  $J = 11.5$  Hz, 2 H), 1.15 (qd,  $J = 11.5, 3.5$  Hz, 2 H). LC–MS (method F)  $m/z$ : 356 [(M + H) $^+$ ];  $R_t$ : 0.65 min; 99% purity.

**5-(5-Chloro-1-((tetrahydro-2H-pyran-4-yl)methyl)-1H-benzo[d]imidazol-2-yl)-1,3-dimethylpyridin-2(1H)-one (22j).** 41 mg, 0.11 mmol, 23% yield.  $^1\text{H NMR}$  (600 MHz,  $\text{DMSO}-d_6$ ):  $\delta$  8.15 (s, 1 H), 7.77–7.71 (m, 2 H), 7.67 (s, 1 H), 7.29 (d,  $J = 8.5$  Hz, 1 H), 4.29 (d,  $J = 7.5$  Hz, 2 H), 3.71 (d,  $J = 11.5$  Hz, 2 H), 3.56 (s, 3 H), 3.10 (t,  $J = 11.5$  Hz, 2 H), 2.10 (s, 3 H), 1.98–1.89 (m, 1 H), 1.22–1.09 (m, 4 H). LC–MS (method F)  $m/z$ : 372, 374 [(M + H) $^+$ ];  $R_t$ : 0.79 min; 99% purity.

**5-(6-Chloro-1-((tetrahydro-2H-pyran-4-yl)methyl)-1H-benzo[d]imidazol-2-yl)-1,3-dimethylpyridin-2(1H)-one (22k).** 19 mg, 0.05 mmol, 11% yield.  $^1\text{H NMR}$  (600 MHz,  $\text{DMSO}-d_6$ ):  $\delta$  8.15 (s, 1 H), 7.89 (s, 1 H), 7.74 (s, 1 H), 7.62 (d,  $J = 8.5$  Hz, 1 H), 7.23 (d,  $J = 8.5$  Hz, 1 H), 4.29 (d,  $J = 7.5$  Hz, 2 H), 3.71 (dd,  $J = 11.5, 3.5$  Hz, 2 H), 3.55 (s, 3 H), 3.11 (t,  $J = 11.5$  Hz, 2 H), 2.10 (s, 3 H), 1.93 (t,  $J = 11.5, 7.5, 3.5$  Hz, 1 H), 1.20 (dd,  $J = 11.5$  Hz, 2 H), 1.14 (qd,  $J = 11.5, 3.5$  Hz, 2 H). LC–MS (method F)  $m/z$ : 372, 374 [(M + H) $^+$ ];  $R_t$ : 0.78 min; 99% purity.

**2-(1,5-Dimethyl-6-oxo-1,6-dihydropyridin-3-yl)-1-((tetrahydro-2H-pyran-4-yl)methyl)-1H-benzo[d]imidazole-5-carboxamide (22l).** 30 mg, 0.08 mmol, 16% yield.  $^1\text{H NMR}$  (600 MHz,  $\text{DMSO}-d_6$ ):  $\delta$  8.18 (s, 1 H), 8.16 (s, 1 H), 7.98 (br s, 1 H), 7.83 (d,  $J = 8.5$  Hz, 1 H), 7.75 (s, 1 H), 7.73 (d,  $J = 8.5$  Hz, 1 H), 7.26 (br s, 1 H), 4.30 (d,  $J = 7.5$  Hz, 2 H), 3.71 (dd,  $J = 11.5, 3.5$  Hz, 2 H), 3.56 (s, 3 H), 3.11 (t,  $J = 11.5$  Hz, 2 H), 2.11 (s, 3 H), 1.95 (t,  $J = 11.5, 7.5, 3.5$  Hz, 1 H), 1.23–1.12 (m, 4 H). LC–MS (method F)  $m/z$ : 381 [(M + H) $^+$ ];  $R_t$ : 0.49 min; 100% purity.

**2-(1,5-Dimethyl-6-oxo-1,6-dihydropyridin-3-yl)-1-((tetrahydro-2H-pyran-4-yl)methyl)-1H-benzo[d]imidazole-6-carboxamide (22m).** 1 mg, 0.003 mmol, 1% yield.  $^1\text{H NMR}$  (600 MHz,  $\text{DMSO}-d_6$ ):  $\delta$  8.22 (s, 1 H), 8.18 (s, 1 H), 8.00 (br s, 1 H), 7.79 (d,  $J = 8.5$  Hz, 1 H), 7.77 (s, 1 H), 7.63 (d,  $J = 8.5$  Hz, 1 H), 7.35 (br s, 1 H), 4.32 (d,  $J = 7.5$  Hz, 2 H), 3.72 (dd,  $J = 11.5, 3.5$  Hz, 2 H), 3.56 (s, 3 H), 3.12 (t,  $J = 11.5$  Hz, 2 H), 2.11 (s, 3 H), 2.00 (t,  $J = 11.5, 7.5, 3.5$  Hz, 1 H), 1.24–1.13 (m, 4 H). LC–MS (method F)  $m/z$ : 381 [(M + H) $^+$ ];  $R_t$ : 0.47 min; 100% purity.

**2-(1,5-Dimethyl-6-oxo-1,6-dihydropyridin-3-yl)-1-((tetrahydro-2H-pyran-4-yl)methyl)-1H-benzo[d]imidazole-5-carbonitrile (22n).** 54 mg, 0.15 mmol, 31% yield.  $^1\text{H NMR}$  (600 MHz,  $\text{DMSO}-d_6$ ):  $\delta$  8.21 (s, 1 H), 8.16 (s, 1 H), 7.94 (d,  $J = 8.5$  Hz, 1 H), 7.77 (s, 1 H), 7.67 (d,  $J = 8.5$  Hz, 1 H), 4.36 (d,  $J = 7.5$  Hz, 2 H), 3.71 (dd,  $J = 11.5, 3.5$  Hz, 2 H), 3.56 (s, 3 H), 3.10 (td,  $J = 11.5, 3.5$  Hz, 2 H), 2.11 (s, 3

H), 1.93 (t,  $J = 11.5, 7.5, 3.5$  Hz, 1 H), 1.22–1.12 (m, 4 H). LC–MS (method F)  $m/z$ : 363 [(M + H)<sup>+</sup>];  $R_t$ : 0.74 min; 97% purity.

**2-(1,5-Dimethyl-6-oxo-1,6-dihydropyridin-3-yl)-1-((tetrahydro-2H-pyran-4-yl)methyl)-1H-benzod[*d*]imidazole-6-carbonitrile (22o).** 36 mg, 0.10 mmol, 20% yield. <sup>1</sup>H NMR (600 MHz, DMSO-*d*<sub>6</sub>):  $\delta$  8.40 (s, 1 H), 8.24–8.22 (m, 1 H), 7.79 (s, 1 H), 7.77 (d,  $J = 8.5$  Hz, 1 H), 7.60 (d,  $J = 8.5$  Hz, 1 H), 4.37 (d,  $J = 7.5$  Hz, 2 H), 3.72 (dd,  $J = 11.5, 3.5$  Hz, 2 H), 3.56 (s, 3 H), 3.12 (td,  $J = 11.5, 3.5$  Hz, 2 H), 2.11 (s, 3 H), 1.97 (t,  $J = 11.5, 7.5, 3.5$  Hz, 1 H), 1.22–1.13 (m, 4 H). LC–MS (method F)  $m/z$ : 363 [(M + H)<sup>+</sup>];  $R_t$ : 0.74 min; 95% purity.

**1,3-Dimethyl-5-(5-(methylsulfonyl)-1-((tetrahydro-2H-pyran-4-yl)methyl)-1H-benzod[*d*]imidazol-2-yl)pyridin-2(1H)-one (22p).** 11 mg, 0.03 mmol, 6% yield. <sup>1</sup>H NMR (600 MHz, DMSO-*d*<sub>6</sub>):  $\delta$  8.20 (d,  $J = 2.5$  Hz, 1 H), 8.16–8.15 (m, 1 H), 7.99 (d,  $J = 8.5$  Hz, 1 H), 7.81 (d,  $J = 8.5$  Hz, 1 H), 7.77 (s, 1 H), 4.37 (d,  $J = 7.5$  Hz, 2 H), 3.72 (dd,  $J = 11.5, 3.5$  Hz, 2 H), 3.57 (s, 3 H), 3.24 (s, 3 H), 3.11 (td,  $J = 11.5, 3.5$  Hz, 2 H), 2.11 (s, 3 H), 1.95 (t,  $J = 11.5, 7.5, 3.5$  Hz, 1 H), 1.24–1.13 (m, 4 H). LC–MS (method F)  $m/z$ : 416 [(M + H)<sup>+</sup>];  $R_t$ : 0.64 min; 99% purity.

**5-(5-(Cyclobutylamino)-1-((tetrahydro-2H-pyran-4-yl)methyl)-1H-benzod[*d*]imidazol-2-yl)-1,3-dimethylpyridin-2(1H)-one (23a).** A suspension of 5-(5-bromo-1-((tetrahydro-2H-pyran-4-yl)methyl)-1H-benzod[*d*]imidazol-2-yl)-1,3-dimethylpyridin-2(1H)-one **22a** (50 mg, 0.12 mmol), NaO<sup>t</sup>Bu (34.6 mg, 0.36 mmol), BrettPhos (6.5 mg, 0.01 mmol), and BrettPhos Pd G1 precatalyst (9.5 mg, 0.01 mmol) in 1,4-dioxane (1 mL) was prepared in a vial containing cyclobutylamine hydrochloride (15 mg, 0.14 mmol). A stirrer bar was added, and the vial was sealed, sonicated, and heated in a microwave at 110 °C for 30 min. The reaction was allowed to cool and loaded onto a 1 g C18 SPE cartridge (preconditioned with MeCN). The cartridge was flushed with MeCN (2 mL) and MeOH (2 mL), and the solvent was removed under a stream of nitrogen. The sample was dissolved in DMSO (1 mL) and purified by MDAP (method B). The solvent was removed using a plate dryer to give the title compound (5 mg, 0.01 mmol, 9% yield). <sup>1</sup>H NMR (600 MHz, DMSO-*d*<sub>6</sub>):  $\delta$  8.04 (s, 1 H), 7.69 (s, 1 H), 7.34 (d,  $J = 8.5$  Hz, 1 H), 6.61–6.57 (m, 2 H), 5.57 (d,  $J = 7.0$  Hz, 1 H), 4.14 (d,  $J = 7.5$  Hz, 2 H), 3.88–3.79 (m, 1 H), 3.71 (d,  $J = 11.5$  Hz, 2 H), 3.54 (s, 3 H), 3.10 (t,  $J = 11.5$  Hz, 2 H), 2.38–2.31 (m, 2 H), 2.09 (s, 3 H), 1.97–1.88 (m, 1 H), 1.86–1.77 (m, 2 H), 1.77–1.69 (m, 2 H), 1.20 (d,  $J = 11.5$  Hz, 2 H), 1.11 (q,  $J = 11.5$  Hz, 2 H); LC–MS (method F)  $m/z$ : 407 [(M + H)<sup>+</sup>];  $R_t$ : 0.61 min; 95% purity.

**5-(6-(Cyclobutylamino)-1-((tetrahydro-2H-pyran-4-yl)methyl)-1H-benzod[*d*]imidazol-2-yl)-1,3-dimethylpyridin-2(1H)-one (23b).** A suspension of 5-(6-bromo-1-((tetrahydro-2H-pyran-4-yl)methyl)-1H-benzod[*d*]imidazol-2-yl)-1,3-dimethylpyridin-2(1H)-one **22b** (50 mg, 0.12 mmol), NaO<sup>t</sup>Bu (23.1 mg, 0.24 mmol), BrettPhos (6.5 mg, 0.01 mmol), and BrettPhos Pd G1 precatalyst (9.6 mg, 0.012 mmol), in 1,4-dioxane (1 mL), was prepared in a vial containing cyclobutylamine hydrochloride (12.9 mg, 0.12 mmol). A stirrer bar was added, and the vial was sealed and heated in a microwave at 120 °C for 30 min. The reaction was allowed to cool and loaded onto a 1 g C18 SPE cartridge (preconditioned with MeCN). The cartridge was flushed with MeCN (2 mL) and MeOH (2 mL), and the solvent was removed under a stream of nitrogen. The sample was dissolved in DMSO (1 mL) and purified by MDAP (method B). The solvent was removed using a plate dryer to give the title compound (11 mg, 0.03 mmol, 20% yield). <sup>1</sup>H NMR (400 MHz, DMSO-*d*<sub>6</sub>):  $\delta$  8.00 (d,  $J = 2.5$  Hz, 1 H), 7.69–7.66 (m, 1 H), 7.29 (d,  $J = 8.5$  Hz, 1 H), 6.54–6.50 (m, 2 H), 5.77 (d,  $J = 7.0$  Hz, 1 H), 4.12 (d,  $J = 7.5$  Hz, 2 H), 3.98–3.87 (m, 1 H), 3.72 (d,  $J = 11.5$  Hz, 2 H), 3.57–3.52 (m, 3 H), 3.12 (td,  $J = 11.5, 3.0$  Hz, 2 H), 2.44–2.34 (m, 2 H), 2.09 (s, 3 H), 1.93 (d,  $J = 11.0$  Hz, 1 H), 1.87–1.69 (m, 4 H), 1.28–1.09 (m, 4 H); LC–MS (method F)  $m/z$ : 407 [(M + H)<sup>+</sup>];  $R_t$ : 0.61 min; 97% purity.

**1,3-Dimethyl-5-(5-(pyrrolidin-1-yl)-1-((tetrahydro-2H-pyran-4-yl)methyl)-1H-benzod[*d*]imidazol-2-yl)pyridin-2(1H)-one (23c).** 5-(5-Bromo-1-((tetrahydro-2H-pyran-4-yl)methyl)-1H-benzod[*d*]imidazol-2-yl)-1,3-dimethylpyridin-2(1H)-one **22a** (100 mg, 0.240 mmol), pyrrolidine (0.02 mL, 0.24 mmol), Pd<sub>2</sub>(dba)<sub>3</sub> (9 mg, 0.01 mmol),

JohnPhos (9 mg, 0.03 mmol), and NaO<sup>t</sup>Bu (23 mg, 0.24 mmol) were suspended in toluene (2 mL) within a sealed microwave vial. The reaction was heated in a microwave at 90 °C for 10 min. The reaction mixture was filtered over a Celite pad and washed with EtOAc (20 mL). The solvent was removed in vacuo, and the residue was dissolved in 1:1 DMSO/MeOH (0.6 mL) and purified by MDAP (method B). The solvent was evaporated in vacuo to give the title compound (29 mg, 0.07 mmol, 30% yield). <sup>1</sup>H NMR (400 MHz, CDCl<sub>3</sub>):  $\delta$  7.72 (d,  $J = 2.5$  Hz, 1 H), 7.52–7.49 (m, 1 H), 7.23 (d,  $J = 8.5$  Hz, 1 H), 6.90 (d,  $J = 2.0$  Hz, 1 H), 6.70 (dd,  $J = 8.5, 2.0$  Hz, 1 H), 4.08 (d,  $J = 7.5$  Hz, 2 H), 3.89 (dd,  $J = 11.5, 3.5$  Hz, 2 H), 3.65 (s, 3 H), 3.38–3.32 (m, 4 H), 3.24 (td,  $J = 11.5, 2.0$  Hz, 2 H), 2.25 (s, 3 H), 2.16–2.03 (m, 5 H), 1.40–1.20 (m, 4 H); LC–MS (method A)  $m/z$ : 407 [(M + H)<sup>+</sup>];  $R_t$ : 0.98 min; 97% purity.

**1,3-Dimethyl-5-(6-(pyrrolidin-1-yl)-1-((tetrahydro-2H-pyran-4-yl)methyl)-1H-benzod[*d*]imidazol-2-yl)pyridin-2(1H)-one (23d).** 5-(6-Bromo-1-((tetrahydro-2H-pyran-4-yl)methyl)-1H-benzod[*d*]imidazol-2-yl)-1,3-dimethylpyridin-2(1H)-one **22b** (100 mg, 0.24 mmol), pyrrolidine (0.02 mL, 0.24 mmol), Pd<sub>2</sub>(dba)<sub>3</sub> (8.8 mg, 0.01 mmol), JohnPhos (8.6 mg, 0.03 mmol), and NaO<sup>t</sup>Bu (23.1 mg, 0.24 mmol) were dissolved in toluene (2 mL). The reaction was heated in a microwave at 90 °C for 10 min. The reaction was heated in a microwave at 90 °C for a further 20 min. The cooled reaction mixture was filtered through Celite washing with EtOAc. The filtrate was concentrated, and the crude material was purified by loading onto a 12 g silica column and eluting using a graduating solvent system of 0–30% EtOH in EtOAc. The appropriate fractions were combined, concentrated, and purified by MDAP (method A). Concentration of the collected fractions gave the title compound as a tan solid (22 mg, 0.05 mmol, 23% yield). <sup>1</sup>H NMR (400 MHz, CDCl<sub>3</sub>):  $\delta$  8.00 (s, 1 H), 7.63 (d,  $J = 8.5$  Hz, 1 H), 7.43 (s, 1 H), 6.73 (d,  $J = 8.5$  Hz, 1 H), 6.34 (s, 1 H), 4.09 (d,  $J = 7.5$  Hz, 2 H), 3.92 (dd,  $J = 11.5, 3.5$  Hz, 2 H), 3.67 (s, 3 H), 3.41–3.34 (m, 4 H), 3.26 (t,  $J = 11.5$  Hz, 2 H), 2.25 (s, 3 H), 2.18–2.05 (m, 5 H), 1.42–1.22 (m, 4 H); LC–MS (method F)  $m/z$ : 407 [(M + H)<sup>+</sup>];  $R_t$ : 0.64 min; 100% purity.

**1,3-Dimethyl-5-(5-morpholino-1-((tetrahydro-2H-pyran-4-yl)methyl)-1H-benzod[*d*]imidazol-2-yl)pyridin-2(1H)-one (23e).** 5-(5-Bromo-1-((tetrahydro-2H-pyran-4-yl)methyl)-1H-benzod[*d*]imidazol-2-yl)-1,3-dimethylpyridin-2(1H)-one **22a** (100 mg, 0.24 mmol), morpholine (0.03 mL, 0.34 mmol), Pd<sub>2</sub>(dba)<sub>3</sub> (9 mg, 0.01 mmol), JohnPhos (9 mg, 0.03 mmol), and NaO<sup>t</sup>Bu (23 mg, 0.24 mmol) were suspended in toluene (2 mL) within a sealed microwave vial. The reaction mixture was heated in a microwave at 90 °C for 10 min. The reaction mixture was cooled to rt, filtered over a Celite pad, and washed with EtOAc (20 mL). The solvent was removed in vacuo, and the residue was dissolved in 1:1 DMSO/MeOH (0.6 mL) and purified by MDAP (method B). The solvent was evaporated in vacuo to give the title compound (56 mg, 0.13 mmol, 55% yield). <sup>1</sup>H NMR (400 MHz, CDCl<sub>3</sub>):  $\delta$  7.73 (d,  $J = 2.5$  Hz, 1 H), 7.51–7.48 (m, 1 H), 7.29 (d,  $J = 9.0$  Hz, 1 H), 7.27 (d,  $J = 2.5$  Hz, 1 H), 7.04 (dd,  $J = 9.0, 2.5$  Hz, 1 H), 4.10 (d,  $J = 7.5$  Hz, 2 H), 3.94–3.87 (m, 6 H), 3.66 (s, 3 H), 3.25 (td,  $J = 11.5, 2.0$  Hz, 2 H), 3.20–3.17 (m, 4 H), 2.25 (s, 3 H), 2.09 (t,  $J = 11.5, 7.5, 3.5$  Hz, 1 H), 1.39–1.22 (m, 4 H); LC–MS (method F)  $m/z$ : 423 [(M + H)<sup>+</sup>];  $R_t$ : 0.55 min; 100% purity.

**1,3-Dimethyl-5-(6-morpholino-1-((tetrahydro-2H-pyran-4-yl)methyl)-1H-benzod[*d*]imidazol-2-yl)pyridin-2(1H)-one (23f).** 5-(6-Bromo-1-((tetrahydro-2H-pyran-4-yl)methyl)-1H-benzod[*d*]imidazol-2-yl)-1,3-dimethylpyridin-2(1H)-one **22b** (100 mg, 0.24 mmol), morpholine (0.03 mL, 0.34 mmol), Pd<sub>2</sub>(dba)<sub>3</sub> (9 mg, 0.01 mmol), JohnPhos (9 mg, 0.03 mmol), and NaO<sup>t</sup>Bu (23 mg, 0.24 mmol) were suspended in toluene (2 mL) within a sealed microwave vial. The reaction mixture was heated in a microwave at 90 °C for 10 min. The reaction mixture was allowed to cool to rt, filtered over Celite, and washed with EtOAc (50 mL). The solvent was removed in vacuo, and the sample was dissolved in 1:1 DMSO/MeOH (0.6 mL) and purified by MDAP (method B). The solvent was evaporated in vacuo to give the title compound (29 mg, 0.07 mmol, 29% yield). <sup>1</sup>H NMR (400 MHz, CDCl<sub>3</sub>):  $\delta$  7.70 (d,  $J = 2.5$  Hz, 1 H), 7.65 (d,  $J = 8.5$  Hz, 1 H), 7.49–7.46 (m, 1 H), 7.02 (dd,  $J = 8.5, 2.0$  Hz, 1 H), 6.80 (d,  $J = 2.0$  Hz, 1 H), 4.09 (d,  $J = 7.5$  Hz, 2 H), 3.96–3.88 (m, 6 H), 3.65 (s, 3

H), 3.30–3.20 (m, 6 H), 2.25 (s, 3 H), 2.07 (ttt,  $J = 11.5, 7.5, 3.5$  Hz, 1 H), 1.40–1.23 (m, 4 H); LC–MS (method A)  $m/z$ : 423 [(M + H)<sup>+</sup>];  $R_t$ : 0.76 min; 100% purity.

2-((2-(1,5-Dimethyl-6-oxo-1,6-dihydropyridin-3-yl)-1-((tetrahydro-2H-pyran-4-yl)methyl)-1H-benzo[d]imidazol-5-yl)amino)-N,N-dimethylacetamide (**23g**). 5-(5-Bromo-1-((tetrahydro-2H-pyran-4-yl)methyl)-1H-benzo[d]imidazol-2-yl)-1,3-dimethylpyridin-2(1H)-one **22a** (50 mg, 0.12 mmol), NaO<sup>t</sup>Bu (23.1 mg, 0.24 mmol), BrettPhos (8.3 mg, 0.02 mmol), and BrettPhos Pd G1 precatalyst (4.8 mg, 0.006 mmol) were added to 2-amino-N,N-dimethylacetamide acetate (19 mg, 0.12 mmol) and suspended in 1,4-dioxane (1.5 mL). DIPEA (0.02 mL) was added to the mixture, and the reaction vessel was sealed and heated in a microwave at 110 °C for 30 min. After cooling the reaction to rt, the reaction mixture was loaded onto a 1 g C18 SPE cartridge (preconditioned with MeCN [3 mL]). The cartridge was flushed with MeCN (3 mL), and the solvent was removed under a stream of nitrogen. The sample was dissolved in DMSO (1 mL) and purified by MDAP (method B). The solvent was dried under a stream of nitrogen to give the title compound (25 mg, 0.06 mmol, 43% yield). <sup>1</sup>H NMR (600 MHz, DMSO-*d*<sub>6</sub>): δ 8.05 (s, 1 H), 7.69 (s, 1 H), 7.37 (d,  $J = 8.5$  Hz, 1 H), 6.77–6.73 (m, 2 H), 5.30 (t,  $J = 5.0$  Hz, 1 H), 4.16 (d,  $J = 7.5$  Hz, 2 H), 3.89 (d,  $J = 5.0$  Hz, 2 H), 3.71 (dd,  $J = 11.5, 3.5$  Hz, 2 H), 3.54 (s, 3 H), 3.11 (t,  $J = 11.5$  Hz, 2 H), 3.05 (s, 3 H), 2.89 (s, 3 H), 2.09 (s, 3 H), 1.93 (ttt,  $J = 11.5, 7.5, 3.5$  Hz, 1 H), 1.20 (dd,  $J = 11.5, 3.5$  Hz, 2 H), 1.12 (qd,  $J = 11.5, 3.5$  Hz, 2 H); LC–MS (method F)  $m/z$ : 438 [(M + H)<sup>+</sup>];  $R_t$ : 0.48 min; 95% purity.

2-((2-(1,5-Dimethyl-6-oxo-1,6-dihydropyridin-3-yl)-1-((tetrahydro-2H-pyran-4-yl)methyl)-1H-benzo[d]imidazol-6-yl)amino)-N,N-dimethylacetamide (**23h**). 5-(6-Bromo-1-((tetrahydro-2H-pyran-4-yl)methyl)-1H-benzo[d]imidazol-2-yl)-1,3-dimethylpyridin-2(1H)-one **22b** (50 mg, 0.12 mmol), BrettPhos (8.3 mg, 0.02 mmol), BrettPhos Pd G1 precatalyst (4.8 mg, 0.006 mmol), and NaO<sup>t</sup>Bu (23.1 mg, 0.24 mmol) were added to 2-amino-N,N-dimethylacetamide acetate (19 mg, 0.12 mmol) suspended in 1,4-dioxane (1.5 mL). The reaction vessel was sealed and heated in a microwave at 110 °C for 30 min. After cooling the reaction to rt, BrettPhos (8.3 mg, 0.02 mmol) and BrettPhos Pd G1 precatalyst (4.8 mg, 0.006 mmol) were added. The reaction vessel was sealed and heated in a microwave at 110 °C for 30 min. After cooling the reaction to rt, the reaction mixture was loaded onto a 1 g C18 SPE cartridge (preconditioned with MeCN [3 mL]). The cartridge was flushed with MeCN (3 mL), and the solvent was removed under a stream of nitrogen. The sample was dissolved in DMSO (1 mL) and purified by MDAP (method B). The solvent was evaporated under a stream of nitrogen to give the title compound (12 mg, 0.03 mmol, 21% yield). <sup>1</sup>H NMR (600 MHz, DMSO-*d*<sub>6</sub>): δ 8.03 (s, 1 H), 7.69 (s, 1 H), 7.32 (d,  $J = 8.5$  Hz, 1 H), 6.74 (s, 1 H), 6.68 (d,  $J = 8.5$  Hz, 1 H), 5.47 (t,  $J = 5.0$  Hz, 1 H), 4.14 (d,  $J = 7.5$  Hz, 2 H), 3.94 (d,  $J = 5.0$  Hz, 2 H), 3.73 (dd,  $J = 11.5, 3.5$  Hz, 2 H), 3.54 (s, 3 H), 3.12 (t,  $J = 11.5$  Hz, 2 H), 3.07 (s, 3 H), 2.89 (s, 3 H), 2.09 (s, 3 H), 1.94 (ttt,  $J = 11.5, 7.5, 3.5$  Hz, 1 H), 1.23 (dd,  $J = 11.5, 3.5$  Hz, 2 H), 1.16 (qd,  $J = 11.5, 3.5$  Hz, 2 H); LC–MS (method F)  $m/z$ : 438 [(M + H)<sup>+</sup>];  $R_t$ : 0.48 min; 100% purity.

1,3-Dimethyl-5-(5-(4-methyl-1,4-diazepan-1-yl)-1-((tetrahydro-2H-pyran-4-yl)methyl)-1H-benzo[d]imidazole-2-yl)pyridin-2(1H)-one (**23i**). 5-(5-Bromo-1-((tetrahydro-2H-pyran-4-yl)methyl)-1H-benzo[d]imidazole-2-yl)-1,3-dimethylpyridin-2(1H)-one **22a** (50 mg, 0.12 mmol), NaO<sup>t</sup>Bu (23.1 mg, 0.24 mmol), and RuPhos Pd G2 precatalyst (2.4 mg, 0.003 mmol) were added to 1-methyl-1,4-diazepan (14 mg, 0.12 mmol) in 1,4-dioxane. The reaction vessel was sealed and heated in a microwave at 110 °C for 30 min. After cooling the reaction to rt, the RuPhos Pd G2 precatalyst (2.4 mg, 0.003 mmol) was added to the reaction mixture. The reaction vessel was sealed and heated in a microwave at 110 °C for 30 min. After cooling the reaction to rt, the reaction mixture was loaded onto a 1 g C18 SPE cartridge (preconditioned with MeCN [3 mL]). The cartridge was flushed with MeCN (3 mL), and the solvent was removed under a stream of nitrogen. The sample was dissolved in DMSO (1 mL) and purified by MDAP (method B). The solvent was evaporated under a stream of nitrogen to give the title compound (13 mg, 0.03 mmol,

22% yield). <sup>1</sup>H NMR (600 MHz, DMSO-*d*<sub>6</sub>): δ 8.05 (s, 1 H), 7.70 (s, 1 H), 7.42 (d,  $J = 8.5$  Hz, 1 H), 6.80 (d,  $J = 2.0$  Hz, 1 H), 6.76 (dd,  $J = 8.5, 2.0$  Hz, 1 H), 4.16 (d,  $J = 7.5$  Hz, 2 H), 3.72 (dd,  $J = 11.5, 3.5$  Hz, 2 H), 3.55 (s, 3 H), 3.54–3.51 (m, 2 H), 3.45 (t,  $J = 6.0$  Hz, 2 H), 3.11 (t,  $J = 11.5$  Hz, 2 H), 2.66–2.62 (m, 2 H), 2.48–2.45 (m, 2 H), 2.26 (s, 3 H), 2.09 (s, 3 H), 1.99–1.89 (m, 3 H), 1.22 (dd,  $J = 11.5, 3.5$  Hz, 2 H), 1.13 (qd,  $J = 11.5, 3.5$  Hz, 2 H); LC–MS (method F)  $m/z$ : 450 [(M + H)<sup>+</sup>];  $R_t$ : 0.35 min; 95% purity.

1,3-Dimethyl-5-(6-(4-methyl-1,4-diazepan-1-yl)-1-((tetrahydro-2H-pyran-4-yl)methyl)-1H-benzo[d]imidazol-2-yl)pyridin-2(1H)-one (**23j**). 1-Methyl-1,4-diazepan (14 mg, 0.120 mmol) was dissolved in 1,4-dioxane (1.5 mL) and added to 5-(6-bromo-1-((tetrahydro-2H-pyran-4-yl)methyl)-1H-benzo[d]imidazol-2-yl)-1,3-dimethylpyridin-2(1H)-one **22b** (50 mg, 0.12 mmol), JohnPhos (4.6 mg, 0.02 mmol), NaO<sup>t</sup>Bu (23.1 mg, 0.24 mmol), and Pd<sub>2</sub>(dba)<sub>3</sub> (4.5 mg, 0.005 mmol). The reaction vessel was sealed and heated in a microwave at 110 °C for 20 min. After cooling the reaction to rt, the reaction mixture was loaded onto a 1 g C18 SPE cartridge (preconditioned with MeCN [3 mL]). The cartridge was flushed with MeCN (3 mL), and the solvent was removed under a stream of nitrogen. The sample was dissolved in DMSO (1 mL) and purified by MDAP (method B). The solvent was evaporated under a stream of nitrogen to give the title compound (26 mg, 0.06 mmol, 43% yield). <sup>1</sup>H NMR (600 MHz, DMSO-*d*<sub>6</sub>): δ 8.04 (s, 1 H), 7.69 (s, 1 H), 7.39 (d,  $J = 8.5$  Hz, 1 H), 6.78 (d,  $J = 2.0$  Hz, 1 H), 6.72 (dd,  $J = 8.5, 2.0$  Hz, 1 H), 4.19 (d,  $J = 7.5$  Hz, 2 H), 3.72 (dd,  $J = 11.5, 3.5$  Hz, 2 H), 3.66–3.62 (m, 2 H), 3.54 (s, 3 H), 3.51 (t,  $J = 6.0$  Hz, 2 H), 3.10 (t,  $J = 11.5$  Hz, 2 H), 2.89–2.81 (m, 2 H), 2.71–2.65 (m, 2 H), 2.42 (s, 3 H), 2.09 (s, 3 H), 2.05–1.98 (m, 2 H), 1.91 (ttt,  $J = 11.5, 7.5, 3.5$  Hz, 1 H), 1.21 (dd,  $J = 11.5, 3.5$  Hz, 2 H), 1.16 (qd,  $J = 11.5, 3.5$  Hz, 2 H); LC–MS (method F)  $m/z$ : 450 [(M + H)<sup>+</sup>];  $R_t$ : 0.35 min; 98% purity.

1-(2-(1,5-Dimethyl-6-oxo-1,6-dihydropyridin-3-yl)-1-((tetrahydro-2H-pyran-4-yl)methyl)-1H-benzo[d]imidazol-5-yl)-N-methylpiperidine-4-carboxamide (**23k**). A stock solution of 5-(5-bromo-1-((tetrahydro-2H-pyran-4-yl)methyl)-1H-benzo[d]imidazol-2-yl)-1,3-dimethylpyridin-2(1H)-one **22a** (300 mg, 0.12 mmol) was prepared in 1,4-dioxane (3 mL), and 0.5 mL aliquoted into a vial containing N-methylpiperidine-4-carboxamide (20 mg, 0.14 mmol). To the vial was added 1,4-dioxane (0.5 mL) along with NaO<sup>t</sup>Bu (34.6 mg, 0.36 mmol) and RuPhos Pd G2 precatalyst (18.7 mg, 0.024 mmol). A stirrer bar was added, and the vial was sonicated and capped before heating in a microwave at 110 °C for 30 min. The reaction mixture was allowed to cool and then loaded onto a 1 g C18 SPE cartridge (preconditioned with MeCN). The cartridge was flushed with MeCN (2 mL) and MeOH (2 mL), and the solvent was removed under a stream of nitrogen. The sample was dissolved in DMSO (1 mL) and purified by MDAP (method B). The solvent was removed using a plate dryer to give the title compound (15 mg, 0.03 mmol, 24% yield). <sup>1</sup>H NMR (600 MHz, DMSO-*d*<sub>6</sub>): δ 8.07 (d,  $J = 2.5$  Hz, 1 H), 7.74 (q,  $J = 4.5$  Hz, 1 H), 7.71–7.69 (m, 1 H), 7.50 (d,  $J = 8.5$  Hz, 1 H), 7.07 (d,  $J = 2.0$  Hz, 1 H), 7.01 (dd,  $J = 8.5, 2.0$  Hz, 1 H), 4.20 (d,  $J = 7.5$  Hz, 2 H), 3.71 (dd,  $J = 11.5, 3.5$  Hz, 2 H), 3.61 (d,  $J = 12.0$  Hz, 2 H), 3.55 (s, 3 H), 3.11 (t,  $J = 11.5$  Hz, 2 H), 2.63 (td,  $J = 12.0, 3.5$  Hz, 2 H), 2.58 (d,  $J = 4.5$  Hz, 3 H), 2.21 (tt,  $J = 11.5, 4.0$  Hz, 1 H), 2.10 (s, 3 H), 1.93 (ttt,  $J = 11.5, 7.5, 3.5$  Hz, 1 H), 1.81–1.68 (m, 4 H), 1.21 (dd,  $J = 11.5, 3.5$  Hz, 2 H), 1.13 (qd,  $J = 11.5, 3.5$  Hz, 2 H); LC–MS (method F)  $m/z$ : 478 [(M + H)<sup>+</sup>];  $R_t$ : 0.47 min; 100% purity.

1-(2-(1,5-Dimethyl-6-oxo-1,6-dihydropyridin-3-yl)-1-((tetrahydro-2H-pyran-4-yl)methyl)-1H-benzo[d]imidazol-6-yl)-N-methylpiperidine-4-carboxamide (**23l**). To a vial containing N-methylpiperidine-4-carboxamide (20 mg, 0.14 mmol) was added 1.0 mL of a stock solution of 5-(6-bromo-1-((tetrahydro-2H-pyran-4-yl)methyl)-1H-benzo[d]imidazol-2-yl)-1,3-dimethylpyridin-2(1H)-one **22b** (150 mg, 0.12 mmol) in 1,4-dioxane (3 mL). Pd<sub>2</sub>(dba)<sub>3</sub> (11 mg, 0.01 mmol), NaO<sup>t</sup>Bu (34.6 mg, 0.36 mmol), JohnPhos (7.2 mg, 0.02 mmol), and a stirrer bar were added to the vial, which was sealed, sonicated, and heated in a microwave at 90 °C for 20 min. The reaction mixture was allowed to cool and then loaded onto a 1 g C18 SPE cartridge (preconditioned with MeCN). The cartridge was

flushed with MeCN (2 mL) and MeOH (2 mL), and the solvent was removed under a stream of nitrogen. The sample was dissolved in DMSO (1 mL) and purified by MDAP (method B). The solvent was removed using a plate dryer to give the title compound (18 mg, 0.04 mmol, 28% yield). <sup>1</sup>H NMR (600 MHz, DMSO-*d*<sub>6</sub>): δ 8.06 (d, *J* = 2.5 Hz, 1 H), 7.75–7.68 (m, 2 H), 7.42 (d, *J* = 8.5 Hz, 1 H), 7.10 (d, *J* = 2.0 Hz, 1 H), 6.93 (dd, *J* = 8.5, 2.0 Hz, 1 H), 4.22 (d, *J* = 7.5 Hz, 2 H), 3.75–3.68 (m, 4 H), 3.55 (s, 3 H), 3.11 (td, *J* = 11.5, 2.0 Hz, 2 H), 2.69 (td, *J* = 11.5, 3.5 Hz, 3 H), 2.59 (d, *J* = 4.5 Hz, 4 H), 2.24 (tt, *J* = 11.5, 4.0 Hz, 1 H), 2.10 (s, 3 H), 1.98–1.85 (m, 1 H), 1.85–1.67 (m, 4 H), 1.26–1.10 (m, 5 H); LC–MS (method F) *m/z*: 478 [(M + H)<sup>+</sup>]; *R*<sub>t</sub>: 0.44 min; 100% purity.

**1,3-Dimethyl-5-(5-(4-(methylamino)piperidin-1-yl)-1-((tetrahydro-2H-pyran-4-yl)methyl)-1H-benzo[d]imidazol-2-yl)pyridin-2(1H)-one (23m).** 5-(5-Bromo-1-((tetrahydro-2H-pyran-4-yl)methyl)-1H-benzo[d]imidazol-2-yl)-1,3-dimethylpyridin-2(1H)-one **22a** (50 mg, 0.12 mmol), NaO<sup>t</sup>Bu (23.1 mg, 0.240 mmol), and RuPhos Pd G2 precatalyst (2.4 mg, 0.003 mmol) were added to *tert*-butyl methyl(piperidin-4-yl)carbamate (26 mg, 0.12 mmol) in 1,4-dioxane (1.5 mL). The reaction vessel was sealed and heated in a microwave at 110 °C for 30 min. After cooling the reaction to rt, the RuPhos Pd G2 precatalyst (2.4 mg, 0.003 mmol) was added. The reaction vessel was sealed and heated in a microwave at 110 °C for 30 min. After cooling the reaction to rt, the reaction mixture was loaded onto a 1 g C18 SPE cartridge (preconditioned with MeCN [3 mL]). The cartridge was flushed with MeCN (3 mL), and the solvent was removed under a stream of nitrogen. HCl (4 M) in dioxane (0.5 mL) was added to the sample, and the reaction was left overnight. The solvent was removed under a stream of nitrogen. The sample was dissolved in DMSO (1 mL) and purified by MDAP (method B). The solvent was dried under a stream of nitrogen to give the title compound (12 mg, 0.03 mmol, 20% yield). <sup>1</sup>H NMR (600 MHz, DMSO-*d*<sub>6</sub>): δ 8.07 (s, 1 H), 7.70 (s, 1 H), 7.49 (d, *J* = 9.0 Hz, 1 H), 7.07 (d, *J* = 2.0 Hz, 1 H), 7.00 (dd, *J* = 9.0, 2.0 Hz, 1 H), 4.20 (d, *J* = 7.5 Hz, 2 H), 3.71 (dd, *J* = 11.5, 3.5 Hz, 2 H), 3.57–3.51 (m, 5 H), 3.11 (t, *J* = 11.5 Hz, 2 H), 2.70 (t, *J* = 12.0 Hz, 2 H), 2.47–2.40 (m, 1 H), 2.32 (s, 3 H), 2.09 (s, 3 H), 1.98–1.88 (m, 3 H), 1.44–1.36 (m, 2 H), 1.21 (d, *J* = 11.5 Hz, 2 H), 1.13 (qd, *J* = 11.5, 3.5 Hz, 2 H); LC–MS (method A) *m/z*: 450 [(M + H)<sup>+</sup>]; *R*<sub>t</sub>: 0.74 min; 96% purity.

**1,3-Dimethyl-5-(6-(4-(methylamino)piperidin-1-yl)-1-((tetrahydro-2H-pyran-4-yl)methyl)-1H-benzo[d]imidazol-2-yl)pyridin-2(1H)-one (23n).** *tert*-Butyl methyl(piperidin-4-yl)carbamate (26 mg, 0.12 mmol) was dissolved in 1,4-dioxane (1.5 mL) and added to 5-(6-bromo-1-((tetrahydro-2H-pyran-4-yl)methyl)-1H-benzo[d]imidazol-2-yl)-1,3-dimethylpyridin-2(1H)-one **22b** (50 mg, 0.12 mmol), JohnPhos (4.6 mg, 0.02 mmol), NaO<sup>t</sup>Bu (23.1 mg, 0.24 mmol), and Pd<sub>2</sub>(dba)<sub>3</sub> (4.5 mg, 0.005 mmol). The reaction vessel was sealed and heated in a microwave at 110 °C for 30 min. After cooling the reaction to rt, the reaction mixture was loaded onto a 1 g C18 SPE cartridge (preconditioned with MeCN [3 mL]). The cartridge was flushed with MeCN (3 mL), and the solvent was removed under a stream of nitrogen. HCl (4 M) in dioxane (0.5 mL) was added to the sample, and the reaction was left for 1 h. The solvent was removed under a stream of nitrogen. The sample was dissolved in DMSO (1 mL) and purified by MDAP (method B). The solvent was dried under a stream of nitrogen to give the title compound (13 mg, 0.03 mmol, 21% yield). <sup>1</sup>H NMR (600 MHz, DMSO-*d*<sub>6</sub>): δ 8.05 (s, 1 H), 7.70 (s, 1 H), 7.41 (d, *J* = 9.0 Hz, 1 H), 7.08 (s, 1 H), 6.92 (d, *J* = 9.0 Hz, 1 H), 4.21 (d, *J* = 7.5 Hz, 2 H), 3.71 (dd, *J* = 11.5, 3.5 Hz, 2 H), 3.61 (d, *J* = 12.0 Hz, 2 H), 3.54 (s, 3 H), 3.11 (t, *J* = 11.5 Hz, 2 H), 2.76 (t, *J* = 12.0 Hz, 2 H), 2.44–2.38 (m, 1 H), 2.30 (s, 3 H), 2.09 (s, 3 H), 1.95–1.88 (m, 3 H), 1.43–1.34 (m, 2 H), 1.21 (d, *J* = 11.5 Hz, 2 H), 1.15 (qd, *J* = 11.5, 3.5 Hz, 2 H); LC–MS (method F) *m/z*: 450 [(M + H)<sup>+</sup>]; *R*<sub>t</sub>: 0.35 min; 98% purity.

**1,3-Dimethyl-5-(5-(3-(methylsulfonyl)pyrrolidin-1-yl)-1-((tetrahydro-2H-pyran-4-yl)methyl)-1H-benzo[d]imidazol-2-yl)pyridin-2(1H)-one (23o).** A stock solution of 5-(5-bromo-1-((tetrahydro-2H-pyran-4-yl)methyl)-1H-benzo[d]imidazol-2-yl)-1,3-dimethylpyridin-2(1H)-one **22a** (250 mg, 0.12 mmol) was prepared in 1,4-dioxane (4 mL), and an aliquot (0.8 mL) was added to a vial containing 3-

(methylsulfonyl)pyrrolidine (21 mg, 0.14 mmol). To the vial was added further 1,4-dioxane (0.4 mL) along with the RuPhos Pd G2 precatalyst (18.7 mg, 0.02 mmol) and NaO<sup>t</sup>Bu (34.6 mg, 0.36 mmol). A stirrer bar was added, and the vial was sonicated and capped before heating in a microwave at 110 °C for 30 min. The reaction mixture was allowed to cool and then loaded onto a 1 g C18 SPE cartridge (preconditioned with MeCN). The cartridge was flushed with MeCN (2 mL) and MeOH (2 mL), and the solvent was removed under a stream of nitrogen. The sample was dissolved in DMSO (1 mL) and purified by MDAP (method B). The solvent was removed using a plate dryer to give the title compound (21 mg, 0.04 mmol, 32% yield). <sup>1</sup>H NMR (600 MHz, DMSO-*d*<sub>6</sub>): δ 8.08 (s, 1 H), 7.71 (s, 1 H), 7.51 (d, *J* = 8.5 Hz, 1 H), 6.79 (s, 1 H), 6.73 (d, *J* = 8.5 Hz, 1 H), 4.20 (d, *J* = 7.5 Hz, 2 H), 4.10 (quin, *J* = 7.0 Hz, 1 H), 3.71 (dd, *J* = 11.5, 3.5 Hz, 2 H), 3.65–3.60 (m, 2 H), 3.55 (s, 3 H), 3.47–3.40 (m, 2 H), 3.10 (t, *J* = 11.5 Hz, 2 H), 3.06 (s, 3 H), 2.42–2.37 (m, 1 H), 2.10 (s, 3 H), 1.98–1.89 (m, 1 H), 1.19 (dd, *J* = 11.5, 3.5 Hz, 2 H), 1.13 (qd, *J* = 11.5, 3.5 Hz, 2 H); LC–MS (method F) *m/z*: 485 [(M + H)<sup>+</sup>]; *R*<sub>t</sub>: 0.52 min; 100% purity.

**1,3-Dimethyl-5-(6-(3-(methylsulfonyl)pyrrolidin-1-yl)-1-((tetrahydro-2H-pyran-4-yl)methyl)-1H-benzo[d]imidazol-2-yl)pyridin-2(1H)-one (23p).** A stock solution of 5-(6-bromo-1-((tetrahydro-2H-pyran-4-yl)methyl)-1H-benzo[d]imidazol-2-yl)-1,3-dimethylpyridin-2(1H)-one **22b** (500 mg, 0.12 mmol) was prepared in 1,4-dioxane (5 mL), and an aliquot (0.5 mL) was added to a vial containing 3-(methylsulfonyl)pyrrolidine (18 mg, 0.12 mmol). To the vial was added further 1,4-dioxane (0.5 mL) along with JohnPhos (7.2 mg, 0.02 mmol), NaO<sup>t</sup>Bu (34.6 mg, 0.36 mmol), and Pd<sub>2</sub>(dba)<sub>3</sub> (11.0 mg, 0.01 mmol). A stirrer bar was added, and the vial was sonicated and capped before heating in a microwave at 90 °C for 20 min. The reaction mixture was allowed to cool and then loaded onto a 1 g C18 SPE cartridge (preconditioned with MeCN). The cartridge was flushed with MeCN (2 mL) and MeOH (2 mL), and the solvent was removed under a stream of nitrogen. The sample was purified by MDAP (method B). The solvent was removed using a plate dryer to give the title compound (9 mg, 0.02 mmol, 14% yield). <sup>1</sup>H NMR (600 MHz, DMSO-*d*<sub>6</sub>): δ 8.06 (s, 1 H), 7.71 (s, 1 H), 7.44 (d, *J* = 8.5 Hz, 1 H), 6.77 (s, 1 H), 6.64 (d, *J* = 8.5 Hz, 1 H), 4.22 (d, *J* = 7.5 Hz, 2 H), 4.14 (quin, *J* = 7.0 Hz, 1 H), 3.72 (d, *J* = 11.5 Hz, 2 H), 3.68–3.62 (m, 2 H), 3.55 (s, 3 H), 3.53–3.47 (m, 2 H), 3.11 (t, *J* = 11.5 Hz, 2 H), 3.08 (s, 3 H), 2.44–2.37 (m, 2 H), 2.09 (s, 3 H), 1.98–1.88 (m, 1 H), 1.27–1.10 (m, 4 H); LC–MS (method F) *m/z*: 485 [(M + H)<sup>+</sup>]; *R*<sub>t</sub>: 0.49 min; 99% purity.

**5-(5-(1,1-Dioxidothiomorpholino)-1-((tetrahydro-2H-pyran-4-yl)methyl)-1H-benzo[d]imidazol-2-yl)-1,3-dimethylpyridin-2(1H)-one (23q).** 5-(5-Bromo-1-((tetrahydro-2H-pyran-4-yl)methyl)-1H-benzo[d]imidazol-2-yl)-1,3-dimethylpyridin-2(1H)-one **22a** (100 mg, 0.24 mmol), thiomorpholine 1,1-dioxide (39 mg, 0.29 mmol), Pd<sub>2</sub>(dba)<sub>3</sub> (9 mg, 0.01 mmol), JohnPhos (9 mg, 0.03 mmol), and NaO<sup>t</sup>Bu (23 mg, 0.24 mmol) were suspended in toluene (2 mL) within a sealed microwave vial. The reaction mixture was heated in a microwave at 90 °C for 10 min. The reaction mixture was cooled to rt, filtered over Celite, and washed with EtOAc (50 mL). The solvent was removed in vacuo, and the sample was dissolved in 1:1 DMSO/MeOH (0.6 mL) and purified by MDAP (method B). The solvent was evaporated in vacuo to give the title compound (5 mg, 0.01 mmol, 4% yield). <sup>1</sup>H NMR (400 MHz, CDCl<sub>3</sub>): δ 7.73 (d, *J* = 2.5 Hz, 1 H), 7.50–7.47 (m, 1 H), 7.33–7.29 (m, 2 H), 7.01 (dd, *J* = 8.5, 2.0 Hz, 1 H), 4.11 (d, *J* = 7.5 Hz, 2 H), 3.91 (dd, *J* = 11.5, 3.5 Hz, 2 H), 3.85–3.79 (m, 4 H), 3.66 (s, 3 H), 3.26 (td, *J* = 11.5, 2.0 Hz, 2 H), 3.22–3.17 (m, 4 H), 2.25 (s, 3 H), 2.08 (tt, *J* = 11.5, 7.5, 3.5 Hz, 1 H), 1.39–1.23 (m, 4 H); LC–MS (method A) *m/z*: 471 [(M + H)<sup>+</sup>]; *R*<sub>t</sub>: 0.73 min; 100% purity.

**5-(6-(1,1-Dioxidothiomorpholino)-1-((tetrahydro-2H-pyran-4-yl)methyl)-1H-benzo[d]imidazol-2-yl)-1,3-dimethylpyridin-2(1H)-one (23r).** 5-(6-Bromo-1-((tetrahydro-2H-pyran-4-yl)methyl)-1H-benzo[d]imidazol-2-yl)-1,3-dimethylpyridin-2(1H)-one **22b** (100 mg, 0.24 mmol), thiomorpholine 1,1-dioxide (32.5 mg, 0.24 mmol), NaO<sup>t</sup>Bu (23.1 mg, 0.24 mmol), JohnPhos (9.2 mg, 0.03 mmol), and Pd<sub>2</sub>(dba)<sub>3</sub> (9.0 mg, 0.01 mmol) were suspended in 1,4-dioxane (2

mL). The reaction vessel was sealed and heated in a microwave at 90 °C for 20 min. After cooling the reaction to rt, further NaO<sup>t</sup>Bu (23.1 mg, 0.24 mmol), JohnPhos (9.2 mg, 0.03 mmol), and Pd<sub>2</sub>(dba)<sub>3</sub> (9.0 mg, 0.01 mmol) were added to the reaction vessel. The reaction vessel was sealed and heated in a microwave at 90 °C for 20 min. After cooling the reaction to rt, the reaction mixture was loaded onto a 1 g C18 SPE cartridge (preconditioned with MeCN [3 mL]). The cartridge was flushed with MeCN (3 mL), and the solvent was removed under a stream of nitrogen. The sample was dissolved in DMSO (1 mL) and purified by MDAP (method B). The solvent was dried under a stream of nitrogen to give the title compound (16 mg, 0.03 mmol, 14% yield). <sup>1</sup>H NMR (400 MHz, DMSO-*d*<sub>6</sub>): δ 8.07 (d, *J* = 2.5 Hz, 1 H), 7.72–7.70 (m, 1 H), 7.48 (d, *J* = 8.5 Hz, 1 H), 7.26 (d, *J* = 2.0 Hz, 1 H), 6.99 (dd, *J* = 8.5, 2.0 Hz, 1 H), 4.24 (d, *J* = 7.5 Hz, 2 H), 3.81–3.75 (m, 4 H), 3.72 (dd, *J* = 11.5, 3.5 Hz, 2 H), 3.55 (s, 3 H), 3.23–3.18 (m, 4 H), 3.12 (td, *J* = 11.5, 2.0 Hz, 2 H), 2.10 (s, 3 H), 1.99–1.86 (m, 1 H), 1.27–1.10 (m, 3 H); LC–MS (method F) *m/z*: 471 [(M + H)<sup>+</sup>]; R<sub>t</sub>: 0.52 min; 98% purity.

**5-(5-(3-Hydroxypyrrolidin-1-yl)-1-((tetrahydro-2H-pyran-4-yl)methyl)-1H-benzo[d]imidazol-2-yl)-1,3-dimethylpyridin-2(1H)-one (23s).** Into a vial were added 5-(5-bromo-1-((tetrahydro-2H-pyran-4-yl)methyl)-1H-benzo[d]imidazol-2-yl)-1,3-dimethylpyridin-2(1H)-one **22a** (62 mg, 0.15 mmol), pyrrolidin-3-ol (20 mg, 0.23 mmol), RuPhos Pd G1 precatalyst (12 mg, 0.02 mmol), RuPhos (7.0 mg, 0.02 mmol), and LiHMDS (1 M in THF, 0.36 mL, 0.36 mmol) in 2-MeTHF (0.6 mL). A stirrer bar was added to the vial which was capped and stirred at 65 °C for 4 h. Pyrrolidin-3-ol (20 mg, 0.23 mmol), RuPhos Pd G1 precatalyst (12 mg, 0.02 mmol), RuPhos (7.0 mg, 0.02 mmol), and LiHMDS (1 M in THF, 0.36 mL, 0.36 mmol) were added, and the reaction was heated at 65 °C for 1 h. The sample was purified by MDAP (method B). The solvent was dried under a stream of nitrogen to give the title compound (4.9 mg, 0.01 mmol, 7% yield). <sup>1</sup>H NMR (400 MHz, DMSO-*d*<sub>6</sub>): δ 8.06 (d, *J* = 2.5 Hz, 1 H), 7.72–7.69 (m, 1 H), 7.45 (d, *J* = 8.5 Hz, 1 H), 6.63 (d, *J* = 2.0 Hz, 1 H), 6.60 (dd, *J* = 8.5, 2.0 Hz, 1 H), 4.92–4.89 (m, 1 H), 4.45–4.39 (m, 1 H), 4.18 (d, *J* = 7.5 Hz, 2 H), 3.71 (d, *J* = 11.5 Hz, 2 H), 3.55 (s, 3 H), 3.46 (dd, *J* = 10.0, 5.0 Hz, 1 H), 3.40–3.31 (m, 2 H), 3.41–3.05 (m, 3 H), 2.12–2.03 (m, 4 H), 2.00–1.85 (m, 2 H), 1.26–1.07 (m, 4 H); LC–MS (method F) *m/z*: 423 [(M + H)<sup>+</sup>]; R<sub>t</sub>: 0.51 min; 100% purity.

**5-(6-(3-Hydroxypyrrolidin-1-yl)-1-((tetrahydro-2H-pyran-4-yl)methyl)-1H-benzo[d]imidazol-2-yl)-1,3-dimethylpyridin-2(1H)-one (23t).** In a vial, a suspension of 5-(6-bromo-1-((tetrahydro-2H-pyran-4-yl)methyl)-1H-benzo[d]imidazol-2-yl)-1,3-dimethylpyridin-2(1H)-one **22b** (50 mg, 0.12 mmol), pyrrolidin-3-ol (17 mg, 0.20 mmol), NaO<sup>t</sup>Bu (25 mg, 0.26 mmol), Pd<sub>2</sub>(dba)<sub>3</sub> (11 mg, 0.01 mmol), and JohnPhos (8 mg, 0.03 mmol) in 1,4-dioxane (1 mL) was prepared. The vial was sealed and heated in a microwave at 90 °C for 20 min. The reaction mixture was allowed to cool and then loaded onto a 1 g C18 SPE cartridge (preconditioned with MeCN [2 mL]). The cartridge was flushed with MeCN (2 mL) and MeOH (2 mL). The washes were combined, and the solvent was removed under a stream of nitrogen. The sample was dissolved in DMSO (1 mL) and purified by MDAP (method B). The solvent was removed using a plate dryer to give the title compound (23 mg, 0.06 mmol, 46% yield). <sup>1</sup>H NMR (400 MHz, DMSO-*d*<sub>6</sub>): δ 8.04 (d, *J* = 2.5 Hz, 1 H), 7.71–7.69 (m, 1 H), 7.39 (d, *J* = 8.5 Hz, 1 H), 6.57 (d, *J* = 2.0 Hz, 1 H), 6.53 (dd, *J* = 8.5, 2.0 Hz, 1 H), 4.94 (d, *J* = 5.0 Hz, 1 H), 4.47–4.41 (m, 1 H), 4.18 (d, *J* = 7.5 Hz, 2 H), 3.72 (d, *J* = 11.5 Hz, 2 H), 3.54 (s, 3 H), 3.49 (dd, *J* = 10.0, 5.0 Hz, 1 H), 3.44–3.31 (m, 2 H), 3.19–3.07 (m, 3 H), 2.14–2.04 (m, 4 H), 2.00–1.88 (m, 2 H), 1.26–1.09 (m, 4 H); LC–MS (method F) *m/z*: 423 [(M + H)<sup>+</sup>]; R<sub>t</sub>: 0.48 min; 100% purity.

**5-(1-(1,3-Dimethoxypropan-2-yl)-5-morpholino-1H-benzod[imidazol-2-yl]-1,3-dimethylpyridin-2(1H)-one (24).** 5-(5-Bromo-1-(1,3-dimethoxypropan-2-yl)-1H-benzo[d]imidazol-2-yl)-1,3-dimethylpyridin-2(1H)-one **26** (29.5 g, 70.2 mmol), DavePhos (1.381 g, 3.51 mmol), Pd<sub>2</sub>(dba)<sub>3</sub> (1.285 g, 1.404 mmol), morpholine (12.23 mL, 140 mmol), and 2-MeTHF (150 mL) were combined in a round bottom flask under nitrogen, and then NaO<sup>t</sup>Bu (2 M in THF, 105 mL, 211 mmol) was added. The mixture was heated at 80 °C for 2 h.

The reaction mixture was diluted with brine (200 mL) and extracted with EtOAc (2 × 200 mL). The combined organics were dried and evaporated in vacuo to give a brown gum, which was triturated with EtOAc (200 mL) and then diluted with ether (100 mL), giving a fine, beige precipitate. This was collected by filtration and washed with ether to give the title compound (batch 1, 21.2 g).

The filtrate was evaporated in vacuo to give a brown gum. This was dissolved in DCM (30 mL) and loaded onto a 340 g silica column. Elution was carried out using a gradient of 0–10% MeOH in DCM, and product-containing fractions were evaporated in vacuo. The resulting solid was triturated with ether (100 mL) and collected by filtration to give the title compound (batch 2, 6.5 g).

**5-(5-Bromo-1-(1,3-dimethoxypropan-2-yl)-1H-benzo[d]imidazol-2-yl)-1,3-dimethylpyridin-2(1H)-one 26** (33.2 g, 79.0 mmol), DavePhos (1.554 g, 3.95 mmol), Pd<sub>2</sub>(dba)<sub>3</sub> (1.447 g, 1.580 mmol), and 2-MeTHF (150 mL) were combined in a round bottom flask under nitrogen; then, NaO<sup>t</sup>Bu (2 M in THF, 118 mL, 237 mmol) was added, and the mixture was heated at 80 °C for 2 h. The reaction mixture was diluted with brine (200 mL) and extracted with EtOAc (2 × 200 mL). The combined organics were dried and evaporated in vacuo to give a brown gum, which was triturated with EtOAc (200 mL) and then diluted with ether (100 mL), giving a fine, beige precipitate. This was collected by filtration and washed with ether to give the title compound (batch 3, 31.4 g).

**5-(5-Bromo-1-(1,3-dimethoxypropan-2-yl)-1H-benzo[d]imidazol-2-yl)-1,3-dimethylpyridin-2(1H)-one 26** (20 g, 47.6 mmol), DavePhos (0.936 g, 2.379 mmol), Pd<sub>2</sub>(dba)<sub>3</sub> (0.871 g, 0.952 mmol), morpholine (8.29 mL, 95 mmol), and 2-MeTHF (150 mL) were combined in a round bottom flask under nitrogen; then, NaO<sup>t</sup>Bu (2 M in THF, 71.4 mL, 143 mmol) was added, and the mixture was heated at 80 °C for 2 h. The reaction mixture was diluted with brine (200 mL) and extracted with EtOAc (2 × 300 mL). The combined organics were dried and evaporated in vacuo to give a brown gum. This was combined with batches 1, 2, and 3 and dissolved in DCM (200 mL). The solution was loaded onto a 750 g silica column and eluted with EtOAc (5 column volumes) and then a gradient of 0–25% EtOH in EtOAc (20 column volumes). Product-containing fractions were evaporated in vacuo to give a pale yellow solid. This was dissolved in DCM (500 mL), SiliCycle thiourea silica resin (40 g) was added, and then the mixture was stirred at rt for 1 h. The suspension was filtered, and the filtrate evaporated in vacuo. The resulting foam was triturated with ether (300 mL), and the resulting solid was collected by filtration to give a pale yellow solid (60 g). This was suspended in EtOAc (400 mL) and heated to reflux with stirring for 1 h. The mixture was allowed to cool over 2 h and then further cooled using an ice bath and stirred for 1 h. The suspension was filtered, and the solid was washed with ether (200 mL) to give the title compound as an almost colorless solid (49.8 g, 117 mmol, 59% total yield). mp 174 °C; IR (solid)  $\nu$  (cm<sup>-1</sup>): 2908, 1653, 1611, 1189, 1105, 968; <sup>1</sup>H NMR (400 MHz, DMSO-*d*<sub>6</sub>): δ 8.00 (d, *J* = 2.5 Hz, 1 H), 7.66–7.64 (m, 1 H), 7.63 (d, *J* = 9.0 Hz, 1 H), 7.10 (d, *J* = 2.5 Hz, 1 H), 6.96 (dd, *J* = 9.0, 2.5 Hz, 1 H), 4.77 (tt, *J* = 9.0, 4.5 Hz, 1 H), 3.97 (dd, *J* = 10.5, 9.0 Hz, 2 H), 3.76–3.78 (m, 4 H), 3.75 (dd, *J* = 10.5, 4.5 Hz, 2 H), 3.53 (s, 3 H), 3.16 (s, 6 H), 3.10–3.07 (m, 4 H), 2.08 (s, 3 H); <sup>13</sup>C NMR (150 MHz, DMSO-*d*<sub>6</sub>): δ 161.6, 151.5, 147.4, 144.0, 138.8, 137.3, 128.0, 127.4, 113.4, 112.4, 108.1, 105.1, 69.8, 66.2, 58.3, 56.7, 50.3, 37.4, 16.9; LC–MS (method A) *m/z*: 427 [(M + H)<sup>+</sup>]; R<sub>t</sub>: 0.81 min; 100% purity; HRMS: [(M + H)<sup>+</sup>] calcd for C<sub>23</sub>H<sub>31</sub>N<sub>4</sub>O<sub>4</sub>, 427.2340; found, 427.2340.

**4-Bromo-N-(1,3-dimethoxypropan-2-yl)-2-nitroaniline (25).** 4-Bromo-1-fluoro-2-nitrobenzene (50 g, 227 mmol) and 1,3-dimethoxypropan-2-amine (32.5 g, 273 mmol) were dissolved in acetonitrile (300 mL), and K<sub>2</sub>CO<sub>3</sub> (47.1 g, 341 mmol) was added. The mixture was stirred at 80 °C for 6 h, then the mixture was allowed to cool and stood over the weekend at rt. The mixture was diluted with water (500 mL) and extracted with EtOAc (2 × 500 mL). The organic layer was washed with water (300 mL) and brine (300 mL), dried, and evaporated in vacuo to give the title compound as an orange solid (70 g, 220 mmol, 97% yield). <sup>1</sup>H NMR (400 MHz, CDCl<sub>3</sub>): δ 8.35 (d, *J* = 8.0 Hz, 1 H), 8.31 (d, *J* = 2.5 Hz, 1 H), 7.47 (dd, *J* = 9.0, 2.5 Hz, 1

H), 6.89 (d,  $J = 9.0$  Hz, 1 H), 3.90–3.81 (m, 1 H), 3.62–3.53 (m, 4 H), 3.41 (s, 6 H); LC–MS (method A)  $m/z$ : 319, 321 [(M + H)<sup>+</sup>];  $R_t$ : 1.25 min; 99% purity.

**5-(5-Bromo-1-(1,3-dimethoxypropan-2-yl)-1H-benzo[d]imidazol-2-yl)-1,3-dimethylpyridin-2(1H)-one (26).** 4-Bromo-*N*-(1,3-dimethoxypropan-2-yl)-2-nitroaniline **25** (69 g, 216 mmol) was dissolved in EtOH (400 mL) with heating, and on cooling, the starting material crystallized out. 1,5-Dimethyl-6-oxo-1,6-dihydropyridine-3-carbaldehyde (35.9 g, 238 mmol) was added to the suspension, followed by water (200 mL) and Na<sub>2</sub>S<sub>2</sub>O<sub>4</sub> (94 g, 540 mmol), and the mixture was heated at 90 °C for 18 h. The mixture was evaporated to approximately half its original volume, then diluted with water (200 mL), and extracted with DCM (2 × 300 mL). The combined organics were washed with brine and then dried and evaporated in vacuo. The resulting yellow solid was triturated with EtOAc (200 mL), and the solid was collected by filtration. The solid was washed with ether (200 mL) and dried under vacuum to give the title compound (batch 1, 31 g, 34% yield). <sup>1</sup>H NMR (400 MHz, CDCl<sub>3</sub>): δ 7.90 (d,  $J = 2.0$  Hz, 1 H), 7.87 (d,  $J = 2.0$  Hz, 1 H), 7.68–7.66 (m, 1 H), 7.44 (d,  $J = 9.0$  Hz, 1 H), 7.35 (dd,  $J = 9.0, 2.0$  Hz, 1 H), 4.84 (tt,  $J = 8.0, 5.0$  Hz, 1 H), 3.94 (dd,  $J = 10.0, 8.0$  Hz, 2 H), 3.82 (dd,  $J = 10.0, 5.0$  Hz, 2 H), 3.62 (s, 3 H), 3.28 (s, 6 H), 2.22 (s, 3 H); LC–MS (method A)  $m/z$ : 420, 422 [(M + H)<sup>+</sup>];  $R_t$ : 1.00 min; 98% purity.

The filtrate was evaporated in vacuo, and the residue was dissolved in DCM (100 mL). The solution was loaded onto a 750 g silica column, and elution was carried out using a gradient of 0–10% MeOH in DCM. Product-containing fractions were evaporated in vacuo to give a yellow solid. This was dissolved in hot EtOAc (150 mL), allowed to cool, and left to stand overnight. The resulting solid was collected by filtration; the product was washed with ether (2 × 100 mL), stirring the product/ether mixture to ensure good trituration, and the product was then dried to give the title compound (batch 2, 20 g, 47.6 mmol, 22% yield). <sup>1</sup>H NMR (400 MHz, DMSO-*d*<sub>6</sub>): δ 8.06 (d,  $J = 2.0$  Hz, 1 H), 7.82 (d,  $J = 2.0$  Hz, 1 H), 7.80 (d,  $J = 9.0$  Hz, 1 H), 7.68–7.66 (m, 1 H), 7.35 (dd,  $J = 9.0, 2.0$  Hz, 1 H), 4.86 (tt,  $J = 9.0, 4.5$  Hz, 1 H), 4.00 (dd,  $J = 10.5, 9.0$  Hz, 2 H), 3.76 (dd,  $J = 10.5, 4.5$  Hz, 2 H), 3.16 (s, 6 H), 2.09 (s, 3 H); LC–MS (method A)  $m/z$ : 420, 422 [(M + H)<sup>+</sup>];  $R_t$ : 1.00 min; 100% purity.

**4-((2-(3-(6-((5-(2-((S)-6-(4-Chlorophenyl)-8-methoxy-1-methyl-4H-benzo[f][1,2,4]triazolo[4,3-*a*][1,4]diazepin-4-yl)acetamido)pentyl)amino)-6-oxohexyl)-2-((2E,4E)-5-[3,3-dimethyl-5-sulfo-1-(4-sulfobutyl)-3H-indol-1-ium-2-yl])penta-2,4-dien-1-ylidene)-3-methyl-5-sulfoindolin-1-yl)butane-1-sulfonate (27).** To a solution of *N*-(5-aminopentyl)-2-[(4S)-6-(4-chlorophenyl)-8-methoxy-1-methyl-4H-benzo[f][1,2,4]triazolo[4,3-*a*][1,4]diazepin-4-yl]acetamide<sup>58</sup> (1.7 mg, 3.53 μmol) in DMF (40 μL) was added a solution of Alexa Fluor 647-ONSu (2.16 mg, 1.966 μmol) in DMF (100 μL). The mixture was basified with DIPEA (1 μL, 5.73 μmol) and agitated overnight on a vortex mixer. The reaction mixture was evaporated to dryness. The solid was dissolved in a mixture of acetonitrile/water/acetic acid (5:4:1, <1 mL), filtered, and applied to a Phenomenex Jupiter C18 preparative column. Gradient elution was carried out at a flow rate of 10 mL/min using 0.1% TFA in water (mobile phase A) and 0.1% TFA in acetonitrile/water (9:1) (mobile phase B) 0–10 min 5% mobile phase B, 10–100 min 35% mobile phase B, 100–115 min 100% mobile phase B. The appropriate fractions were combined, evaporated to dryness, and triturated with dry ether, and the blue solid was dried overnight at <0.2 mbar to give the title compound (1.54 mg). HPLC analysis was conducted on a Spherisorb ODS2 column. Gradient elution was carried out using 0.1% TFA in water (mobile phase A) and 0.1% TFA in acetonitrile/water (9:1) (mobile phase B) 0–60 min 1–35% mobile phase B. Estimated purity >95%. Mass analysis was recorded on a Waters micromass ZQ mass spectrometer operating in the positive electrospray ionization mode giving ES<sup>+</sup> = 661.8 corresponding to [(M – C<sub>2</sub>H<sub>5</sub>/2) + H]<sup>+</sup>.

**BRD4 Protein Expression and Purification.** Recombinant human bromodomains BRD4 (1–477) (Y390A) (BD2 mutation to monitor binding to BD1) were expressed in *Escherichia coli* cells using a pET15b vector with a 6-His tag at the *N*-terminal. The His-tagged

bromodomain pellet was resuspended in 50 mM 4-(2-hydroxyethyl)-piperazine-1-ethanesulfonic acid (HEPES) (pH 7.5), 300 mM NaCl, 10 mM imidazole, and 1 μL/mL protease inhibitor cocktail and extracted from the *E. coli* cells using sonication. Purification was carried out using a nickel sepharose high-performance column, and the proteins were washed and then eluted with a linear gradient of 0–500 mM imidazole with buffer 50 mM HEPES (pH 7.5), 150 mM NaCl, and 500 mM imidazole, over 20 column volumes. Final purification was completed by using a Superdex 200 prep grade size exclusion column. Purified protein was stored at –80 °C in 20 mM HEPES (pH 7.5) and 100 mM NaCl. The protein identity was confirmed by peptide mass fingerprinting, and the predicted molecular weight was confirmed by mass spectrometry.

**BRD4 TR-FRET Assay.** All assay components were diluted in a buffer composition of 50 mM HEPES (pH 7.4), 150 mM NaCl, 5% glycerol, 1 mM DTT, and 1 mM 3-[(3-cholamidopropyl)-dimethylammonio]-1-propanesulfonate. The final concentration of bromodomain protein was 10 nM. An Alexa Fluor 647 derivative of I-BET762 (**27**) was used as the competing ligand and was used at a concentration equal to the  $K_d$ . These components were premixed and 5 μL of this reaction mixture was added to wells containing 50 nL of various concentrations of the test compound or DMSO vehicle (0.5% DMSO final) in 384-well black low volume microtiter plates and incubated in the dark for 30 min at rt. The bromodomain protein/fluorescent ligand interaction was detected using TR-FRET following 5 μL addition of a 1.5 nM europium chelate-labeled anti-6His antibody in assay buffer. Time-resolved fluorescence (TRF) was then detected on a TRF laser equipped with a PerkinElmer EnVision multimode plate reader (excitation = 337 nm; emission 1 = 615 nm; emission 2 = 665 nm; dual wavelength bias dichroic = 400, 630 nm). The TR-FRET ratio was calculated using the following equation: ratio = ((acceptor fluorescence at 665 nm)/(donor fluorescence at 615 nm)) × 1000. TR-FRET ratio data were normalized to a mean of 16 replicates per microtiter plate of both 10 μM I-BET151 **4** and 1% DMSO controls, and IC<sub>50</sub> values were determined for each of the compounds tested by fitting the fluorescence ratio data to a four-parameter model:  $y = a + ((b - a)/(1 + (10^x/10^c)^d))$  where “*a*” is the minimum, “*b*” is the Hill slope, “*c*” is the IC<sub>50</sub>, and “*d*” is the maximum.

**Cocrystallization and Structure Determination.** BRD4 BD1-dimethylpyridone benzimidazole **24** complex was cocrystallized with at least 3:1 excess of the compound over protein at 9.0 mg/mL in 120 + 120 nL sitting drops using a 96-well MRC plate. Crystals were grown with a well solution of 0.1 M PCTP pH 8.0, 25% v/v PEG1500 at 20 °C and cryoprotected using the well solution with 20% ethylene glycol prior to flash freezing in liquid nitrogen. Data from a single crystal were collected at 100 K on I03 at the Diamond Light Source at Oxford and processed to 1.30 Å using X-ray detector software (XDS)<sup>80</sup> and AIMLESS.<sup>81</sup> A molecular replacement solution was determined using Phaser and a previously determined in-house structure as a starting model. The P<sub>2</sub>1<sub>2</sub>1<sub>2</sub> cell ( $\alpha = \beta = \gamma = 90^\circ$ ,  $a = 39.493$  Å,  $b = 49.533$  Å,  $c = 58.2133$  Å) has a single molecule in the ASU. Manual model building was performed using COOT<sup>82</sup> and refined using REFMAC<sup>83</sup> within the CCP4 software suite. There was clear difference density for the ligand in the acetylated lysine binding site, allowing the ligand to be unambiguously modeled. Statistics for the data collection and refined co-ordinates are given in the Supporting Information.

**Measurement of LPS-Induced MCP-1 Production from Human WB.** Blood was collected in a tube containing sodium heparin (10 units/mL). 96-well compound plates containing 1 μL test sample in 100% DMSO were prepared (two replicates to account for donor variability). WB (130 μL) was dispensed into each well and incubated for 30 min at 37 °C under a 5% CO<sub>2</sub> atmosphere. LPS (10 μL, *Salmonella typhosa*) made up in phosphate-buffered saline (PBS; 200 ng/mL final assay concentration) was added to each well of the compound plates. After further incubation for 18–24 h at 37 °C under a 5% CO<sub>2</sub> atmosphere, 140 μL of PBS was added to each well. The plates were sealed and centrifuged for 10 min at 1800 rpm at rt. The cell supernatant (20 μL) was placed in a 96-well meso scale

discovery (MSD) plate precoated with a human MCP-1 capture antibody. The plates were sealed and placed on a shaker at 600 rpm for 1.5 h at rt. Anti-human MCP-1 antibody (20  $\mu$ L) labeled with sulfo-TAG was added to each well of the MSD plate (stock 50 $\times$  was diluted 1:50 with diluent 100, final assay concentration was 1  $\mu$ g/mL). The plates were then resealed and shaken for 1.5 h at rt before washing with PBS Tween 0.05% ( $\times 3$ ). 2 $\times$  MSD Read Buffer T (150  $\mu$ L, stock 4 $\times$  MSD Read Buffer T was diluted 50:50 with deionized water) was then added to each well and the plates read on the MSD Sector Imager 6000. Concentration response curves for each compound were generated from the data and an  $IC_{50}$  value was calculated. Human biological samples were sourced ethically and their research use was in accord with the terms of the informed consents under an Institutional Review Board (IRB)/Ethics Committee (EC)-approved protocol.

**Measurement of LPS Induced IL-6 Production from Human WB.** Blood was collected in a tube containing sodium heparin (10 units of heparin/mL of blood). 96-well compound plates containing 1  $\mu$ L of the test sample in 100% DMSO were prepared (two replicates to account for donor variability). WB (130  $\mu$ L) was dispensed into each well of the 96-well compound plates and incubated for 30 min at 37  $^{\circ}$ C under a 5%  $CO_2$  atmosphere. LPS (10  $\mu$ L, *S. typhosa*) made up in PBS with 1% bovine serum albumin (200 ng/mL final assay concentration) was added to each well of the compound plates. The plates were then placed in the humidified primary cell incubator for 18–24 h at 37  $^{\circ}$ C under a 5%  $CO_2$  atmosphere. PBS (140  $\mu$ L) was added to all wells of the compound plates containing blood, and the plates were sealed and shaken on a plate shaker at 600 rpm for 2 min. The plates were then centrifuged for 10 min at 2500 rpm at rt. The cell supernatant (100  $\mu$ L) was removed using a Bomec NX robot. MSD plates precoated with the human IL-6 capture antibody were blocked with MSD diluent 2 for 30 min on a plate shaker (600 rpm at rt). The supernatants were diluted 1:40 in PBS, and 25  $\mu$ L of which was added to 96-well MSD IL-6 plates. The plates were sealed and placed on a shaker at 600 rpm for 1.5 h at rt. Anti-human IL-6 antibody (20  $\mu$ L) labeled with sulfo-TAG was added to each well of the MSD plate (stock 50 $\times$  was diluted 1:50 with diluent 3, final assay concentration is 1  $\mu$ g/mL). The plates were then resealed and shaken for 1 h at rt before washing with PBS Tween 0.05% ( $\times 3$ ). 2 $\times$  MSD Read Buffer T (150  $\mu$ L, stock 4 $\times$  MSD Read Buffer T was diluted 50:50 with deionized water) was then added to each well, and the plates were read on the MSD Sector Imager 6000. Concentration response curves for each compound were generated from the data, and an  $IC_{50}$  value was calculated. Human biological samples were sourced ethically, and their research use was in accord with the terms of the informed consents under an IRB/EC-approved protocol.

**Mouse LPS Model.** Male CD1 mice (Charles River Laboratories, 5 per group) received an iv challenge of LPS (100  $\mu$ g/kg, L3192 *E. coli* 0127:B8) 0.5 h after oral administration of dimethylpyridone benzimidazole **24** (in 1% (w/v) methylcellulose, aq 400). Serial blood samples were collected via tail vein up to 3 h or via cardiac puncture at 5 h (terminal sample) post LPS administration, and the serum harvested from the blood samples was frozen at  $-80$   $^{\circ}$ C. On the day of analysis, the serum was thawed to rt and diluted 1:50 with assay diluent and levels of IL-6 were measured on MSD plates according to the manufacturer's guidelines. Plates were read on an MSD Sector Imager 6000. The mean IL-6 AUC and mean unbound blood AUC values were generated using WinNonlin Phoenix version 6.3. All values statistically analyzed are represented as mean  $\pm$  SD and are compared to the corresponding vehicle-treated group. Levels of significance were calculated by analysis of variance (ANOVA) followed by Dunnett's multiple comparison *t*-test using GraphPad Prism version 5.04 (GraphPad Software, San Diego, CA). Statistical differences were determined as  $p < 0.05$  (\*),  $p < 0.001$  (\*\*\*) as compared to the vehicle-treated group. Animal studies were ethically reviewed and carried out in accordance with Animals (Scientific Procedures) Act 1986 and the GSK Policy on the Care, Welfare and Treatment of Laboratory Animals.

**T Cell-Dependent Immunization Model.** Male CD1 mice (Charles River Laboratories, 8 per group) received a single oral

administration of dimethylpyridone benzimidazole **24** (in 1% (w/v) methylcellulose, aq 400) either QD or QOD over a 14 day dosing period. On day 1 of the study, each mouse received a single bolus ip administration of TNP-KLH (100  $\mu$ g/kg) 0.5 h after oral administration of the compound. Serial blood samples were collected at 0.5 h post oral compound administration via tail vein on days 1, 4, 7, 9, and 11 or via cardiac puncture (terminal sample) on day 14, and the serum harvested from the blood samples was frozen at  $-80$   $^{\circ}$ C. On the day of analysis, the serum was thawed to rt and levels of IgG1 were measured using a TNP ELISA and the plates read on a SpectraMax 190 spectrophotometer.  $C_{50}$  values were generated using WinNonlin Phoenix version 6.3. All values statistically analyzed are represented as mean  $\pm$  SD and are compared to the corresponding vehicle-treated group. Levels of significance were calculated by ANOVA followed by Dunnett's multiple comparison *t*-test using GraphPad Prism version 5.04 (GraphPad Software, San Diego, CA). Statistical differences were determined as  $p < 0.01$  (\*\*), as compared to the vehicle-treated group. Animal studies were ethically reviewed and carried out in accordance with Animals (Scientific Procedures) Act 1986 and the GSK Policy on the Care, Welfare and Treatment of Laboratory Animals.

## ■ ASSOCIATED CONTENT

### 📄 Supporting Information

The Supporting Information is available free of charge at <https://pubs.acs.org/doi/10.1021/acs.jmedchem.9b01670>.

Affinity screening of the encoded library method, BRD4 FP assay method, representative compound spectra, full assay data table, representative BCP selectivity data for dimethylpyridone benzimidazole **20a**, chromLog $D_{7,4}$  method, solubility methods and data, X-ray powder diffraction (XRPD) method and data, mouse in vivo pharmacokinetic data for 2,6-dimethylphenol benzimidazole **10a**, dose prediction calculations, in vitro clearance data for 5-dimethylamine **22c** and 5-morpholine **23e**, bromodomain binding assay panel data, NanoBRET method and data, X-ray crystallization methods and data, and developability and cross screening panel data (PDF)

Molecular formula strings and biological data for final compounds (CSV)

### Accession Codes

Cocrystal structures of BRD4 BD1 in the complex with compounds **10**, **20a**, and **24** and cocrystal structures of BRD2 BD1 in the complex with compounds **16** and **17** are deposited under the accession codes 6TPX, 6TPY, 6TPZ, 6TQ1, and 6TQ2, in the Protein Data Bank, respectively. Authors will release the atomic coordinates upon article publication.

## ■ AUTHOR INFORMATION

### Corresponding Author

\*E-mail: [christopher.x.wellaway@gsk.com](mailto:christopher.x.wellaway@gsk.com).

### ORCID

Christopher R. Wellaway: 0000-0003-0077-3452

Paul Bamborough: 0000-0001-9479-2894

David J. Hirst: 0000-0001-9969-2104

Philip G. Humphreys: 0000-0002-8614-7155

Rishi R. Shah: 0000-0002-5018-1730

### Present Address

<sup>§</sup>Research and Early Development, Respiratory, Inflammation and Autoimmunity (RIA) BioPharmaceuticals R&D, AstraZeneca, SE-431 83 Mölndal, Sweden.

## Author Contributions

The manuscript was written through contributions of all authors. All authors have given approval to the final version of the manuscript.

## Notes

The authors declare no competing financial interest.

## ACKNOWLEDGMENTS

We are grateful to Graham Inglis, Emmanuel Demont, and Cesar Molina for review and proof-reading of the manuscript. We thank Kate Dennis, Alan Ferrie, Iain Reid, Yang Zhuli and colleagues at WuXi, and GVK for supporting laboratory work.

## ABBREVIATIONS

BAZ2A, bromodomain adjacent to zinc finger domain 2A; BCP, bromodomain-containing proteins; BD1, first (N-terminal) bromodomain; BD2, second (C-terminal) bromodomain; BET, bromodomain and extraterminal; BOP, (benzotriazol-1-yloxy)tris(dimethylamino)phosphonium hexafluorophosphate; BRET, bioluminescence resonance energy transfer; CHAPS, 3-[(3-cholamidopropyl)dimethylammonio]-1-propanesulfonate; dba, dibenzylideneacetone; DEL, DNA-encoded small-molecule library; DIPEA, diisopropylethylamine; EDC,  $N^1$ -((ethylimino)methylene)- $N^3,N^3$ -dimethylpropane-1,3-diamine; ELT, encoded library technology; HATU, 1-[bis(dimethylamino)methylene]-1H-1,2,3-triazolo[4,5-b]pyridinium 3-oxide hexafluorophosphate; HEPES, 4-(2-hydroxyethyl) piperazine-1-ethanesulfonic acid; Heps, hepatocytes; HOBt, 1H-benzo[d][1,2,3]triazol-1-ol; HPB, hydroxypropyl betacyclodextrin; IL-6, interleukin 6; IVC, in vitro clearance; KAc, N-acetyl lysine; MCP-1, monocyte chemoattractant protein 1; MDAP, mass-directed autoperformative high-performance liquid chromatography; 2-MeTHF, 2-methyl tetrahydrofuran; Mics, microsomes; MMP, matched molecular pair; NMC, nuclear protein in testis midline carcinoma; PFI, property forecast index; PKPD, pharmacokinetic/pharmacodynamic; PPA, polyphosphoric acid; PROTAC, proteolysis targeting chimera; PTM, post-translational modification; TNP-KLH, trinitrophenyl-keyhole limpet hemocyanin; TRF, time-resolved fluorescence; WB, whole blood; XRPD, X-ray powder diffraction

## REFERENCES

- (1) Taverna, S. D.; Li, H.; Ruthenburg, A. J.; Allis, C. D.; Patel, D. J. How chromatin-binding modules interpret histone modifications: lessons from professional pocket pickers. *Nat. Struct. Mol. Biol.* **2007**, *14*, 1025–1040.
- (2) Romero, F. A.; Taylor, A. M.; Crawford, T. D.; Tsui, V.; Côté, A.; Magnuson, S. Disrupting acetyl-lysine recognition: progress in the development of bromodomain inhibitors. *J. Med. Chem.* **2016**, *59*, 1271–1298.
- (3) Filippakopoulos, P.; Picaud, S.; Mangos, M.; Keates, T.; Lambert, J.-P.; Barsyte-Lovejoy, D.; Felletar, I.; Volkmer, R.; Müller, S.; Pawson, T.; Gingras, A.-C.; Arrowsmith, C. H.; Knapp, S. Histone recognition and large-scale structural analysis of the human bromodomain family. *Cell* **2012**, *149*, 214–231.
- (4) Yu, L.; Wang, Z.; Zhang, Z.; Ren, X.; Lu, X.; Ding, K. Small-molecule BET inhibitors in clinical and preclinical development and their therapeutic potential. *Curr. Top. Med. Chem.* **2015**, *15*, 776–794.
- (5) Liu, Z.; Wang, P.; Chen, H.; Wold, E. A.; Tian, B.; Brasier, A. R.; Zhou, J. Drug discovery targeting bromodomain-containing protein 4 (BRD4). *J. Med. Chem.* **2017**, *60*, 4533–4558.
- (6) McLure, K. G.; Gesner, E. M.; Tsujikawa, L.; Kharenko, O. A.; Attwell, S.; Campeau, E.; Wasiak, S.; Stein, A.; White, A.; Fontano, E.;

Suto, R. K.; Wong, N. C. W.; Wagner, G. S.; Hansen, H. C.; Young, P. R. RVX-208, an inducer of ApoA-I in humans, is a BET bromodomain antagonist. *PLoS One* **2013**, *8*, No. e83190.

- (7) Picaud, S.; Wells, C.; Felletar, I.; Brotherton, D.; Martin, S.; Savitsky, P.; Diez-Dacal, B.; Philpott, M.; Bountra, C.; Lingard, H.; Fedorov, O.; Müller, S.; Brennan, P. E.; Knapp, S.; Filippakopoulos, P. RVX-208, an inhibitor of BET transcriptional regulators with selectivity for the second bromodomain. *Proc. Natl. Acad. Sci. U.S.A.* **2013**, *110*, 19754–19759.

- (8) Gacias, M.; Gerona-Navarro, G.; Plotnikov, A. N.; Zhang, G.; Zeng, L.; Kaur, J.; Moy, G.; Rusinova, E.; Rodriguez, Y.; Matikainen, B.; Vincek, A.; Joshua, J.; Casaccia, P.; Zhou, M.-M. Selective chemical modulation of gene transcription favors oligodendrocyte lineage progression. *Chem. Biol.* **2014**, *21*, 841–854.

- (9) Law, R. P.; Atkinson, S. J.; Bamborough, P.; Chung, C.-w.; Demont, E. H.; Gordon, L. J.; Lindon, M.; Prinjha, R. K.; Watson, A. J. B.; Hirst, D. J. Discovery of tetrahydroquinoxalines as bromodomain and extra-terminal domain (BET) inhibitors with selectivity for the second bromodomain. *J. Med. Chem.* **2018**, *61*, 4317–4334.

- (10) Galdeano, C.; Ciulli, A. Selectivity on-target of bromodomain chemical probes by structure-guided medicinal chemistry and chemical biology. *Future Med. Chem.* **2016**, *8*, 1655–1680.

- (11) Raux, B.; Voitovich, Y.; Derviaux, C.; Lugari, A.; Rebuffet, E.; Milhas, S.; Priet, S.; Roux, T.; Trinquet, E.; Guillemot, J.-C.; Knapp, S.; Brunel, J.-M.; Fedorov, A. Y.; Collette, Y.; Roche, P.; Betzi, S.; Combes, S.; Morelli, X. Exploring selective inhibition of the first bromodomain of the human bromodomain and extra-terminal domain (BET) proteins. *J. Med. Chem.* **2016**, *59*, 1634–1641.

- (12) Tanaka, M.; Roberts, J. M.; Seo, H.-S.; Souza, A.; Paulk, J.; Scott, T. G.; Deangelo, S. L.; Dhe-paganon, S.; Bradner, J. E. Design and characterization of bivalent BET inhibitors. *Nat. Chem. Biol.* **2016**, *12*, 1089–1096.

- (13) Waring, M. J.; Chen, H.; Rabow, A. A.; Walker, G.; Bobby, R.; Boiko, S.; Bradbury, R. H.; Callis, R.; Clark, E.; Dale, I.; Daniels, D. L.; Dulak, A.; Flavell, L.; Holdgate, G.; Jowitt, T. A.; Kikhney, A.; McAlister, M.; Méndez, J.; Ogg, D.; Patel, J.; Petteruti, P.; Robb, G. R.; Robers, M. B.; Saif, S.; Stratton, N.; Svergun, D. I.; Wang, W.; Whittaker, D.; Wilson, D. M.; Yao, Y. Potent and selective bivalent inhibitors of BET bromodomains. *Nat. Chem. Biol.* **2016**, *12*, 1097–1104.

- (14) Rhyasen, G. W.; Hattersley, M. M.; Yao, Y.; Dulak, A.; Wang, W.; Petteruti, P.; Dale, I. L.; Boiko, S.; Cheung, T.; Zhang, J.; Wen, S.; Castriotta, L.; Lawson, D.; Collins, M.; Bao, L.; Ahdesmaki, M. J.; Walker, G.; O'Connor, G.; Yeh, T. C.; Rabow, A. A.; Dry, J. R.; Reimer, C.; Lyne, P.; Mills, G. B.; Fawell, S. E.; Waring, M. J.; Zinda, M.; Clark, E.; Chen, H. AZD5153: a novel bivalent BET bromodomain inhibitor highly active against hematologic malignancies. *Mol. Cancer Ther.* **2016**, *15*, 2563–2574.

- (15) Lu, J.; Qian, Y.; Altieri, M.; Dong, H.; Wang, J.; Raina, K.; Hines, J.; Winkler, J. D.; Crew, A. P.; Coleman, K.; Crews, C. M. Hijacking the E3 ubiquitin ligase cereblon to efficiently target BRD4. *Chem. Biol.* **2015**, *22*, 755–763.

- (16) Zengerle, M.; Chan, K.-H.; Ciulli, A. Selective small molecule induced degradation of the BET bromodomain protein BRD4. *ACS Chem. Biol.* **2015**, *10*, 1770–1777.

- (17) Raina, K.; Lu, J.; Qian, Y.; Altieri, M.; Gordon, D.; Rossi, A. M. K.; Wang, J.; Chen, X.; Dong, H.; Siu, K.; Winkler, J. D.; Crew, A. P.; Crews, C. M.; Coleman, K. G. PROTAC-induced BET protein degradation as a therapy for castration-resistant prostate cancer. *Proc. Natl. Acad. Sci. U.S.A.* **2016**, *113*, 7124–7129.

- (18) Zhou, B.; Hu, J.; Xu, F.; Chen, Z.; Bai, L.; Fernandez-Salas, E.; Lin, M.; Liu, L.; Yang, C.-Y.; Zhao, Y.; McEachern, D.; Przybranowski, S.; Wen, B.; Sun, D.; Wang, S. Discovery of a small-molecule degrader of bromodomain and extra-terminal (BET) proteins with picomolar cellular potencies and capable of achieving tumor regression. *J. Med. Chem.* **2018**, *61*, 462–481.

- (19) Chan, K.-H.; Zengerle, M.; Testa, A.; Ciulli, A. Impact of target warhead and linkage vector on inducing protein degradation:

comparison of bromodomain and extra-terminal (BET) degraders derived from triazolodiazepine (JQ1) and tetrahydroquinoline (I-BET726) BET inhibitor scaffolds. *J. Med. Chem.* **2018**, *61*, 504–513.

(20) Kharenko, O. A.; Patel, R. G.; Brown, S. D.; Calosing, C.; White, A.; Lakshminarasimhan, D.; Suto, R. K.; Duffy, B. C.; Kitchen, D. B.; McLure, K. G.; Hansen, H. C.; van der Horst, E. H.; Young, P. R. Design and characterization of novel covalent bromodomain and extra-terminal domain (BET) inhibitors targeting a methionine. *J. Med. Chem.* **2018**, *61*, 8202–8211.

(21) Nicodeme, E.; Jeffrey, K. L.; Schaefer, U.; Beinke, S.; Dewell, S.; Chung, C.-w.; Chandwani, R.; Marazzi, L.; Wilson, P.; Coste, H.; White, J.; Kirilovsky, J.; Rice, C. M.; Lora, J. M.; Prinjha, R. K.; Lee, K.; Tarakhovskiy, A. Suppression of inflammation by a synthetic histone mimic. *Nature* **2010**, *468*, 1119–1123.

(22) Mirguet, O.; Gosmini, R.; Toum, J.; Clément, C. A.; Barnathan, M.; Brusq, J.-M.; Mordaunt, J. E.; Grimes, R. M.; Crowe, M.; Pineau, O.; Ajakane, M.; Daugan, A.; Jeffrey, P.; Cutler, L.; Haynes, A. C.; Smithers, N. N.; Chung, C.-w.; Bamborough, P.; Uings, I. J.; Lewis, A.; Witherington, J.; Parr, N.; Prinjha, R. K.; Nicodème, E. Discovery of epigenetic regulator I-BET762: lead optimization to afford a clinical candidate inhibitor of the BET bromodomains. *J. Med. Chem.* **2013**, *56*, 7501–7515.

(23) Filippakopoulos, P.; Qi, J.; Picaud, S.; Shen, Y.; Smith, W. B.; Fedorov, O.; Morse, E. M.; Keates, T.; Hickman, T. T.; Felletar, L.; Philpott, M.; Munro, S.; McKeown, M. R.; Wang, Y.; Christie, A. L.; West, N.; Cameron, M. J.; Schwartz, B.; Heightman, T. D.; La Thangue, N.; French, C. A.; Wiest, O.; Kung, A. L.; Knapp, S.; Bradner, J. E. Selective inhibition of BET bromodomains. *Nature* **2010**, *468*, 1067–1073.

(24) Matzuk, M. M.; McKeown, M. R.; Filippakopoulos, P.; Li, Q.; Ma, L.; Agno, J. E.; Lemieux, M. E.; Picaud, S.; Yu, R. N.; Qi, J.; Knapp, S.; Bradner, J. E. Small-molecule inhibition of BRDT for male contraception. *Cell* **2012**, *150*, 673–684.

(25) Tang, X.; Peng, R.; Phillips, J. E.; Deguzman, J.; Ren, Y.; Apparsundaram, S.; Luo, Q.; Bauer, C. M.; Fuentes, M. E.; DeMartino, J. A.; Tyagi, G.; Garrido, R.; Hogaboam, C. M.; Denton, C. P.; Holmes, A. M.; Kitson, C.; Stevenson, C. S.; Budd, D. C. Assessment of Brd4 inhibition in idiopathic pulmonary fibrosis lung fibroblasts and in vivo models of lung fibrosis. *Am. J. Pathol.* **2013**, *183*, 470–479.

(26) Tang, X.; Peng, R.; Ren, Y.; Apparsundaram, S.; Deguzman, J.; Bauer, C. M.; Hoffman, A. F.; Hamilton, S.; Liang, Z.; Zeng, H.; Fuentes, M. E.; Demartino, J. A.; Kitson, C.; Stevenson, C. S.; Budd, D. C. BET bromodomain proteins mediate downstream signaling events following growth factor stimulation in human lung fibroblasts and are involved in bleomycin-induced pulmonary fibrosis. *Mol. Pharmacol.* **2013**, *83*, 283–293.

(27) Spiltoir, J. I.; Stratton, M. S.; Cavañin, M. A.; Demos-Davies, K.; Reid, B. G.; Qi, J.; Bradner, J. E.; McKinsey, T. A. BET acetyl-lysine binding proteins control pathological cardiac hypertrophy. *J. Mol. Cell. Cardiol.* **2013**, *63*, 175–179.

(28) Bailey, D.; Jahagirdar, R.; Gordon, A.; Hafiane, A.; Campbell, S.; Chatur, S.; Wagner, G. S.; Hansen, H. C.; Chiacchia, F. S.; Johansson, J.; Krimbou, L.; Wong, N. C. W.; Genest, J. RVX-208: a small molecule that increases apolipoprotein A-I and high-density lipoprotein cholesterol in vitro and in vivo. *J. Am. Coll. Cardiol.* **2010**, *55*, 2580–2589.

(29) Jahagirdar, R.; Zhang, H.; Azhar, S.; Tobin, J.; Attwell, S.; Yu, R.; Wu, J.; McLure, K. G.; Hansen, H. C.; Wagner, G. S.; Young, P. R.; Srivastava, R. A. K.; Wong, N. C. W.; Johansson, J. A novel BET bromodomain inhibitor, RVX-208, shows reduction of atherosclerosis in hyperlipidemic ApoE deficient mice. *Atherosclerosis* **2014**, *236*, 91–100.

(30) Dawson, M. A.; Prinjha, R. K.; Dittmann, A.; Giotopoulos, G.; Bantscheff, M.; Chan, W.-I.; Robson, S. C.; Chung, C.-w.; Hopf, C.; Savitski, M. M.; Huthmacher, C.; Gudgin, E.; Lugo, D.; Beinke, S.; Chapman, T. D.; Roberts, E. J.; Soden, P. E.; Auger, K. R.; Mirguet, O.; Doehner, K.; Delwel, R.; Burnett, A. K.; Jeffrey, P.; Drewes, G.; Lee, K.; Huntly, B. J. P.; Kouzarides, T. Inhibition of BET recruitment

to chromatin as an effective treatment for MLL-fusion leukaemia. *Nature* **2011**, *478*, 529–533.

(31) Mirguet, O.; Lamotte, Y.; Donche, F.; Toum, J.; Gellibert, F.; Bouillot, A.; Gosmini, R.; Nguyen, V.-L.; Delannée, D.; Seal, J.; Blandel, F.; Boullay, A.-B.; Boursier, E.; Martin, S.; Brusq, J.-M.; Krysa, G.; Riou, A.; Tellier, R.; Costaz, A.; Huet, P.; Dudit, Y.; Trottet, L.; Kirilovsky, J.; Nicodeme, E. From ApoA1 upregulation to BET family bromodomain inhibition: discovery of I-BET151. *Bioorg. Med. Chem. Lett.* **2012**, *22*, 2963–2967.

(32) Seal, J.; Lamotte, Y.; Donche, F.; Bouillot, A.; Mirguet, O.; Gellibert, F.; Nicodeme, E.; Krysa, G.; Kirilovsky, J.; Beinke, S.; McCleary, S.; Rioja, I.; Bamborough, P.; Chung, C.-w.; Gordon, L.; Lewis, T.; Walker, A. L.; Cutler, L.; Lugo, D.; Wilson, D. M.; Witherington, J.; Lee, K.; Prinjha, R. K. Identification of a novel series of BET family bromodomain inhibitors: binding mode and profile of I-BET151 (GSK1210151A). *Bioorg. Med. Chem. Lett.* **2012**, *22*, 2968–2972.

(33) Fish, P. V.; Filippakopoulos, P.; Bish, G.; Brennan, P. E.; Bunnage, M. E.; Cook, A. S.; Federov, O.; Gerstenberger, B. S.; Jones, H.; Knapp, S.; Marsden, B.; Nocka, K.; Owen, D. R.; Philpott, M.; Picaud, S.; Primiano, M. J.; Ralph, M. J.; Sciammetta, N.; Trzuppek, J. D. Identification of a chemical probe for bromo and extra C-terminal bromodomain inhibition through optimization of a fragment-derived hit. *J. Med. Chem.* **2012**, *55*, 9831–9837.

(34) Wyce, A.; Ganji, G.; Smitheman, K. N.; Chung, C.-w.; Korenchuk, S.; Bai, Y.; Barbash, O.; Le, B.; Craggs, P. D.; McCabe, M. T.; Kennedy-Wilson, K. M.; Sanchez, L. V.; Gosmini, R. L.; Parr, N.; McHugh, C. F.; Dhanak, D.; Prinjha, R. K.; Auger, K. R.; Tummino, P. J. BET inhibition silences expression of MYCN and BCL2 and induces cytotoxicity in neuroblastoma tumor models. *PLoS One* **2013**, *8*, No. e72967.

(35) Gosmini, R.; Nguyen, V. L.; Toum, J.; Simon, C.; Brusq, J.-M. G.; Krysa, G.; Mirguet, O.; Riou-Eymard, A. M.; Boursier, E. V.; Trottet, L.; Bamborough, P.; Clark, H.; Chung, C.-w.; Cutler, L.; Demont, E. H.; Kaur, R.; Lewis, A. J.; Schilling, M. B.; Soden, P. E.; Taylor, S.; Walker, A. L.; Walker, M. D.; Prinjha, R. K.; Nicodème, E. The Discovery of I-BET726 (GSK1324726A), a Potent Tetrahydroquinoline ApoA1 Up-Regulator and Selective BET Bromodomain Inhibitor. *J. Med. Chem.* **2014**, *57*, 8111–8131.

(36) Shapiro, G. I.; Dowlati, A.; LoRusso, P. M.; Eder, J. P.; Anderson, A.; Do, K. T.; Kagey, M. H.; Sirard, C.; Bradner, J. E.; Landau, S. B. Abstract A49: Clinically efficacy of the BET bromodomain inhibitor TEN-010 in an open-label substudy with patients with documented NUT-midline carcinoma (NMC). *Mol. Cancer Ther.* **2015**, *14*, A49.

(37) Siu, K. T.; Ramachandran, J.; Yee, A. J.; Eda, H.; Santo, L.; Panaroni, C.; Mertz, J. A.; Sims, R. J., III; Cooper, M. R.; Raje, N. Preclinical activity of CPI-0610, a novel small-molecule bromodomain and extra-terminal protein inhibitor in the therapy of multiple myeloma. *Leukemia* **2017**, *31*, 1760–1769.

(38) Albrecht, B. K.; Gehling, V. S.; Hewitt, M. C.; Vaswani, R. G.; Côté, A.; Leblanc, Y.; Nasveschuk, C. G.; Bellon, S.; Bergeron, L.; Campbell, R.; Cantone, N.; Cooper, M. R.; Cummings, R. T.; Jayaram, H.; Joshi, S.; Mertz, J. A.; Neiss, A.; Normant, E.; O'Meara, M.; Pardo, E.; Poy, F.; Sandy, P.; Supko, J.; Sims, R. J., III; Harmange, J.-C.; Taylor, A. M.; Audia, J. E. Identification of a benzoisoxazoloazepine inhibitor (CPI-0610) of the bromodomain and extra-terminal (BET) family as a candidate for human clinical trials. *J. Med. Chem.* **2016**, *59*, 1330–1339.

(39) Hewitt, M. C.; Leblanc, Y.; Gehling, V. S.; Vaswani, R. G.; Côté, A.; Nasveschuk, C. G.; Taylor, A. M.; Harmange, J.-C.; Audia, J. E.; Pardo, E.; Cummings, R.; Joshi, S.; Sandy, P.; Mertz, J. A.; Sims, R. J., 3rd; Bergeron, L.; Bryant, B. M.; Bellon, S.; Poy, F.; Jayaram, H.; Tang, Y.; Albrecht, B. K. Development of methyl isoxazoloazepines as inhibitors of BET. *Bioorg. Med. Chem. Lett.* **2015**, *25*, 1842–1848.

(40) Taylor, A. M.; Vaswani, R. G.; Gehling, V. S.; Hewitt, M. C.; Leblanc, Y.; Audia, J. E.; Bellon, S.; Cummings, R. T.; Côté, A.; Harmange, J.-C.; Jayaram, H.; Joshi, S.; Lora, J. M.; Mertz, J. A.; Neiss, A.; Pardo, E.; Nasveschuk, C. G.; Poy, F.; Sandy, P.; Setser, J.

W.; Sims, R. J., 3rd; Tang, Y.; Albrecht, B. K. Discovery of benzotriazololo[4,3-d][1,4]diazepines as orally active inhibitors of BET bromodomains. *ACS Med. Chem. Lett.* **2016**, *7*, 145–150.

(41) Gehling, V. S.; Hewitt, M. C.; Vaswani, R. G.; Leblanc, Y.; Côté, A.; Nasveschuk, C. G.; Taylor, A. M.; Harmange, J.-C.; Audia, J. E.; Pardo, E.; Joshi, S.; Sandy, P.; Mertz, J. A.; Sims, R. J., 3rd; Bergeron, L.; Bryant, B. M.; Bellon, S.; Poy, F.; Jayaram, H.; Sankaranarayanan, R.; Yellapantula, S.; Bangalore Srinivasamurthy, N.; Birudukota, S.; Albrecht, B. K. Discovery, design, and optimization of isoxazole azepine BET inhibitors. *ACS Med. Chem. Lett.* **2013**, *4*, 835–840.

(42) Herait, P. E.; Berthon, C.; Thieblemont, C.; Raffoux, E.; Magarotto, V.; Stathis, A.; Thomas, X.; Leleu, X.; Gomez-Roca, C.; Odore, E.; Roumier, C.; Bourdel, F.; Quesnel, B.; Zucca, E.; Michallet, M.; Recher, C.; Cvitkovic, E.; Rezai, K.; Preudhomme, C.; Facon, T.; Palumbo, A.; Dombret, H. Abstract CT231: BET-bromodomain inhibitor OTX015 shows clinically meaningful activity at nontoxic doses: interim results of an ongoing phase I trial in hematologic malignancies. *Cancer Res.* **2014**, *74*, CT231.

(43) Stathis, A.; Zucca, E.; Bekradda, M.; Gomez-Roca, C.; Delord, J.-P.; Rouge, T. d. L. M.; Uro-Coste, E.; de Braud, F.; Pelosi, G.; French, C. A. Clinical response of carcinomas harboring the BRD4-NUT oncoprotein to the targeted bromodomain inhibitor OTX015/MK-8628. *Cancer Discovery* **2016**, *6*, 492–500.

(44) Gaudio, E.; Tarantelli, C.; Ponzoni, M.; Odore, E.; Rezai, K.; Bernasconi, E.; Cascione, L.; Rinaldi, A.; Stathis, A.; Riveiro, E.; Cvitkovic, E.; Zucca, E.; Bertoni, F. Bromodomain inhibitor OTX015 (MK-8628) combined with targeted agents shows strong in vivo antitumor activity in lymphoma. *Oncotarget* **2016**, *7*, 58142–58147.

(45) Vázquez, R.; Riveiro, M. E.; Astorgues-Xerri, L.; Odore, E.; Rezai, K.; Erba, E.; Panini, N.; Rinaldi, A.; Kwee, I.; Beltrame, L.; Bekradda, M.; Cvitkovic, E.; Bertoni, F.; Frapolli, R.; D'Incalci, M. The bromodomain inhibitor OTX015 (MK-8628) exerts anti-tumor activity in triple-negative breast cancer models as single agent and in combination with everolimus. *Oncotarget* **2017**, *8*, 7598–7613.

(46) McDaniel, K. F.; Wang, L.; Soltwedel, T.; Fidanze, S. D.; Hasvold, L. A.; Liu, D.; Mantei, R. A.; Pratt, J. K.; Sheppard, G. S.; Bui, M. H.; Favre, E. J.; Huang, X.; Li, L.; Lin, X.; Wang, R.; Warder, S. E.; Wilcox, D.; Albert, D. H.; Magoc, T. J.; Rajaraman, G.; Park, C. H.; Hutchins, C. W.; Shen, J. J.; Edalji, R. P.; Sun, C. C.; Martin, R.; Gao, W.; Wong, S.; Fang, G.; Elmore, S. W.; Shen, Y.; Kati, W. M. Discovery of *N*-(4-(2,4-difluorophenoxy)-3-(6-methyl-7-oxo-6,7-dihydro-1*H*-pyrrolo[2,3-*c*]pyridin-4-yl)phenyl)ethanesulfonamide (ABBV-075/Mivebresib), a potent and orally available bromodomain and extraterminal domain (BET) family bromodomain inhibitor. *J. Med. Chem.* **2017**, *60*, 8369–8384.

(47) Dose escalation study of GSK2820151 in subjects with advanced or recurrent solid tumors; Clinical trials <https://clinicaltrials.gov/ct2/show/NCT02630251> (accessed Nov 30, 2015).

(48) Young, R. J.; Green, D. V. S.; Luscombe, C. N.; Hill, A. P. Getting physical in drug discovery II: the impact of chromatographic hydrophobicity measurements and aromaticity. *Drug Discovery Today* **2011**, *16*, 822–830.

(49) Bayliss, M. K.; Butler, J.; Feldman, P. L.; Green, D. V. S.; Leeson, P. D.; Palovich, M. R.; Taylor, A. J. Quality guidelines for oral drug candidates: dose, solubility and lipophilicity. *Drug Discovery Today* **2016**, *21*, 1719–1727.

(50) Franzini, R. M.; Neri, D.; Scheuermann, J. DNA-encoded chemical libraries: advancing beyond conventional small-molecule libraries. *Acc. Chem. Res.* **2014**, *47*, 1247–1255.

(51) Kleiner, R. E.; Dumelin, C. E.; Liu, D. R. Small-molecule discovery from DNA-encoded chemical libraries. *Chem. Soc. Rev.* **2011**, *40*, 5707–5717.

(52) Clark, M. A.; Acharya, R. A.; Arico-Muendel, C. C.; Belyanskaya, S. L.; Benjamin, D. R.; Carlson, N. R.; Centrella, P. A.; Chiu, C. H.; Creaser, S. P.; Cuozzo, J. W.; Davie, C. P.; Ding, Y.; Franklin, G. J.; Franzen, K. D.; Geffer, M. L.; Hale, S. P.; Hansen, N. J. V.; Israel, D. I.; Jiang, J.; Kavarana, M. J.; Kelley, M. S.; Kollmann, C. S.; Li, F.; Lind, K.; Mataruse, S.; Medeiros, P. F.; Messer, J. A.; Myers,

P.; O'Keefe, H.; Oliff, M. C.; Rise, C. E.; Satz, A. L.; Skinner, S. R.; Svendsen, J. L.; Tang, L.; van Vloten, K.; Wagner, R. W.; Yao, G.; Zhao, B.; Morgan, B. A. Design, synthesis and selection of DNA-encoded small-molecule libraries. *Nat. Chem. Biol.* **2009**, *5*, 647–654.

(53) Deng, H.; Zhou, J.; Sundersingh, F. S.; Summerfield, J.; Somers, D.; Messer, J. A.; Satz, A. L.; Ancellin, N.; Arico-Muendel, C. C.; Bedard, K. L.; Beljean, A.; Belyanskaya, S. L.; Bingham, R.; Smith, S. E.; Boursier, E.; Carter, P.; Centrella, P. A.; Clark, M. A.; Chung, C.-w.; Davie, C. P.; Delorey, J. L.; Ding, Y.; Franklin, G. J.; Grady, L. C.; Herry, K.; Hobbs, C.; Kollmann, C. S.; Morgan, B. A.; Kaushansky, L. J.; Zhou, Q. Discovery, SAR, and x-ray binding mode study of BCATm inhibitors from a novel DNA-encoded library. *ACS Med. Chem. Lett.* **2015**, *6*, 919–924.

(54) Deng, H.; Zhou, J.; Sundersingh, F.; Messer, J. A.; Somers, D. O.; Ajakane, M.; Arico-Muendel, C. C.; Beljean, A.; Belyanskaya, S. L.; Bingham, R.; Blazensky, E.; Boullay, A.-B.; Boursier, E.; Chai, J.; Carter, P.; Chung, C.-W.; Daugan, A.; Ding, Y.; Herry, K.; Hobbs, C.; Humphries, E.; Kollmann, C.; Nguyen, V. L.; Nicodeme, E.; Smith, S. E.; Dodic, N.; Ancellin, N. Discovery and optimization of potent, selective, and in vivo efficacious 2-aryl benzimidazole BCATm inhibitors. *ACS Med. Chem. Lett.* **2016**, *7*, 379–384.

(55) Ding, Y.; Chai, J.; Centrella, P. A.; Gondo, C.; DeLorey, J. L.; Clark, M. A. Development and synthesis of DNA-encoded benzimidazole library. *ACS Comb. Sci.* **2018**, *20*, 251–255.

(56) Yang, D.; Fokas, D.; Li, J.; Yu, L.; Baldino, C. A versatile method for the synthesis of benzimidazoles from o-nitroanilines and aldehydes in one step via a reductive cyclization. *Synthesis* **2005**, 47–56.

(57) Zhang, G.; Plotnikov, A. N.; Rusinova, E.; Shen, T.; Morohashi, K.; Joshua, J.; Zeng, L.; Mujtaba, S.; Ohlmeyer, M.; Zhou, M.-M. Structure-guided design of potent diazobenzene inhibitors for the BET bromodomains. *J. Med. Chem.* **2013**, *56*, 9251–9264.

(58) Chung, C.-w.; Coste, H.; White, J. H.; Mirguet, O.; Wilde, J.; Gosmini, R. L.; Delves, C.; Magny, S. M.; Woodward, R.; Hughes, S. A.; Boursier, E. V.; Flynn, H.; Bouillot, A. M.; Bamborough, P.; Brusq, J.-M. G.; Gellibert, F. J.; Jones, E. J.; Riou, A. M.; Homes, P.; Martin, S. L.; Uings, I. J.; Toum, J.; Clément, C. A.; Boullay, A.-B.; Grimley, R. L.; Blandel, F. M.; Prinjha, R. K.; Lee, K.; Kirilovsky, J.; Nicodeme, E. Discovery and characterization of small molecule inhibitors of the BET family bromodomains. *J. Med. Chem.* **2011**, *54*, 3827–3838.

(59) Holenz, J.; Stoy, P. Advances in lead generation. *Bioorg. Med. Chem. Lett.* **2019**, *29*, 517–524.

(60) Chung, C.-w.; Dean, A. W.; Woolven, J. M.; Bamborough, P. Fragment-based discovery of bromodomain inhibitors part 1: inhibitor binding modes and implications for lead discovery. *J. Med. Chem.* **2012**, *55*, 576–586.

(61) Bamborough, P.; Diallo, H.; Goodacre, J. D.; Gordon, L.; Lewis, A.; Seal, J. T.; Wilson, D. M.; Woodrow, M. D.; Chung, C.-w. Fragment-based discovery of bromodomain inhibitors part 2: optimization of phenylisoxazole sulfonamides. *J. Med. Chem.* **2012**, *55*, 587–596.

(62) Bogdan, A.; Kati, W. M.; McDaniel, K. F.; Park, C. H.; Sheppard, G. S.; Wang, L. Preparation of Pyridinyl Containing Compounds as Bromodomain Inhibitors for Therapy. U.S. Patent 20150158873A1, 2015.

(63) Engelhardt, H.; Martin, L.; Smethurst, C. Preparation of Substituted Pyridinones as Anticancer Agents. WO2015022332A1, 2015.

(64) Wang, L.; Frey, R. R.; Hansen, T. M.; Liu, D.; McClellan, W. J.; McDaniel, K. F.; Pratt, J. K.; Wada, C. K. Preparation of Multicyclic Compounds as Bromodomain Inhibitors. WO2015085925A1, 2015.

(65) Engelhardt, H. Benzimidazole Derivatives as BRD4 Inhibitors and their Preparation and Use for the Treatment of Cancer. WO2015169962A1, 2015.

(66) Wang, L.; Pratt, J. K.; Soltwedel, T.; Sheppard, G. S.; Fidanze, S. D.; Liu, D.; Hasvold, L. A.; Mantei, R. A.; Holms, J. H.; McClellan, W. J.; Wendt, M. D.; Wada, C.; Frey, R.; Hansen, T. M.; Hubbard, R.; Park, C. H.; Li, L.; Magoc, T. J.; Albert, D. H.; Lin, X.; Warder, S. E.; Kovar, P.; Huang, X.; Wilcox, D.; Wang, R.; Rajaraman, G.; Petros, A.

M.; Hutchins, C. W.; Panchal, S. C.; Sun, C.; Elmore, S. W.; Shen, Y.; Kati, W. M.; McDaniel, K. F. Fragment-based, structure-enabled discovery of novel pyridones and pyridone macrocycles as potent bromodomain and extra-terminal domain (BET) family bromodomain inhibitors. *J. Med. Chem.* **2017**, *60*, 3828–3850.

(67) Postepska-Igielska, A.; Kronic, D.; Schmitt, N.; Greulich-Bode, K. M.; Boukamp, P.; Grummt, I. The chromatin remodelling complex NoRC safeguards genome stability by heterochromatin formation at telomeres and centromeres. *EMBO Rep.* **2013**, *14*, 704–710.

(68) Hosea, N. A.; Collard, W. T.; Cole, S.; Maurer, T. S.; Fang, R. X.; Jones, H.; Kakar, S. M.; Nakai, Y.; Smith, B. J.; Webster, R.; Beaumont, K. Prediction of human pharmacokinetics from preclinical information: comparative accuracy of quantitative prediction approaches. *Clin. Pharmacol.* **2009**, *49*, 513–533.

(69) Mahmood, I.; Balian, J. D. Interspecies scaling: predicting clearance of drugs in humans. Three different approaches. *Xenobiotica* **1996**, *26*, 887–895.

(70) Tallant, C.; Valentini, E.; Fedorov, O.; Overvoorde, L.; Ferguson, F. M.; Filippakopoulos, P.; Svergun, D. I.; Knapp, S.; Ciulli, A. Molecular basis of histone tail recognition by human TIP5 PHD finger and bromodomain of the chromatin remodeling complex NoRC. *Structure* **2015**, *23*, 80–92.

(71) Wuitschik, G.; Rogers-Evans, M.; Buckl, A.; Bernasconi, M.; Märki, M.; Godel, T.; Fischer, H.; Wagner, B.; Parrilla, I.; Schuler, F.; Schneider, J.; Alker, A.; Schweizer, W. B.; Müller, K.; Carreira, E. M. Spirocyclic oxetanes: synthesis and properties. *Angew. Chem., Int. Ed.* **2008**, *47*, 4512–4515.

(72) Bagdanoff, J. T.; Jain, R.; Han, W.; Zhu, S.; Madiera, A.-M.; Lee, P. S.; Ma, X.; Poon, D. Tetrahydropyrrolo-diazepenones as inhibitors of ERK2 kinase. *Bioorg. Med. Chem. Lett.* **2015**, *25*, 3788–3792.

(73) Stepan, A. F.; Kauffman, G. W.; Keefer, C. E.; Verhoest, P. R.; Edwards, M. Evaluating the differences in cycloalkyl ether metabolism using the design parameter “lipophilic metabolism efficiency” (LipMetE) and a matched molecular pairs analysis. *J. Med. Chem.* **2013**, *56*, 6985–6990.

(74) Gottschall, D. W.; Theodorides, V. J.; Wang, R. The metabolism of benzimidazole anthelmintics. *Parasitol. Today* **1990**, *6*, 115–124.

(75) Wiltshire, H. R.; Sutton, B. M.; Heeps, G.; Betty, A. M.; Angus, D. W.; Harris, S. R.; Worth, E.; Welker, H. A. Metabolism of the calcium antagonist, mibefradil (POSICORTM, Ro 40-5967). Part III. Comparative pharmacokinetics of mibefradil and its major metabolites in rat, marmoset, cynomolgus monkey and man. *Xenobiotica* **1997**, *27*, 557–571.

(76) Craig, P. N. Interdependence between physical parameters and selection of substituent groups for correlation studies. *J. Med. Chem.* **1971**, *14*, 680–684.

(77) Robers, M. B.; Dart, M. L.; Woodroffe, C. C.; Zimprich, C. A.; Kirkland, T. A.; Machleidt, T.; Kupcho, K. R.; Levin, S.; Hartnett, J. R.; Zimmerman, K.; Niles, A. L.; Ohana, R. F.; Daniels, D. L.; Slater, M.; Wood, M. G.; Cong, M.; Cheng, Y.-Q.; Wood, K. V. Target engagement and drug residence time can be observed in living cells with BRET. *Nat. Commun.* **2015**, *6*, 10091.

(78) Bandukwala, H. S.; Gagnon, J.; Togher, S.; Greenbaum, J. A.; Lamperti, E. D.; Parr, N. J.; Molesworth, A. M. H.; Smithers, N.; Lee, K.; Witherington, J.; Tough, D. F.; Prinjha, R. K.; Peters, B.; Rao, A. Selective inhibition of CD4+ T-cell cytokine production and autoimmunity by BET protein and c-Myc inhibitors. *Proc. Natl. Acad. Sci. U.S.A.* **2012**, *109*, 14532–14537.

(79) Schilderink, R.; Bell, M.; Reginato, E.; Patten, C.; Rioja, I.; Hilbers, F. W.; Kabala, P. A.; Reedquist, K. A.; Tough, D. F.; Tak, P. P.; Prinjha, R. K.; de Jonge, W. J. BET bromodomain inhibition reduces maturation and enhances tolerogenic properties of human and mouse dendritic cells. *Mol. Immunol.* **2016**, *79*, 66–76.

(80) Kabsch, W. XDS. *Acta Crystallogr., Sect. D: Biol. Crystallogr.* **2010**, *66*, 125–132.

(81) Evans, P. R.; Murshudov, G. N. How good are my data and what is the resolution? *Acta Crystallogr., Sect. D: Biol. Crystallogr.* **2013**, *69*, 1204–1214.

(82) Emsley, P.; Cowtan, K. Coot: model-building tools for molecular graphics. *Acta Crystallogr., Sect. D: Biol. Crystallogr.* **2004**, *60*, 2126–2132.

(83) Murshudov, G. N.; Vagin, A. A.; Dodson, E. J. Refinement of macromolecular structures by the maximum-likelihood method. *Acta Crystallogr., Sect. D: Biol. Crystallogr.* **1997**, *53*, 240–255.